

NASA
TP
1316
c.1

NASA Technical Paper 1316

LOAN COPY: RET
AFWL TECHNICAL
KIRTLAND AFB,

0134418



TECH LIBRARY KAFB, NM

Wind-Tunnel Investigation at Supersonic Speeds of a Canard-Controlled Missile With Fixed and Free-Rolling Tail Fins

A. B. Blair, Jr.

SEPTEMBER 1978

NASA



NASA Technical Paper 1316

Wind-Tunnel Investigation at Supersonic Speeds of a Canard-Controlled Missile With Fixed and Free-Rolling Tail Fins

A. B. Blair, Jr.
*Langley Research Center
Hampton, Virginia*



National Aeronautics
and Space Administration

**Scientific and Technical
Information Office**

1978

A wind-tunnel investigation was made at free-stream Mach numbers from 1.70 to 2.86 to determine the effects of fixed and free-rolling tail-fin afterbodies on the static longitudinal and lateral aerodynamic characteristics of a cruciform canard-controlled missile model. The effect of small canard roll- and yaw-control deflections was also investigated.

The results indicate that the fixed and free-rolling tail configurations have about the same lift-curve slope and longitudinal stability level at low angles of attack. For the free-rolling tail configuration, the canards provide conventional roll control with no roll-control reversal at low angles of attack. The free-rolling tail configuration reduced induced roll due to model roll angle and canard yaw control.

INTRODUCTION

It is well documented that missile configurations which utilize forward surfaces to provide control experience the problem of induced rolling moments at supersonic Mach numbers. One approach to the solution of this problem, which is described in reference 1, uses a free-rolling tail-fin afterbody on a canard-controlled missile model to reduce induced rolling moments.

The idea of using free-rolling tail fins is not new. From 1950 to 1960, the NASA and its predecessor, NACA, investigated a number of roll-control devices in free flight as part of their aerodynamic control research program for missiles and airplanes. For some of these tests, a free-rolling tail-fin assembly was used on the missile airframes, not only to stabilize the models longitudinally but also to eliminate unwanted, induced rolling moments that were generated by the various roll controls under investigation (e.g., ref. 2). In many cases, the free-rolling tails were on nonmaneuvering missile systems (e.g., boost-glide trajectories at low angles of attack). More recently (1960 to 1973), the U.S. Navy has conducted research on bomb-shaped bodies (free-fall stores) with free-rolling tail fins (refs. 3 and 4) as a means of reducing dispersion and of increasing accuracy by eliminating the effect of flow asymmetries over the tail fins.

The present investigation was conducted to provide some insight into the effectiveness of the free-rolling tail concept for the reduction or elimination of large induced rolling moments that are generally experienced by maneuvering canard-controlled missile configurations at supersonic speeds. In an effort to reduce or eliminate these induced rolling moments, an experimental wind-tunnel investigation has been made to determine the effect of a free-rolling (no fin cant) cruciform tail on the stability and control characteristics of a canard-controlled missile. The results of a similar test conducted by the U.S. Navy with canted free-rolling tail fins can be found in reference 5. The rolling tail concept also offers the potential of enabling the canards to provide some

measure of roll control, either increased roll-damping or roll-attitude control at low angles of attack. There is a growing need to give canard-controlled missile configurations more simplicity and modular flexibility. The free-rolling tail concept may satisfy these requirements by allowing a missile configuration to have a single control system utilizing a cruciform canard control system for pitch, yaw, and roll control.

The tests were conducted in the Langley Unitary Plan wind tunnel at Mach numbers from 1.70 to 2.86. The nominal angle-of-attack range was -30 to 250 at model (canard) roll angles of 0° to 45° and at a Reynolds number of 6.6×10^6 per meter (2.0×10^6 per foot). Results of these tests include the effects of small roll- and yaw-control deflections of the canards on the longitudinal and lateral aerodynamic characteristics of the model with a fixed and free-rolling tail-fin afterbody.

SYMBOLS

The aerodynamic coefficient data are referred to the body-axis system except for lift and drag which are referred to the stability-axis system. The moment reference was located aft of the model nose at 49.0 percent of the reference body length.

Measurements and calculations were made in the U.S. Customary Units. Measurements are presented in the International System of Units (SI), with the equivalent values given parenthetically in U.S. Customary Units (ref. 6).

A reference area; maximum cross-sectional area of body, 0.003425 m² (0.036870 ft²)

C_A axial-force coefficient, Axial force/qA

C_{A,b} base axial-force coefficient, Base axial force/qA

C_D drag coefficient, Drag/qA

C_{D,b} base drag coefficient, Base drag/qA

C_L lift coefficient, Lift/qA

C_{Lα} lift-curve slope, per degree

C_l rolling-moment coefficient, Rolling moment/qAd

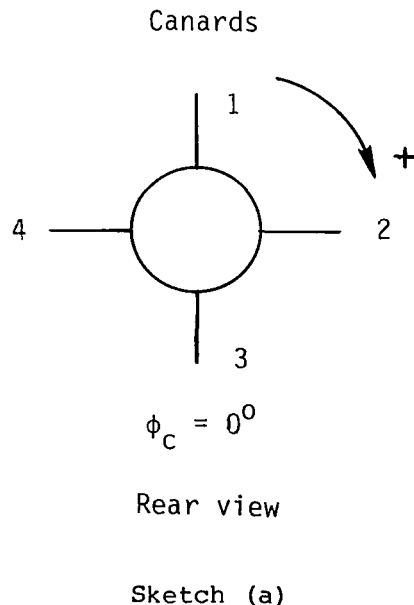
C_m pitching-moment coefficient, Pitching moment/qAd

C_N normal-force coefficient, Normal force/qA

C_n yawing-moment coefficient, Yawing moment/qAd

C_y side-force coefficient, Side force/qA

d	reference diameter, 6.604 cm (2.600 in.)
l	reference body length, 99.060 cm (39.000 in.)
M	Mach number
q	free-stream dynamic pressure, N/m^2 (psfa)
α	angle of attack, deg
δ_{roll}	differential deflections of two canards (canards 2 and 4, shown in sketch (a)) for roll control; individual canards are deflected indicated amount; negative to provide counterclockwise rotation when viewed from rear, deg
δ_{yaw}	yaw-control deflection of two canards (canards 1 and 3, shown in sketch (a)); positive for leading edge right when viewed from rear, deg
ϕ_C	model roll angle; positive clockwise when viewed from rear (for $\phi_C = 0^\circ$, canards are in vertical and horizontal planes), deg
$\dot{\phi}_{tail}$	roll rate of tail-fin afterbody; positive clockwise when viewed from rear, rpm
$\partial C_m / \partial C_L$	static longitudinal stability parameter



APPARATUS AND TESTS

Wind Tunnel

The investigation was conducted in the low Mach number test section of the Langley Unitary Plan wind tunnel, which is a variable-pressure, continuous-flow facility. The test section is approximately 2.13 m (7 ft) long and 1.22 m (4 ft) square. The nozzle leading to the test section is of the asymmetric sliding-block type, which permits a continuous variation in Mach number from about 1.5 to 2.9. (See ref. 7.)

Model

Dimensional details of the model are shown in figure 1(a) and a model photograph is shown in figure 2. The model was a cruciform missile configuration that consisted of a cylindrical body with canards, aft tail fins, and a tangent ogive nose of fineness ratio 3.0. The complete model body had a fineness ratio of 15. The canards and tail fins had slab cross sections with beveled leading and trailing edges. In order for the model to have a free-rolling tail-fin assembly, the tail-fin afterbody was mounted on a set of low-friction ball bearings and was free to rotate through 360° (lock screw out). For the fixed-tail configuration (lock screw in), the tail fins were locked in line with the canards. For both the fixed and free-rolling tail configurations, the canards were deflected to provide roll control and yaw control. The tail fins were not deflected (zero cant angle) and the tail-fin assembly had no braking system.

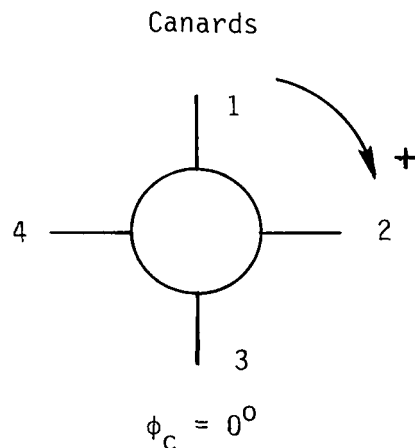
Test Conditions

Tests were performed at the following tunnel conditions:

Mach number	Stagnation temperature		Stagnation pressure		Reynolds number	
	K	°F	kPa	psfa	per meter	per foot
1.70	339	150	56.4	1178	6.6×10^6	2.0×10^6
2.16	339	150	68.5	1430	6.6	2.0
2.36	339	150	75.7	1580	6.6	2.0
2.86	339	150	98.4	2056	6.6	2.0

The dewpoint temperature measured at stagnation pressure was maintained below 239 K (-30° F) to assure negligible condensation effects. All tests were performed with boundary-layer transition strips measured streamwise on both sides of the canards and tail fins and located 3.05 cm (1.20 in.) aft of the body nose and 1.02 cm (0.40 in.) aft of the leading edges. The transition strips were approximately 0.157 cm wide (0.062 in.) and were composed of No. 50 sand grains sprinkled in acrylic plastic. (See ref. 8.)

d	reference diameter, 6.604 cm (2.600 in.)
l	reference body length, 99.060 cm (39.000 in.)
M	Mach number
q	free-stream dynamic pressure, N/m^2 (psfa)
α	angle of attack, deg
δ_{roll}	differential deflections of two canards (canards 2 and 4, shown in sketch (a)) for roll control; individual canards are deflected indicated amount; negative to provide counterclockwise rotation when viewed from rear, deg
δ_{yaw}	yaw-control deflection of two canards (canards 1 and 3, shown in sketch (a)); positive for leading edge right when viewed from rear, deg
ϕ_C	model roll angle; positive clockwise when viewed from rear (for $\phi_C = 0^\circ$, canards are in vertical and horizontal planes), deg
$\dot{\phi}_{tail}$	roll rate of tail-fin afterbody; positive clockwise when viewed from rear, rpm
$\partial C_m / \partial C_L$	static longitudinal stability parameter



Rear view

Sketch (a)

APPARATUS AND TESTS

Wind Tunnel

The investigation was conducted in the low Mach number test section of the Langley Unitary Plan wind tunnel, which is a variable-pressure, continuous-flow facility. The test section is approximately 2.13 m (7 ft) long and 1.22 m (4 ft) square. The nozzle leading to the test section is of the asymmetric sliding-block type, which permits a continuous variation in Mach number from about 1.5 to 2.9. (See ref. 7.)

Model

Dimensional details of the model are shown in figure 1(a) and a model photograph is shown in figure 2. The model was a cruciform missile configuration that consisted of a cylindrical body with canards, aft tail fins, and a tangent ogive nose of fineness ratio 3.0. The complete model body had a fineness ratio of 15. The canards and tail fins had slab cross sections with beveled leading and trailing edges. In order for the model to have a free-rolling tail-fin assembly, the tail-fin afterbody was mounted on a set of low-friction ball bearings and was free to rotate through 360° (lock screw out). For the fixed-tail configuration (lock screw in), the tail fins were locked in line with the canards. For both the fixed and free-rolling tail configurations, the canards were deflected to provide roll control and yaw control. The tail fins were not deflected (zero cant angle) and the tail-fin assembly had no braking system.

Test Conditions

Tests were performed at the following tunnel conditions:

Mach number	Stagnation temperature		Stagnation pressure		Reynolds number	
	K	°F	kPa	psfa	per meter	per foot
1.70	339	150	56.4	1178	6.6×10^6	2.0×10^6
2.16	339	150	68.5	1430	6.6	2.0
2.36	339	150	75.7	1580	6.6	2.0
2.86	339	150	98.4	2056	6.6	2.0

The dewpoint temperature measured at stagnation pressure was maintained below 239 K (-30° F) to assure negligible condensation effects. All tests were performed with boundary-layer transition strips measured streamwise on both sides of the canards and tail fins and located 3.05 cm (1.20 in.) aft of the body nose and 1.02 cm (0.40 in.) aft of the leading edges. The transition strips were approximately 0.157 cm wide (0.062 in.) and were composed of No. 50 sand grains sprinkled in acrylic plastic. (See ref. 8.)

The primary method for controlling tail-fin rotational speed was by limiting the model angle of attack. In the early stages of this test program, tail-fin rotational speed was nominally limited to 200 rpm as a safety precaution; however, this limit was extended to 500 rpm as more confidence was gained. In order to satisfy these limits, only small canard deflections were made.

Measurements

Aerodynamic forces and moments on the model were measured by means of a six-component electrical strain-gage balance which was housed within the model. The balance was attached to a sting which was, in turn, rigidly fastened to the model support system. Balance-chamber pressure (base pressure) was measured by means of a single static-pressure orifice located in the vicinity of the balance. One light-emitting diode with a photo-transistor receiver pick-up mounted on the sting was used in conjunction with a color-coded ring at the base of the model to record tail-fin afterbody revolutions. The accuracy of this recording system was ± 20 rpm. No attempt was made to measure the afterbody torque that was produced by the internal ball-bearing friction, viscous-layer skin friction, or aerodynamic damping.

Corrections

The angles of attack have been corrected for deflection of the balance and sting due to aerodynamic loads. In addition, angles of attack have been corrected for tunnel-flow misalignment. The drag and axial-force coefficient data have been adjusted to free-stream static pressure acting over the model base. Typical measured values of base axial-force and drag coefficients are presented in figure 3.

PRESENTATION OF RESULTS

Figure

Effect of free-rolling tail on longitudinal aerodynamic characteristics of model with zero control deflection at -	
$\phi_C = 0^\circ$	4
$\phi_C = 45^\circ$	5
Effect of canards on longitudinal aerodynamic characteristics of model with free-rolling tail at $\phi_C = 0^\circ$	6
Effect of free-rolling tail on lateral aerodynamic characteristics of model with zero control deflection at -	
$\phi_C = 0^\circ$	7
$\phi_C = 26.6^\circ$	8
$\phi_C = 45^\circ$	9

Effect of canards on lateral aerodynamic characteristics of model with free-rolling tail at $\phi_C = 0^\circ$	10
Roll-control characteristics of model with fixed and free-rolling tail at -	
$\phi_C = 0^\circ$	11
$\phi_C = 45^\circ$	12
Yaw-control characteristics of model with fixed and free-rolling tail at $\phi_C = 0^\circ$	13

Summary of test data from free-rolling tail configuration with -	
Zero control deflection	I
Canard off	II
Two canards differentially deflected 0.5° each for negative roll control	III
Vertical canards deflected 5° for positive yaw control	IV

DISCUSSION

Longitudinal Aerodynamic Characteristics

The longitudinal aerodynamic characteristics of the model with zero control deflection are presented in figures 4 and 5 for $\phi_C = 0^\circ$ and 45° , respectively. In general, at low angles of attack ($\alpha \leq 4^\circ$), both the fixed and free-rolling tail configurations have about the same lift-curve slope C_{L_α} and stability

level $\partial C_m / \partial C_L$. At the higher angles of attack for $\phi_C = 0^\circ$, the free-rolling tail configuration has more nonlinear pitching-moment coefficient characteristics with a slight pitch-up tendency and, in general, less restoring moment than the fixed-tail configuration. These aerodynamic differences between the two configurations for the $\phi_C = 45^\circ$ case (fig. 5) are less pronounced, with the pitching-moment curves becoming more nearly linear with increases in Mach number for the free-rolling tail configuration. However, the fixed-tail configuration now exhibits the pitch-up tendency that characterized the free-rolling tail configuration at $\phi_C = 0^\circ$. This pitch-up trend is typical for a missile with cruciform tail fins in the \times -position ($\phi_C = 45^\circ$) at supersonic speeds. Flow-field effects, in conjunction with adverse panel-to-panel interference between the windward and leeward tail-fin surfaces, result in a small overall reduction in tail lift capability. This loss of lift for the fixed-tail configuration ($\phi_C = 45^\circ$) can be seen in the lift-coefficient curves presented in figure 5 and for the free-rolling tail configuration at $\phi_C = 0^\circ$ in figure 4. Visual observation has shown that for $\phi_C = 0^\circ$, the free-rolling tail fins are generally interdigitated to the canards (\times -position) when rotation stops and are therefore in a similar flow environment as the fixed-tail case when $\phi_C = 45^\circ$. This loss in tail lift would account for the pitch-up tendency.

yaw-control capability than the fixed-tail configuration. Again, the aero lockup is delayed to higher angles of attack. (See table IV.)

CONCLUSIONS

A wind-tunnel investigation was made at free-stream Mach numbers from 1.70 to 2.86 to determine the effects of fixed and free-rolling tail-fin afterbodies on the static longitudinal and lateral aerodynamic characteristics of a cruciform canard-controlled missile model. The effect of small canard roll- and yaw-control deflections was also investigated. The results of the investigation are as follows:

1. The fixed and free-tail configurations have about the same lift-curve slope and longitudinal stability level at low angles of attack.
2. For the free-rolling tail configuration, the canards provide conventional roll control with no roll-control reversal at low angles of attack.
3. The free-rolling tail configuration reduced induced roll due to model roll angle and canard yaw control.

Langley Research Center
National Aeronautics and Space Administration
Hampton, VA 23665
August 9, 1978

REFERENCES

1. Sawyer, Wallace C.; Jackson, Charlie M., Jr.; and Blair, A. B., Jr.: Aerodynamic Technologies for the Next Generation of Missiles. Paper presented at the AIAA/ADPA Tactical Missile Conference (Gaithersburg, Maryland), Apr. 27-28, 1977.
2. Schult, Eugene D.: Free-Flight Measurements of the Rolling Effectiveness and Operating Characteristics of a Bellows-Actuated Split-Flap Aileron on a 60° Delta Wing at Mach Numbers Between 0.8 and 1.8. NACA RM L54H17, 1954.
3. Regan, Frank J.; and Falusi, Mary E.: The Static and Magnus Aerodynamic Characteristics of the M823 Research Store Equipped With Fixed and Freely Spinning Stabilizers. NOLTR 72-291, U.S. Navy, Dec. 1, 1972. (Available from DDC as AD 751 658.)
4. Regan, F. J.; Shannon, J. H. W.; and Tanner, F. J.: The Joint N.O.L./R.A.E./W.R.E. Research Programme on Bomb Dynamics. Part III. A Low-Drag Bomb With Freely Spinning Stabilizers. WRE-Report-904 (WR&D), Australian Def. Sci. Serv., June 1973.
5. Darling, John A.: Elimination of the Induced Roll of a Canard Control Configuration by Use of a Freely Spinning Tail. NOLTR 72-197, U.S. Navy, Aug. 16, 1972.
6. Mechtly, E. A.: The International System of Units - Physical Constants and Conversion Factors (Second Revision). NASA SP-7012, 1973.
7. Schaefer, William T., Jr.: Characteristics of Major Active Wind Tunnels at the Langley Research Center. NASA TM X-1130, 1965.
8. Stallings, Robert L., Jr.; and Lamb, Milton: Effects of Roughness Size on the Position of Boundary-Layer Transition and on the Aerodynamic Characteristics of a 55° Swept Delta Wing at Supersonic Speeds. NASA TP-1027, 1977.
9. Spahr, J. Richard; and Dickey, Robert R.: Wind-Tunnel Investigation of the Vortex Wake and Downwash Field Behind Triangular Wings and Wing-Body Combinations at Supersonic Speeds. NACA RM A53D10, 1953.
10. Dillenius, Marnix F. E.; and Nielsen, Jack N.: Prediction of Aerodynamics of Missiles at High Angles of Attack in Supersonic Flow. NEAR TR 99 (Contract No. N00014-74-C-0050); Nielsen Eng. & Res., Inc., Oct. 1975. (Available from DDC as AD A018 680.)
11. Hardy, Samuel R.: Subsonic Wind Tunnel Tests of a Canard-Control Missile Configuration in Pure Rolling Motion. NSWC/DL TR-3615, U.S. Navy, June 1977. (Available from DDC as AD A044 957.)

TABLE I.- SUMMARY OF TEST DATA FROM FREE-ROLLING TAIL CONFIGURATION
WITH ZERO CONTROL DEFLECTION

M	α , deg	ϕ_c , deg	Tail-fin roll rate, rpm ^a		Remarks
			Counterclockwise		
1.70	-1.9	0	115		
	-.8		122		
	0		115		
	1.2		127		
	2.2		97		
	4.4		88		
	6.6		80		
	8.9		0	Stopped rolling	
	11.1		0	Aero lockup	
	13.5		0	Very small oscillation angle	
	↓				
	17.9		0		
1.70	-2.0	26.6	108		
	-.5		133		
	-.1		121		
	1.1		127		
	2.1		116		
	4.5		12	Rotated very slowly	
	6.6		116	Roll rate apparently increasing with α	
1.70	-2.4	45	105		
	-.9		112		
	0		123		
	.9		112		
	2.2		124		
	4.4		0	Stopped rolling	
	6.5		0	Very small oscillation angle	
	8.8		21	Rotated very slowly	
	↓				
	17.8		0	Aero lockup	
2.16	-1.2	0	120		
	.1		114		
	1.0		112		
	2.2		110		
	3.3		96		
	5.5		75		
	7.7		0	Stopped rolling; aero lockup	
	↓				
	24.7		0		

^aWhen viewed from the rear.

TABLE I.- Continued

M	α , deg	ϕ_C , deg	Tail-fin roll rate, rpm ^a		Remarks
			Counterclockwise		
2.16	-1.0	26.4	121		
	-.1		122		
	.9		130		
	2.1		107		
	3.2		96		
	5.4		0	Stopped rolling	
	7.5		0		
	7.8		199	Roll rate apparently increasing with α	
2.16	-1.4	45	100		
	-.1		104		
	1.0		99		
	2.1		100		
	3.2		87		
	5.4		0	Stopped rolling	
	7.5		0		
	9.9		114	Started rolling	
	12.0		128		
	14.1		195	Roll rate increasing with α	
2.36	-1.5	0	143		
	-.2		129		
	.9		83		
	2.0		78		
	2.9		72		
	5.2		37		
	7.3		27		
	9.6		0	Stopped rolling; aero lockup	
	↓				
	23.7		0	Large oscillation angle	
2.36	-1.5	26.6	80		
	0		94		
	.9		98		
	2.0		61		
	3.1		0	Stopped rolling	
	5.3		0		
	7.4		194	Roll rate apparently increasing with α	

^aWhen viewed from the rear.

TABLE I.- Continued

M	α , deg	ϕ_c , deg	Tail-fin roll rate, rpm ^a	Remarks
			Counterclockwise	
2.36	-1.0	45	56	Stopped rolling Started rolling Roll rate increasing with α
	.3		70	
	1.3		100	
	2.4		56	
	3.5		54	
	5.6		0	
	7.7		33	
	9.9		118	
	12.0		161	
	14.4		167	
	16.5		122	
	18.7		0	
	↓			
	23.8		0	Stopped rolling; aero lockup
2.86	-2.9	0	23	Low roll rates
	-1.6		71	
	-.5		64	
	.7		62	
	1.8		36	
	3.8		0	
	↓			
	22.0		0	
2.86	-2.8	26.5	33	Oscillated; 2 or 3 revolutions Started rolling Stopped rolling Started rolling Stopped rolling Roll rate apparently increasing with α
	-1.5		49	
	-.6		51	
	.6		0	
	1.8		50	
	3.7		0	
	5.9		0	
	8.0		131	
	10.0		0	
	11.5		230	

^aWhen viewed from the rear.

TABLE I.- Concluded

M	α , deg	ϕ_C , deg	Tail-fin roll rate, rpm ^a		Remarks
			Counterclockwise		
2.86	-2.5	45	27	Low roll rates	
	-1.5		51		
	-.5		93		
	.7		50		
	1.7		0	Stopped rolling	
	3.9		0	Small oscillation angle	
	5.9		0		
	8.1		75	Started rolling	
	10.3		120	Steady rolling	
	12.6		124		
	14.6		0	Stopped rolling	
	17.0		0		
	19.1		0		
	20.2		157	Started rolling	

^aWhen viewed from the rear.

TABLE II.- SUMMARY OF TEST DATA FROM FREE-ROLLING TAIL CONFIGURATION
WITH CANARD OFF

M	α , deg	ϕ_C , deg	Tail-fin roll rate, rpm ^a	Remarks
			Clockwise	
1.70	-2.0	0	54	Very low roll rates
	-.9		37	
	0		39	
	1.0		46	
	2.1		47	
	4.0		31	
	6.0		31	Stopped and started to roll
	8.0		0	
	10.0		0	
	12.1		30	
	14.2		28	Aero lockup
	16.4		26	
2.16	-1.6	0	33	Very low and steady roll rates
	-.9		34	
	-.1		31	
	1.0		47	
	2.0		20	
	3.0		30	
	5.0		23	Stopped rolling
	7.0		0	
	9.1		0	
	11.3		0	
	13.4		26	Stopped; started; oscillated
	↓			
	23.2		27	Rolled hesitantly and irregularly

^aWhen viewed from the rear.

TABLE II.- Concluded

M	α , deg	ϕ_c , deg	Tail-fin roll rate, rpm ^a	Remarks
			Clockwise	
2.36	-1.2	0	74	Low roll rates
	-.3		47	
	.8		86	
	1.8		52	
	2.8		102	
	4.9		88	Stopped; started; and oscillated Rolled hesitantly and irregularly
	6.9		45	
	9.0		0	
	↓			
	23.0		42	
2.86	-2.5	0	39	Low roll rates
	↓			
	5.6		28	
	7.8		0	Stopped rolling
	9.8		0	Oscillated through small angle
	↓			
	21.6		0	

^aWhen viewed from the rear.

TABLE III.- SUMMARY OF TEST DATA FROM FREE-ROLLING TAIL CONFIGURATION
WITH TWO CANARDS DIFFERENTIALLY DEFLECTED 0.5°
EACH FOR NEGATIVE ROLL CONTROL

M	α , deg	ϕ_c , deg	Tail-fin roll rate, rpm ^a		Remarks
			Clockwise		
1.70	-2.2	0	98		
	-1.1		96		
	0		90		
	1.2		100		
	2.4		114		
	4.5		123		
	6.6		131		
	8.9		97		
	11.1		0	Stopped rolling; aero lockup	
	↓				
	17.9		0	Small oscillation angle	
1.70	-2.3	45	102		
	-1.3		81		
	-.1		83		
	1.3		105		
	2.2		104		
	4.3		128		
	↓				
	10.8		207	Roll rate increasing with α ; $\alpha > 11^\circ$; rpm > 500	
2.16	-1.2	0	93		
	0		97		
	1.1		109		
	2.2		122		
	3.3		136		
	5.5		154		
	7.6		164	Steady rolling	
	↓				
	16.7		138		
	18.9		0	Stopped rolling; aero lockup	
	↓				
	24.8		0		

^aWhen viewed from the rear.

TABLE III.- Continued

M	α , deg	ϕ_C , deg	Tail-fin roll rate, rpm ^a	Remarks
			Clockwise	
2.16	-1.3	45	82	Steady rolling
	0		84	
	1.0		95	
	2.1		95	
	3.3		104	
	5.4		150	
	7.6		207	Stopped rolling; aero lockup
	↓			
	12.0		151	
	14.3		0	
	↓			
	24.5		0	
2.36	-1.3	0	109	Stopped rolling; aero lockup
	-.1		121	
	.8		103	
	2.0		95	
	3.1		147	
	5.2		123	
	7.3		110	
	9.6		0	
	↓			
	24.4		0	
2.36	-1.0	45	88	Stopped rolling; aero lockup
	.4		71	
	1.3		105	
	2.3		93	
	3.4		108	
	5.6		168	
	7.8		178	
	10.0		156	
	12.2		0	
	↓			
	24.2		0	

^aWhen viewed from the rear.

TABLE III.- Concluded

M	α , deg	ϕ_C , deg	Tail-fin roll rate, rpm ^a		Remarks
			Clockwise		
2.86	-2.7	0	51		
	-1.5		67		
	-.4		87		
	.7		104		
	2.1		80		
	3.8		99		
	5.9		123		Steady rolling
	↓				
	14.7		133		
	17.0		0		Stopped rolling; aero lockup
	↓				
	22.6		0		
2.86	-2.6	45	84		Low roll rates
	-1.5		58		
	-.5		65		
	.6		71		
	1.7		73		
	3.8		105		Steady rolling
	↓				
	10.3		42		
	12.5		0		Stopped rolling; aero lockup
	↓				
	22.5		0		

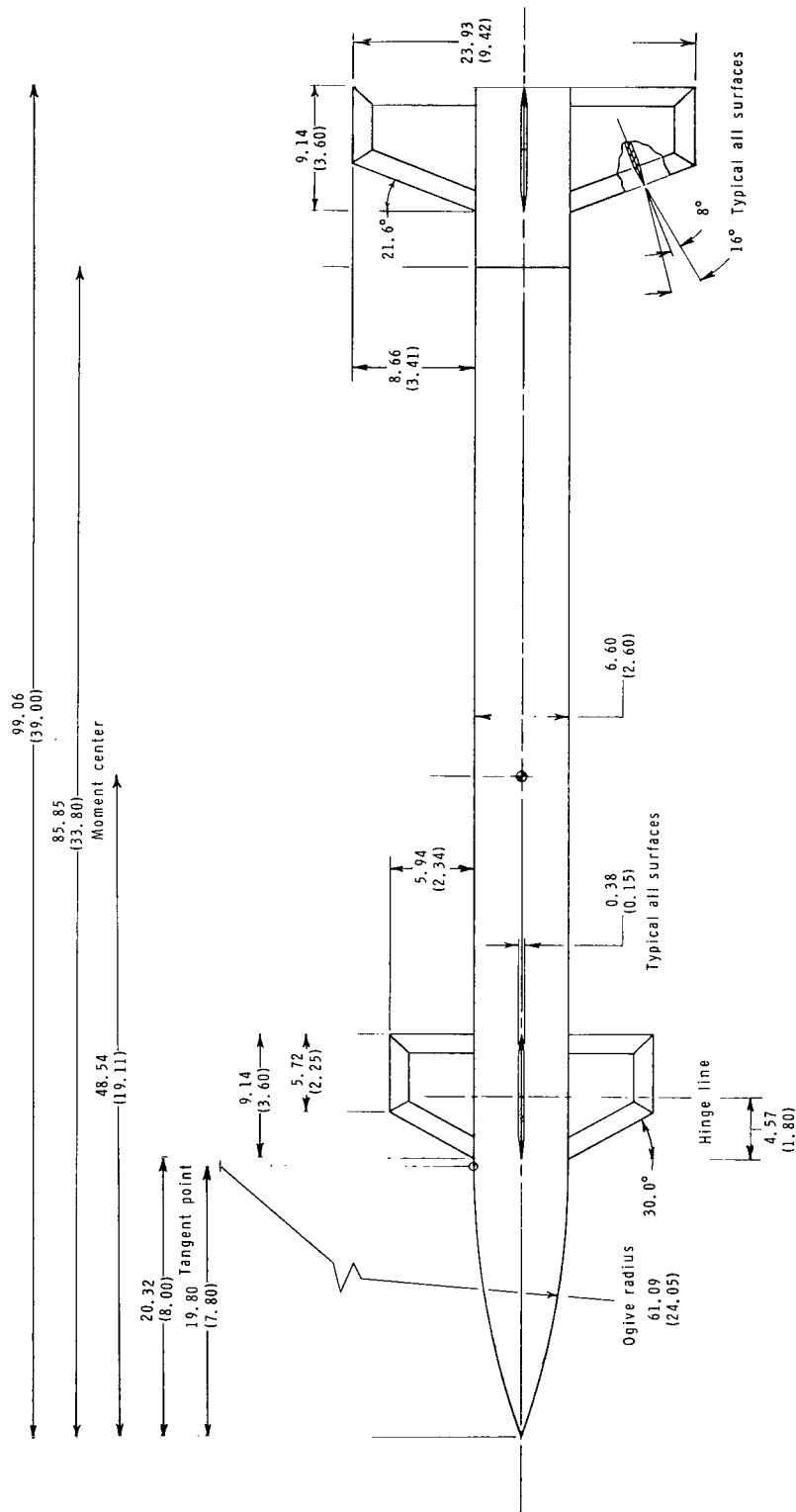
^aWhen viewed from the rear.

TABLE IV.- SUMMARY OF TEST DATA FROM FREE-ROLLING TAIL CONFIGURATION

WITH VERTICAL CANARDS DEFLECTED 5° FOR POSITIVE YAW CONTROL

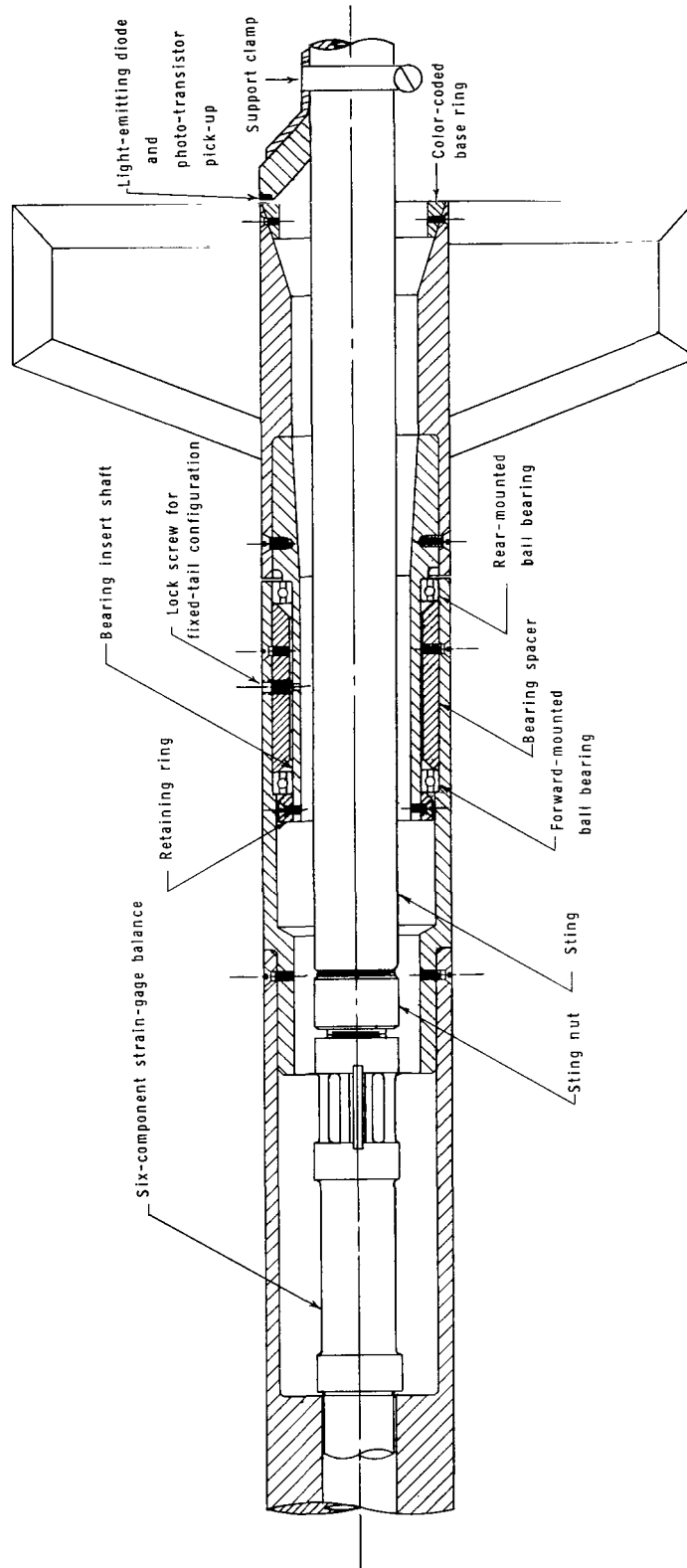
M	α , deg	ϕ_C , deg	Tail-fin roll rate, rpm ^a		Remarks
			Clockwise	Counterclockwise	
1.70	-2.2	0	360		
	-1.1		134		
	0			80	Roll direction changed
	1.0			314	Roll rate increasing with α
	2.1			463	Excessive roll rate
2.16	-1.3	0	152		
	0			53	Low roll rate
	1.1			240	
	2.2			430	
	3.3			517	
	6.2			522	Excessive roll rate
2.36	-1.3	0	191		
	-.2			36	Very low roll rate both directions
	.9			187	Roll rate increasing with α
	2.0			360	
	3.0			500	
	6.7			590	Excessive roll rate
2.86	-2.7	0	351		
	-1.5		177		
	-.5		55		
	.6			84	Roll direction changed
	1.7			206	Roll rate increasing with α
	3.9			439	
	5.8			527	
	8.3			507	
	10.3			354	
	12.5			94	
	14.1			0	Stopped rolling; "stable" aero lockup
	↓				
	22.7			0	

^aWhen viewed from the rear.



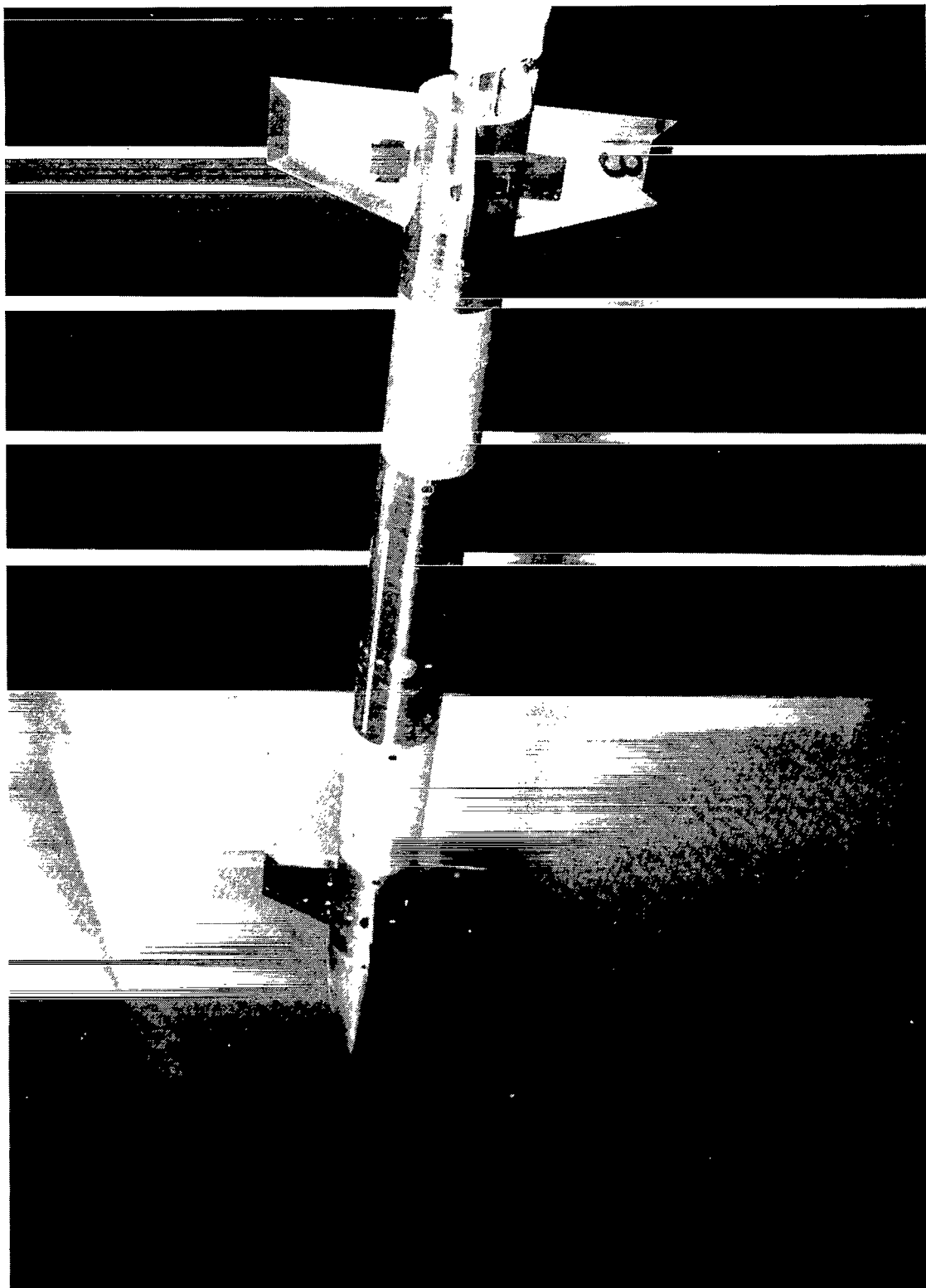
(a) Complete model.

Figure 1.- Model details. All dimensions are in centimeters (inches) unless otherwise indicated.



(b) Ball-bearing spindle assembly and sting support.

Figure 1.- Concluded.



L-76-3409

Figure 2.- Model.

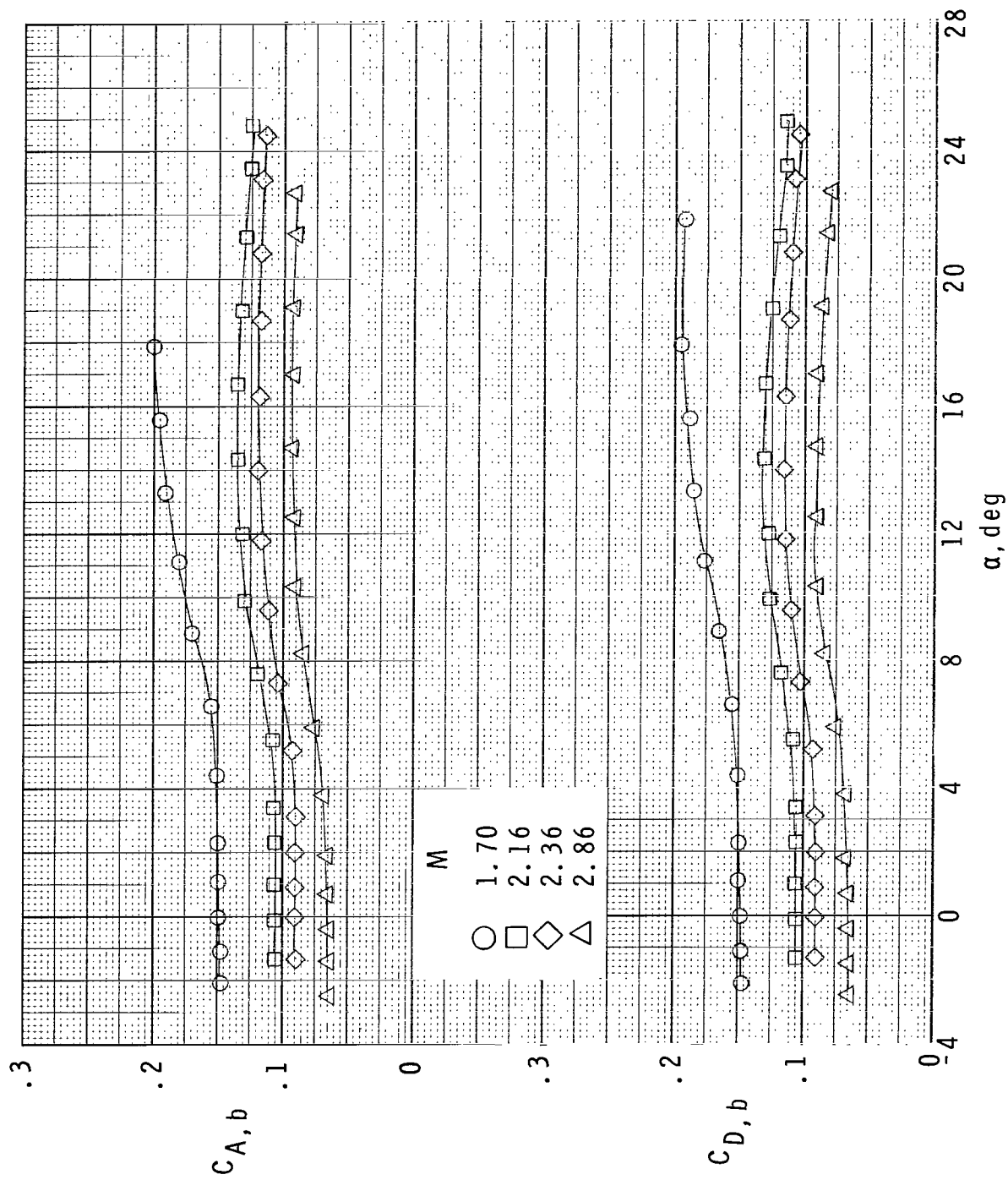
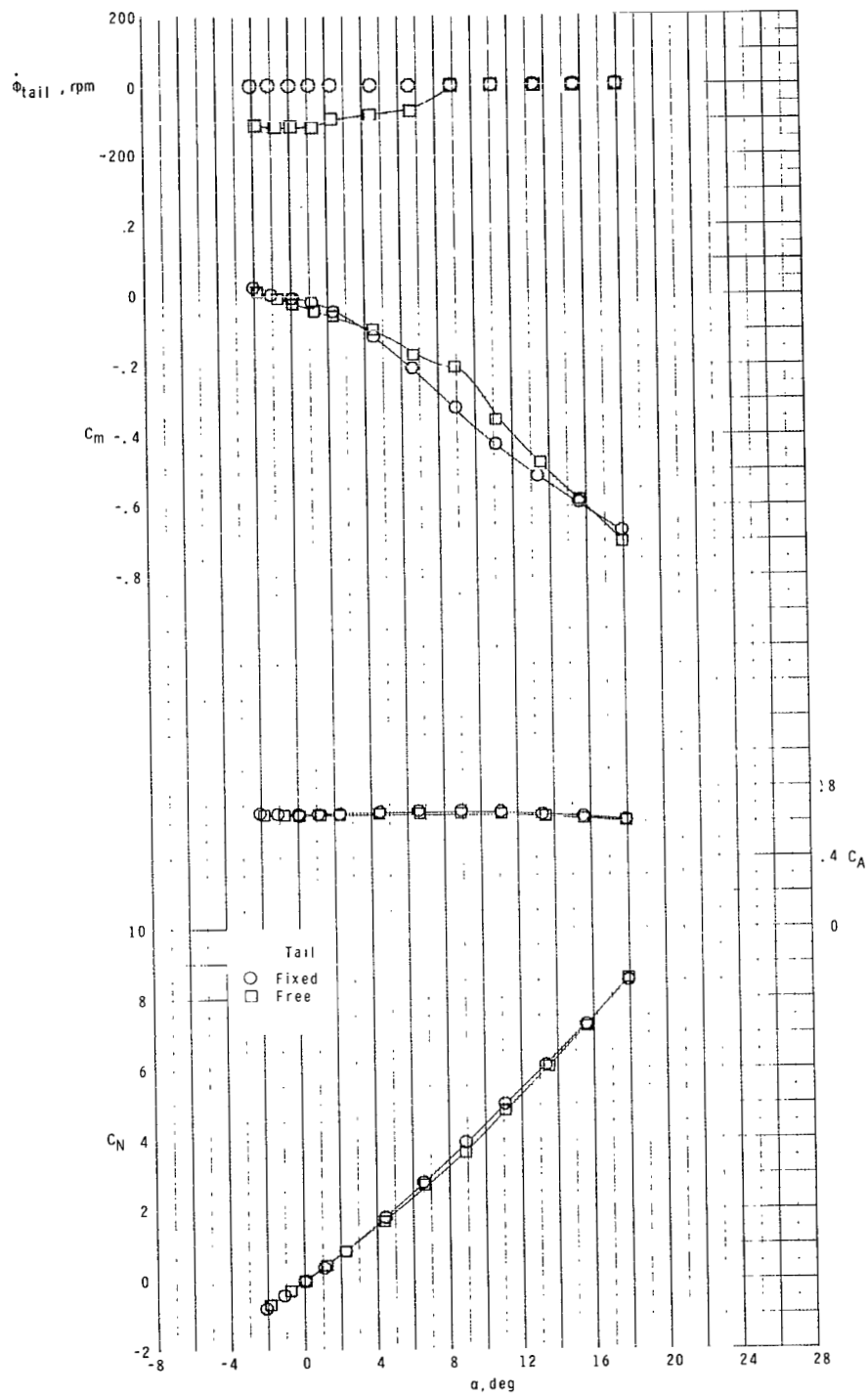
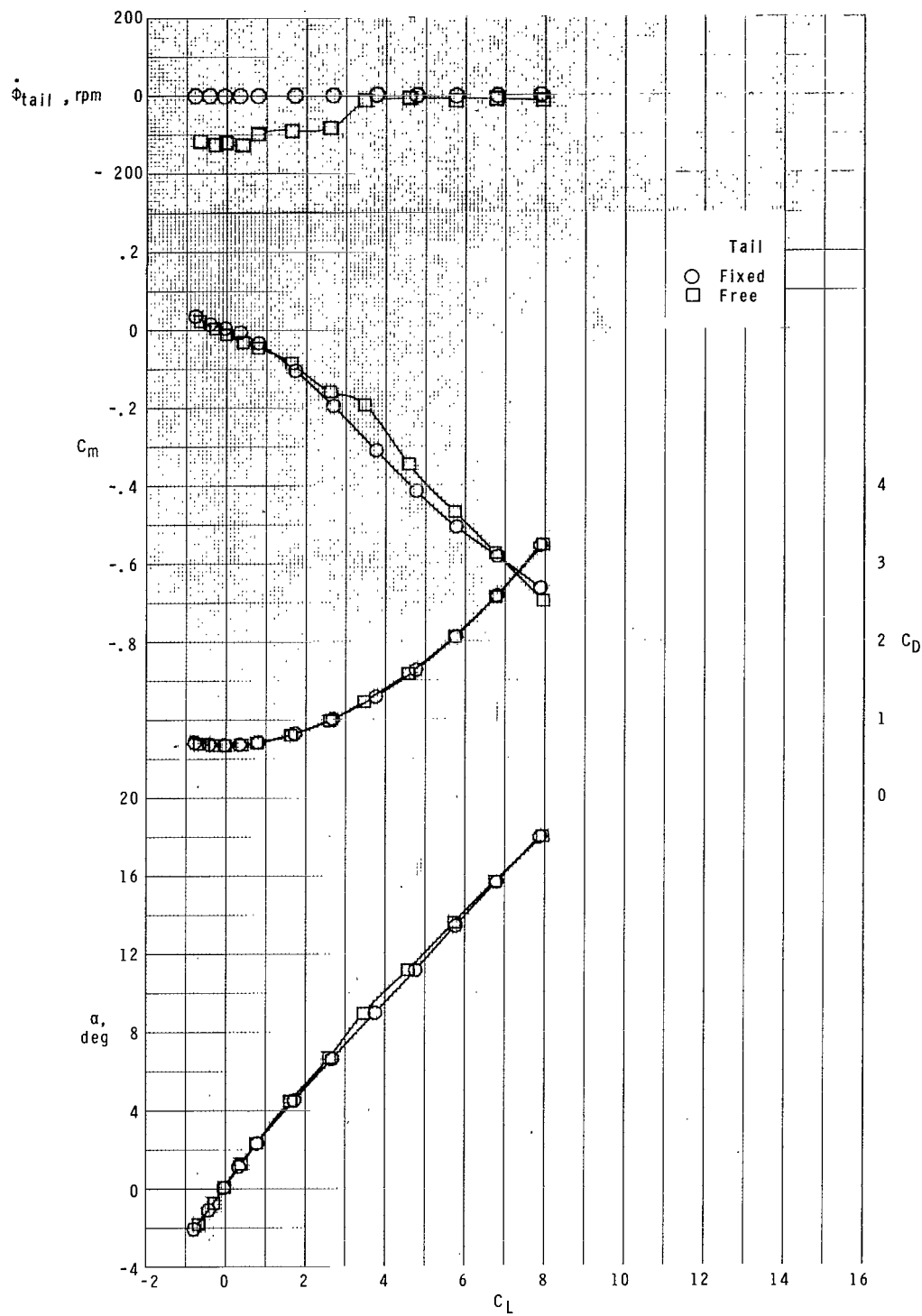


Figure 3.- Typical variation of measured $C_{A,b}$ and $C_{D,b}$ with angle of attack.



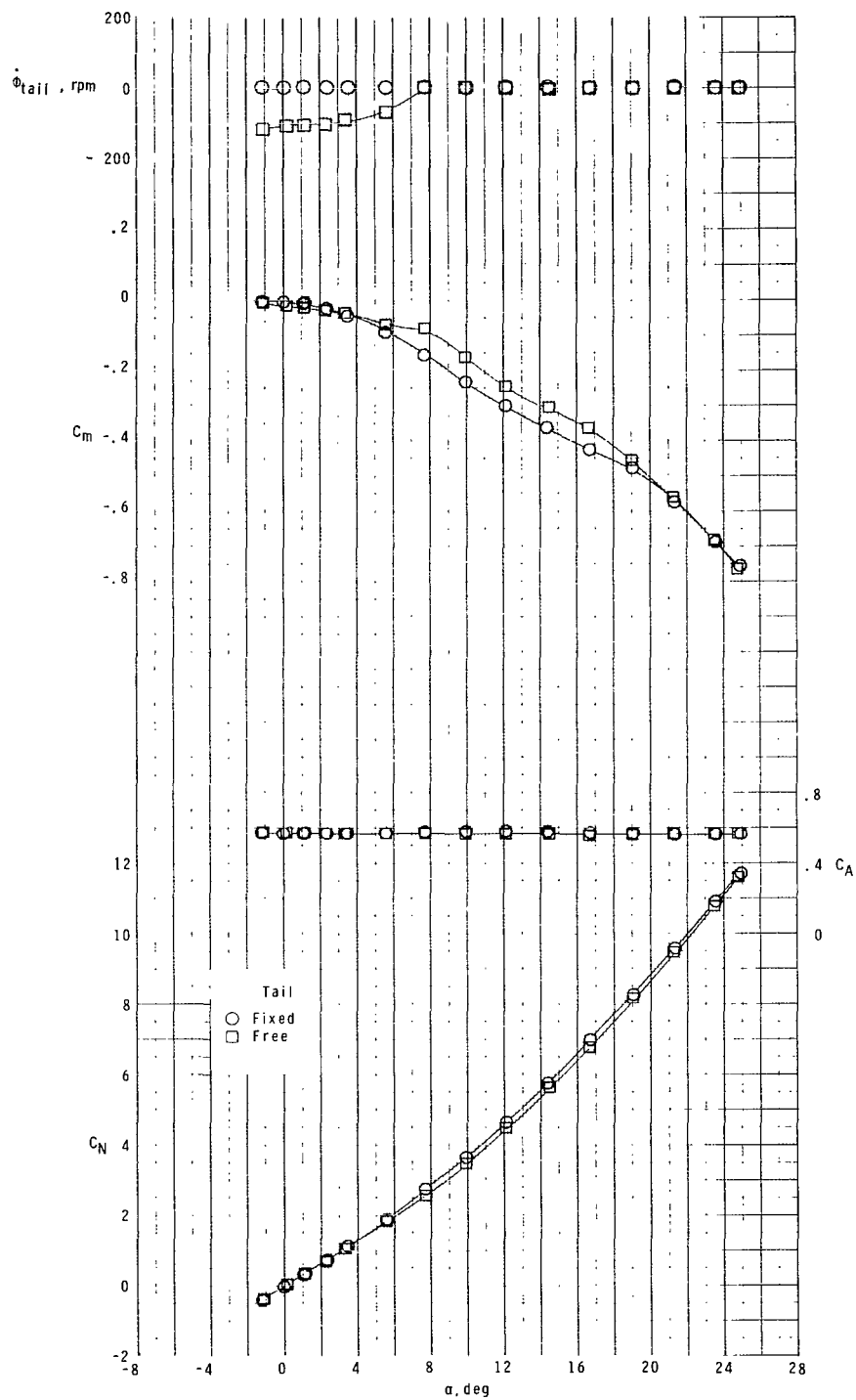
(a) $M = 1.70$.

Figure 4.- Effect of free-rolling tail on longitudinal aerodynamic characteristics of model with zero control deflection at $\phi_C = 0^\circ$.



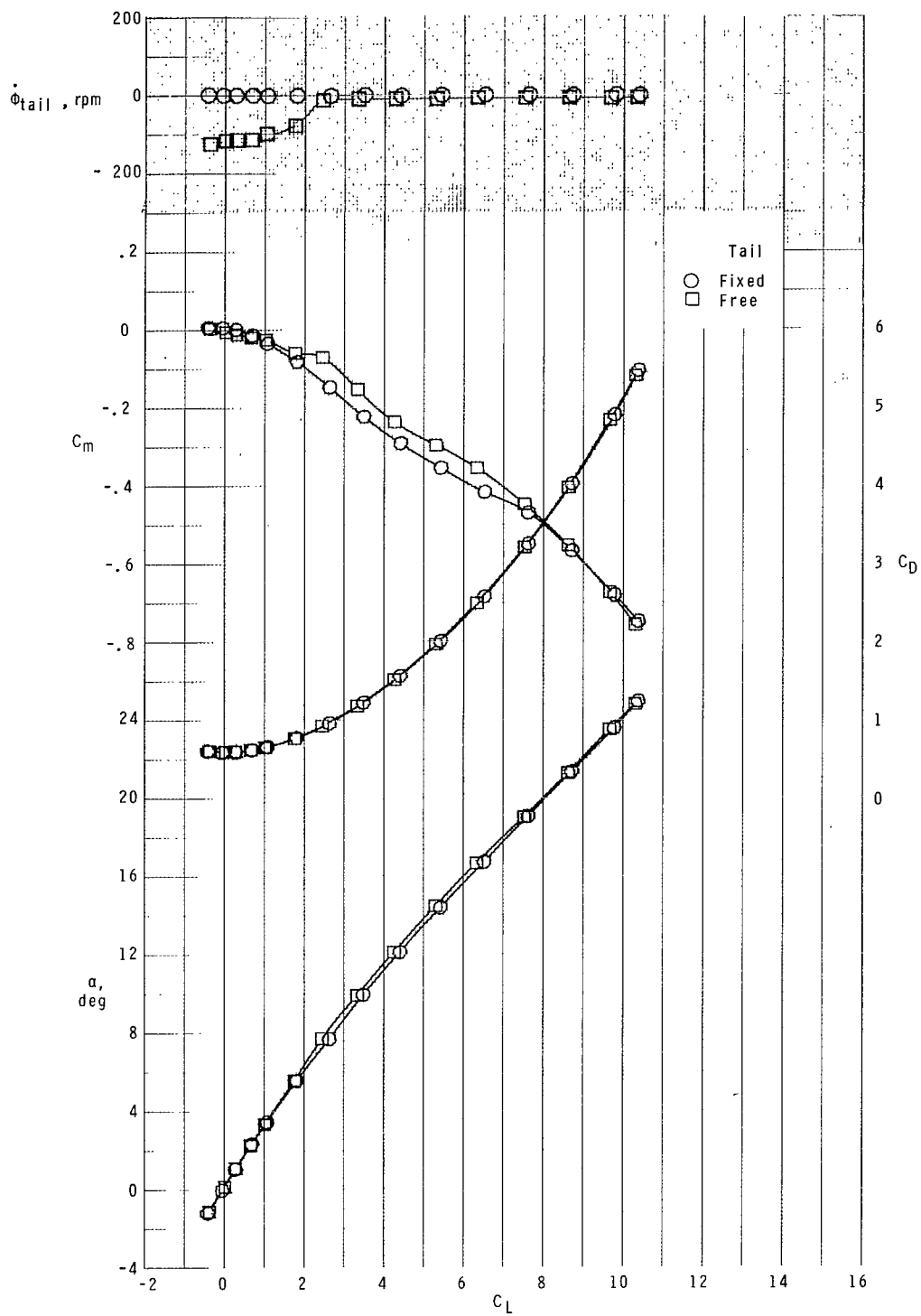
(a) Concluded.

Figure 4.- Continued.



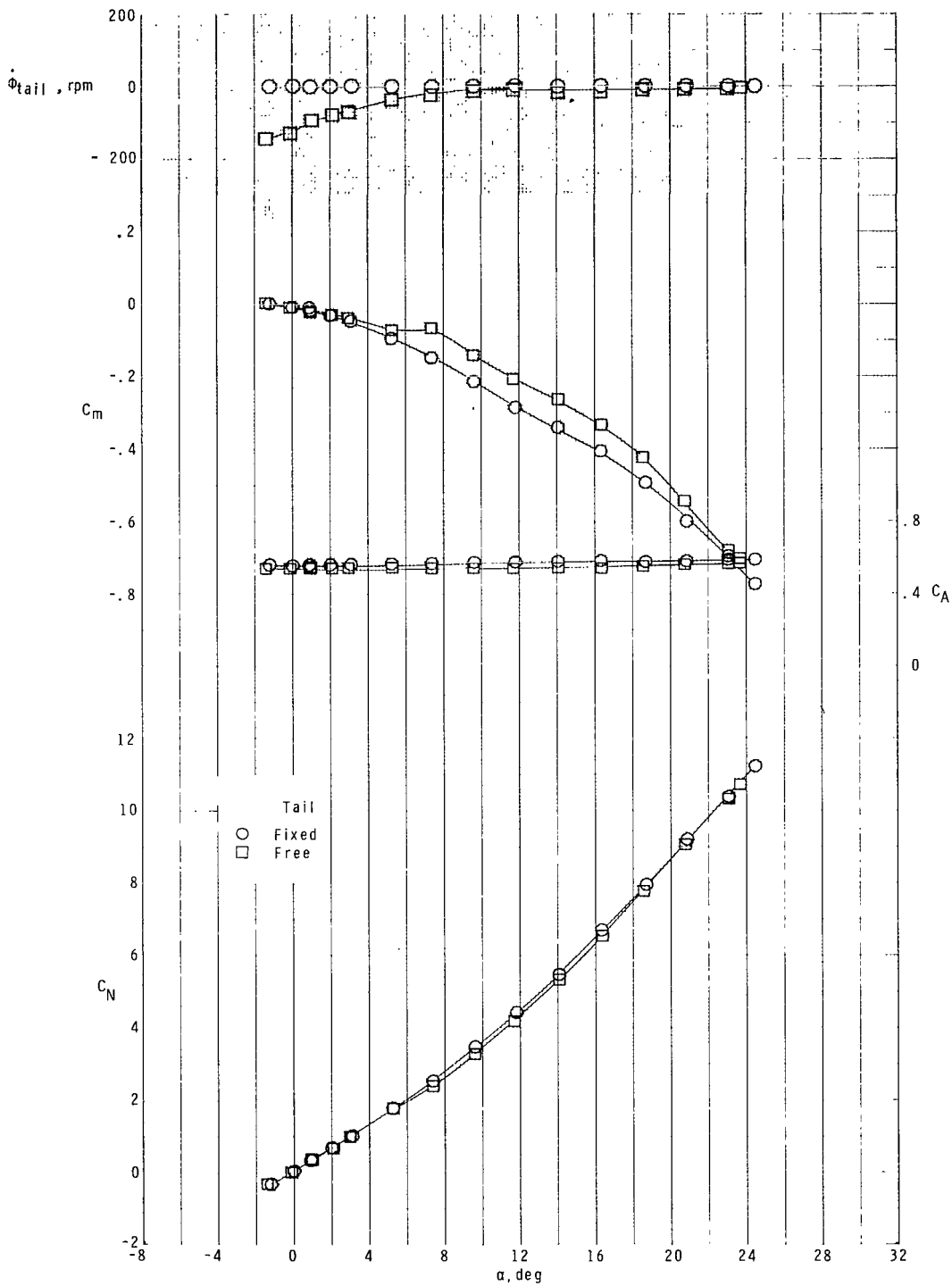
(b) $M = 2.16$.

Figure 4.- Continued.



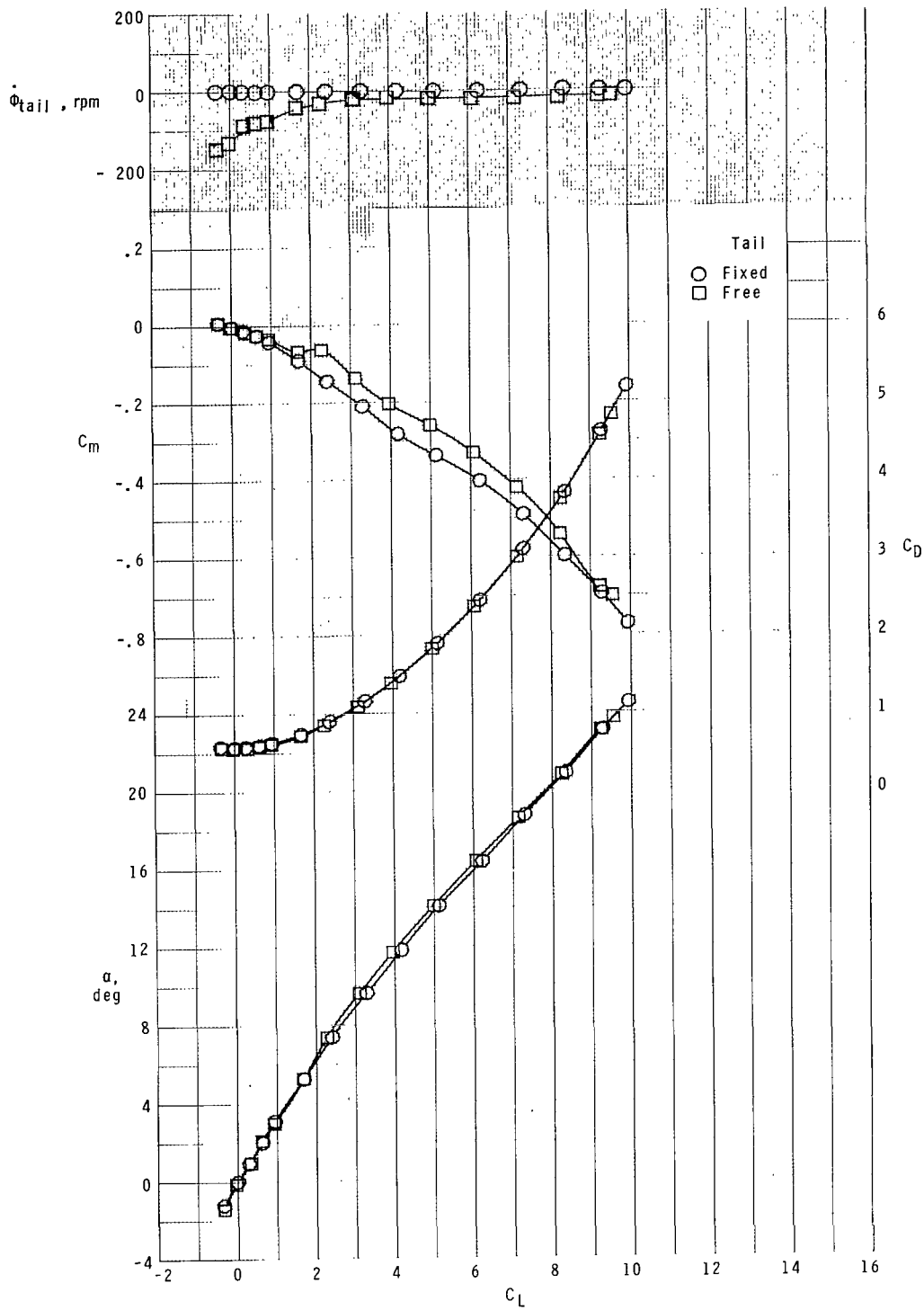
(b) Concluded.

Figure 4.- Continued.



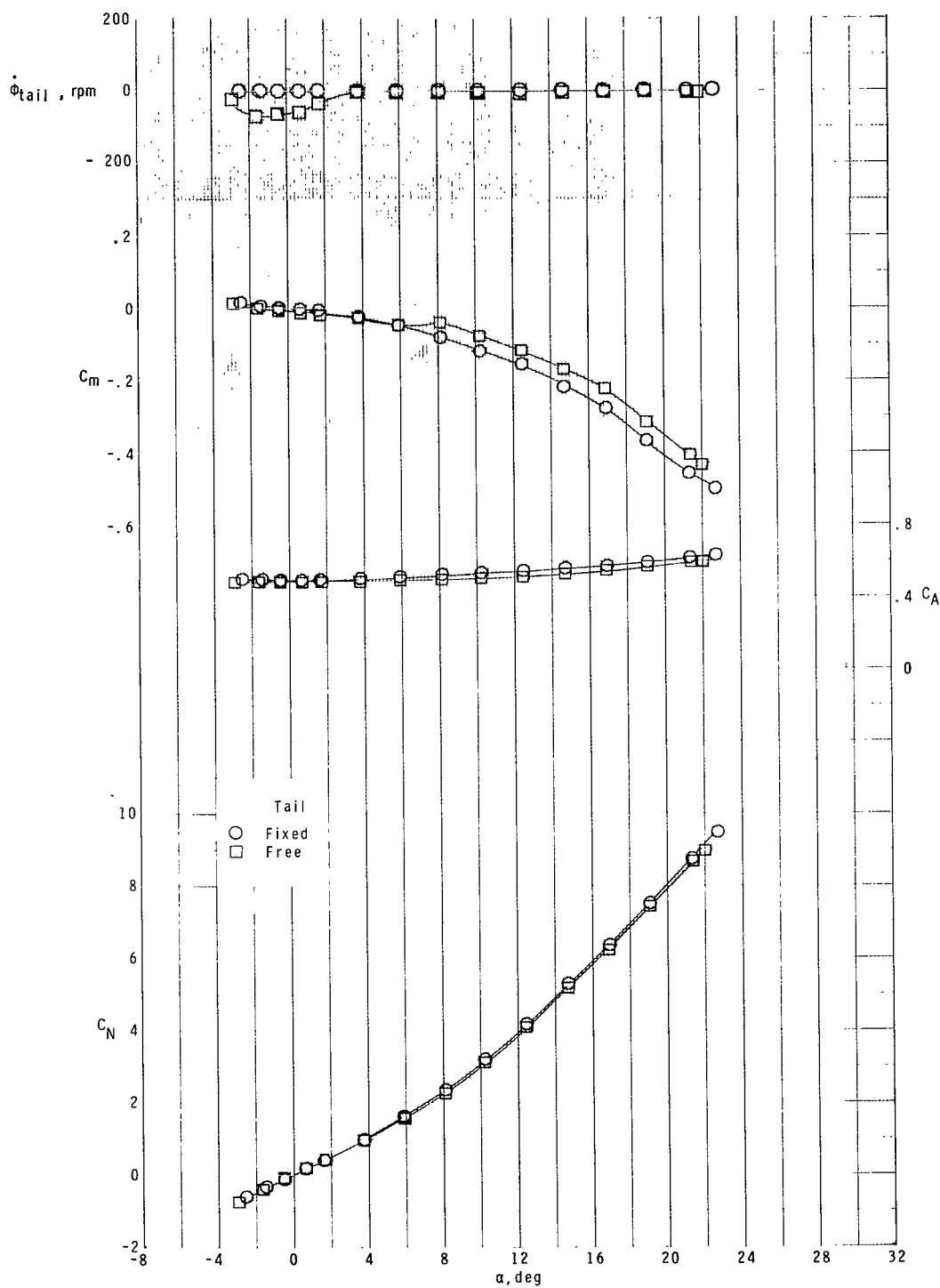
(c) $M = 2.36$.

Figure 4.- Continued.



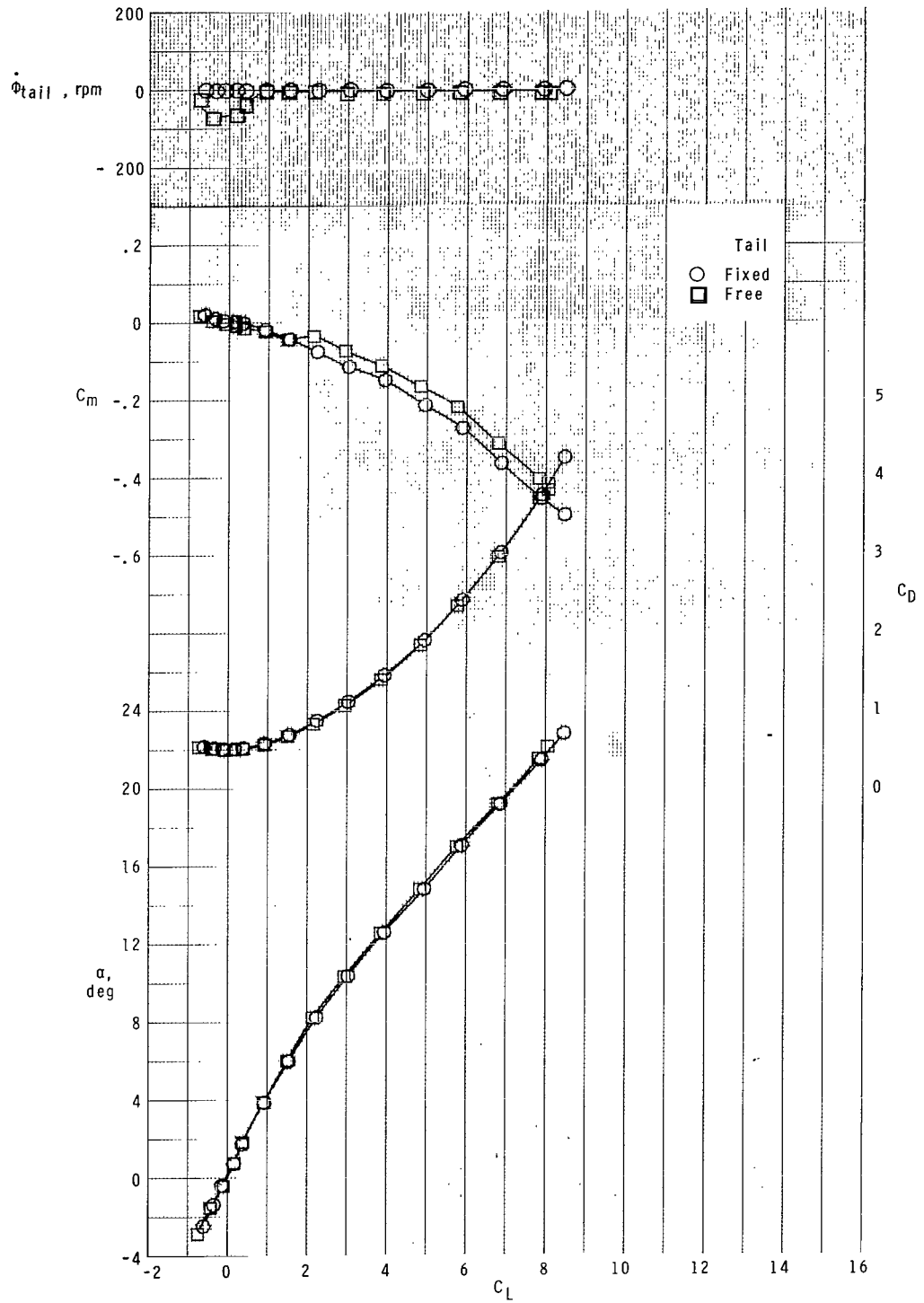
(c) Concluded.

Figure 4.- Continued.



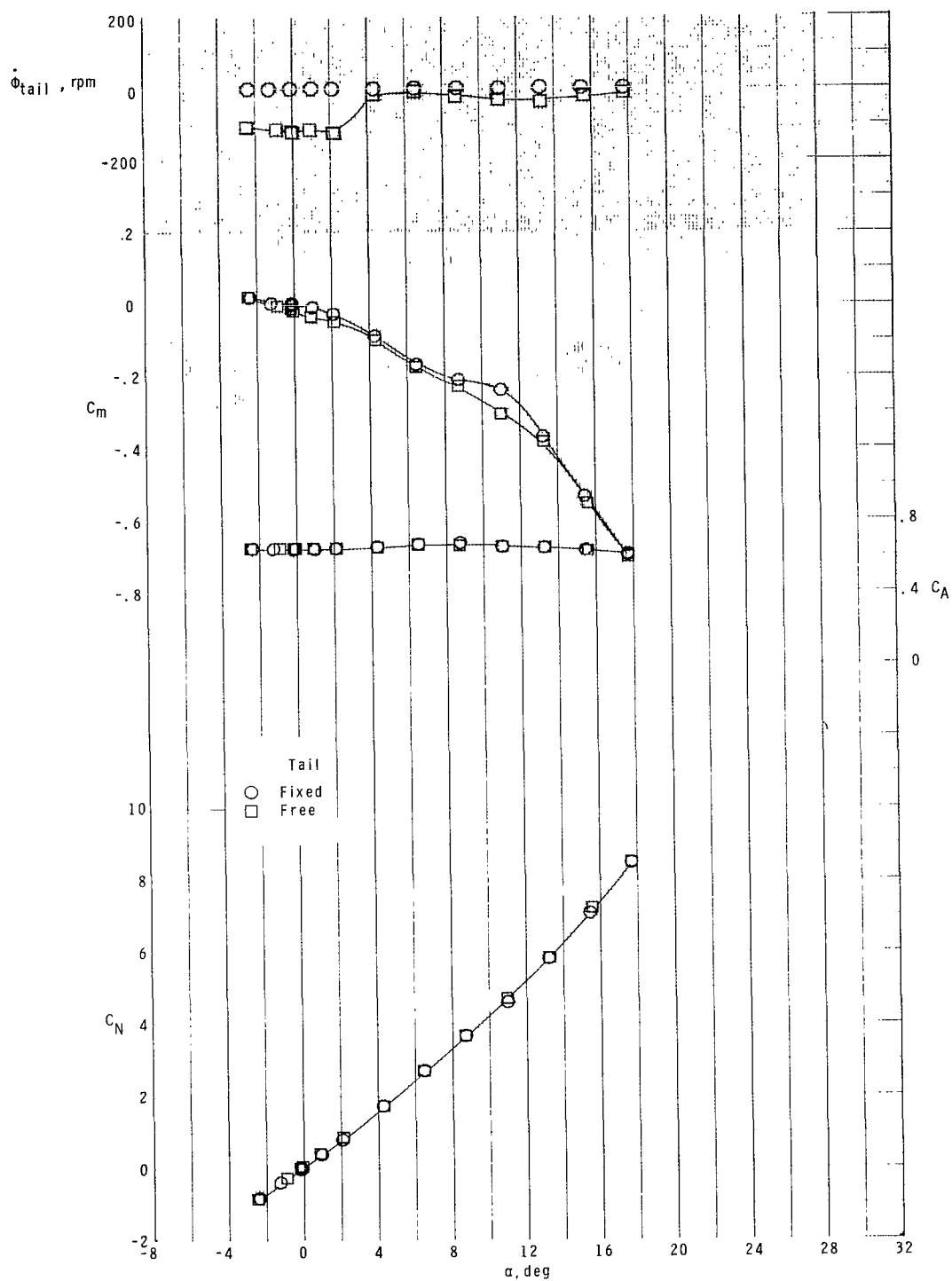
(d) $M = 2.86$.

Figure 4.- Continued.



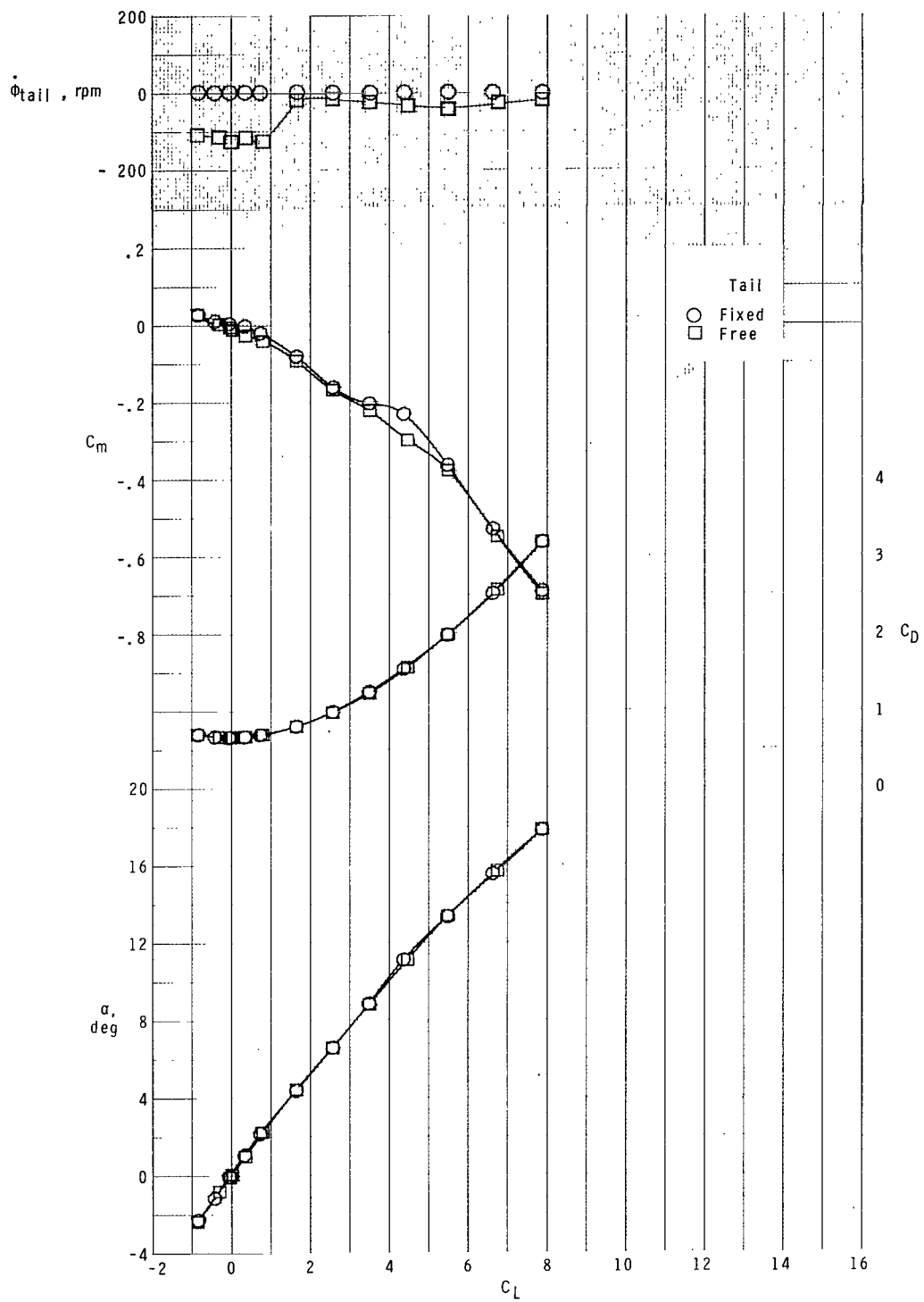
(d) Concluded.

Figure 4.- Concluded.



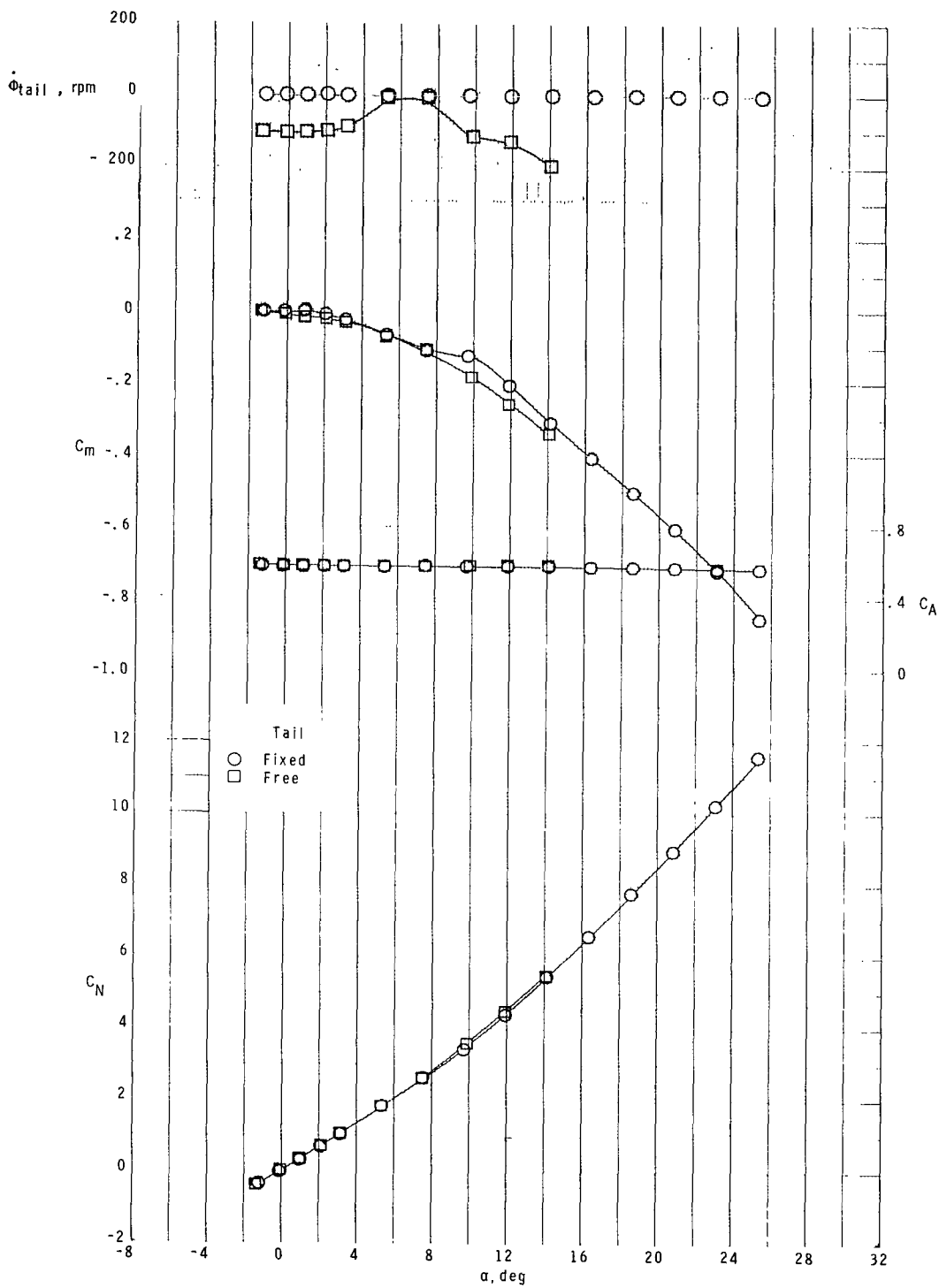
(a) $M = 1.70$.

Figure 5.- Effect of free-rolling tail on longitudinal aerodynamic characteristics of model with zero control deflection at $\phi_C = 45^\circ$.



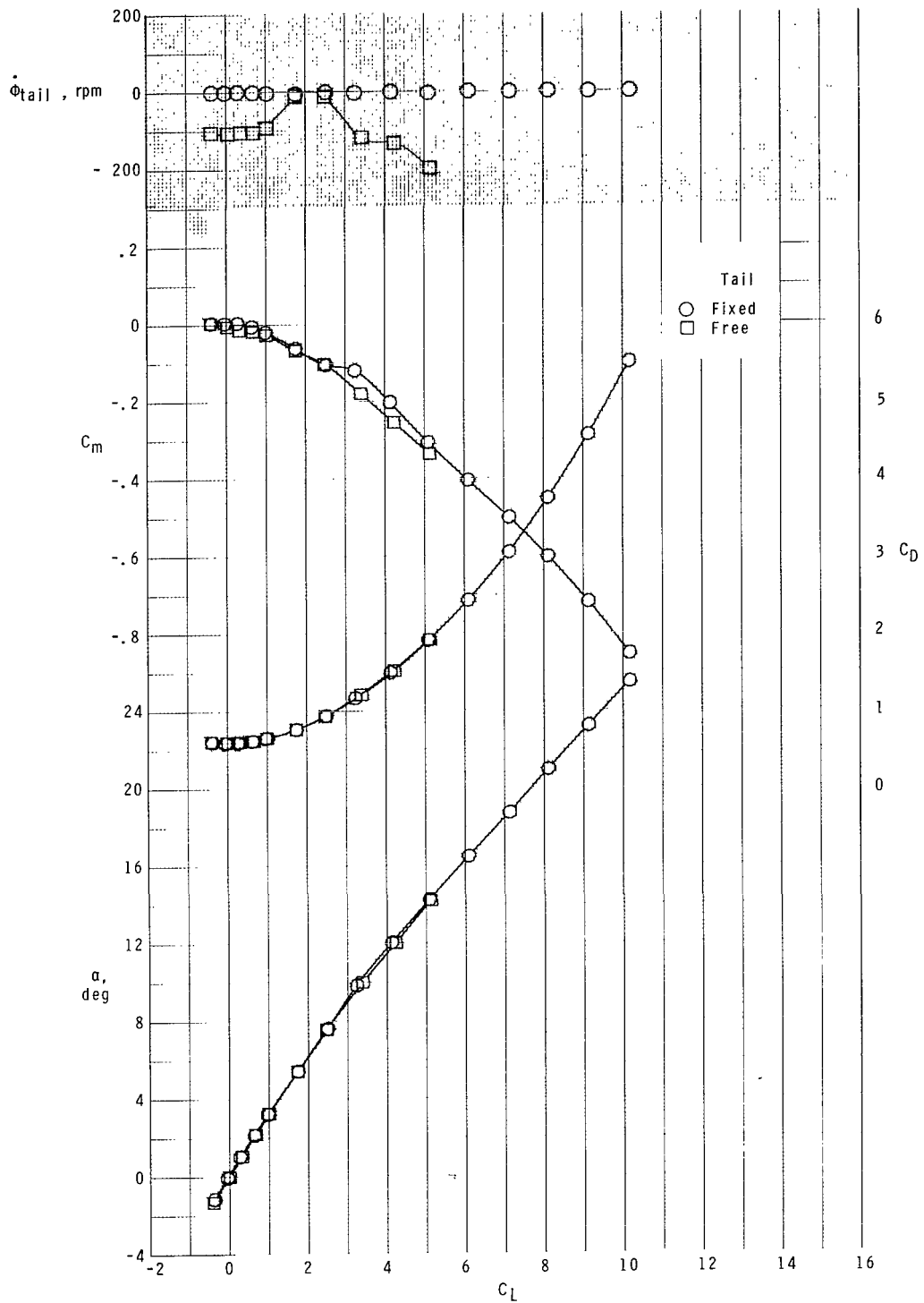
(a) Concluded.

Figure 5.- Continued.



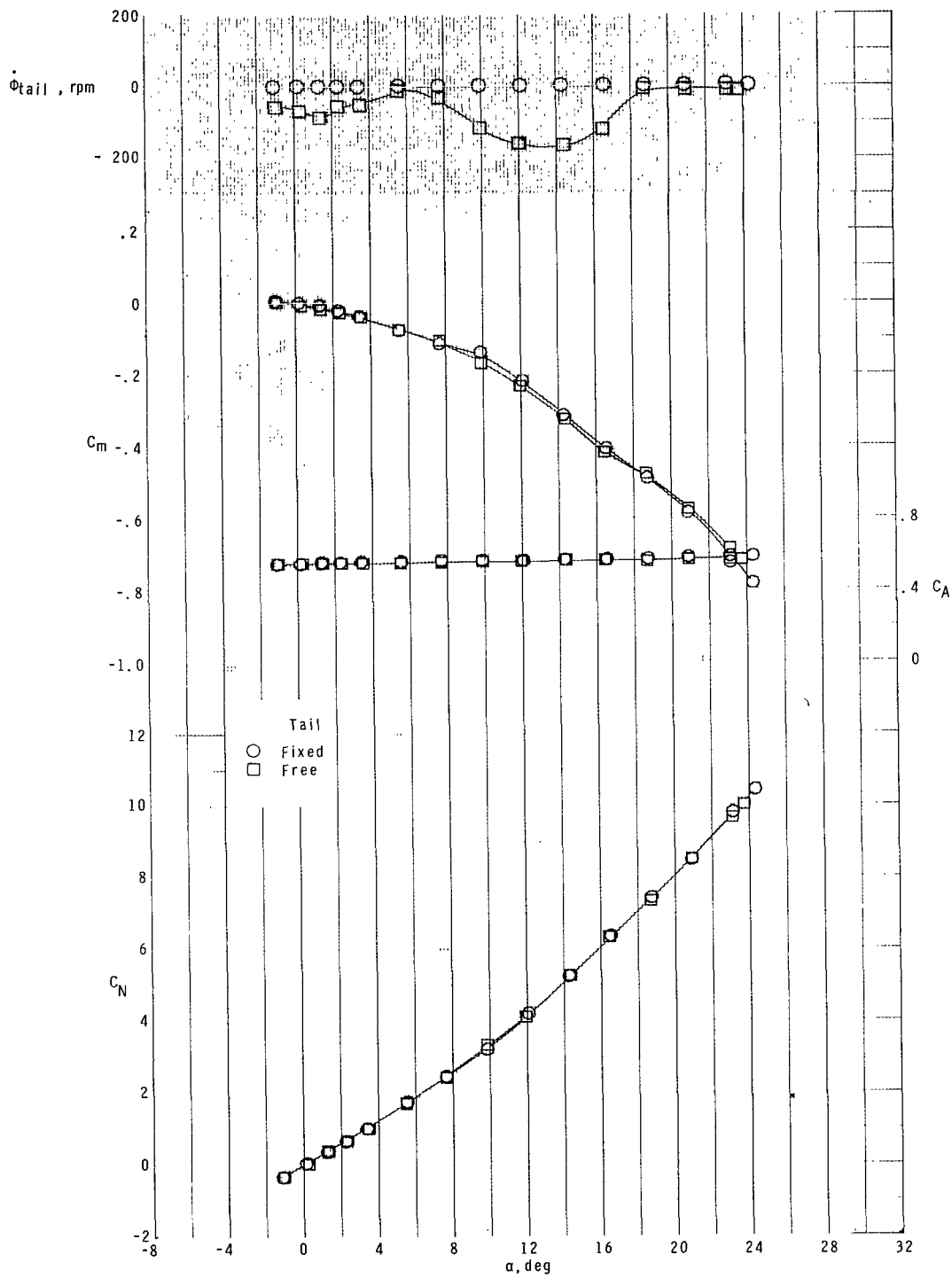
(b) $M \approx 2.16$.

Figure 5.- Continued.



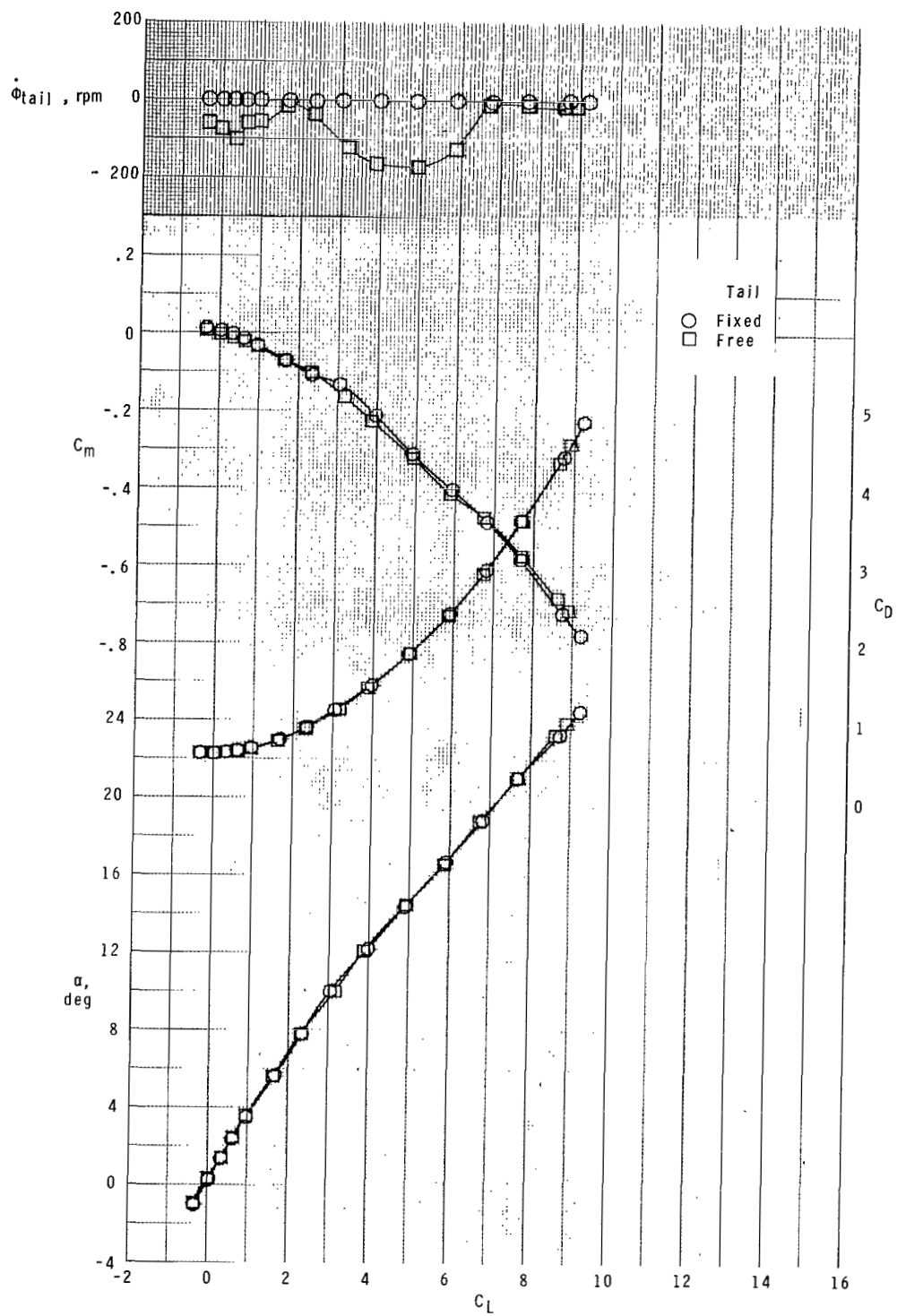
(b) Concluded.

Figure 5.- Continued.



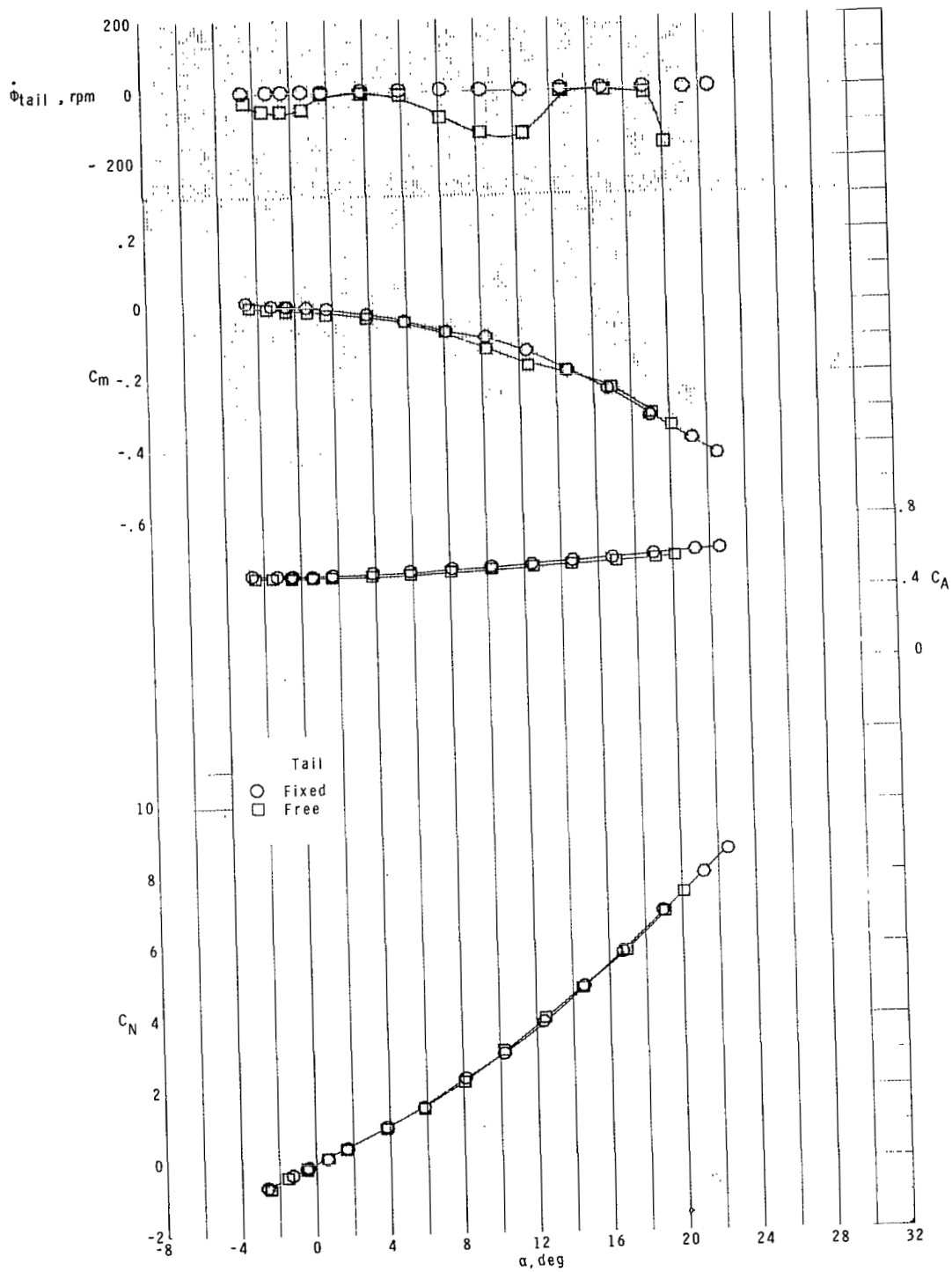
(c) $M = 2.36$.

Figure 5.- Continued.



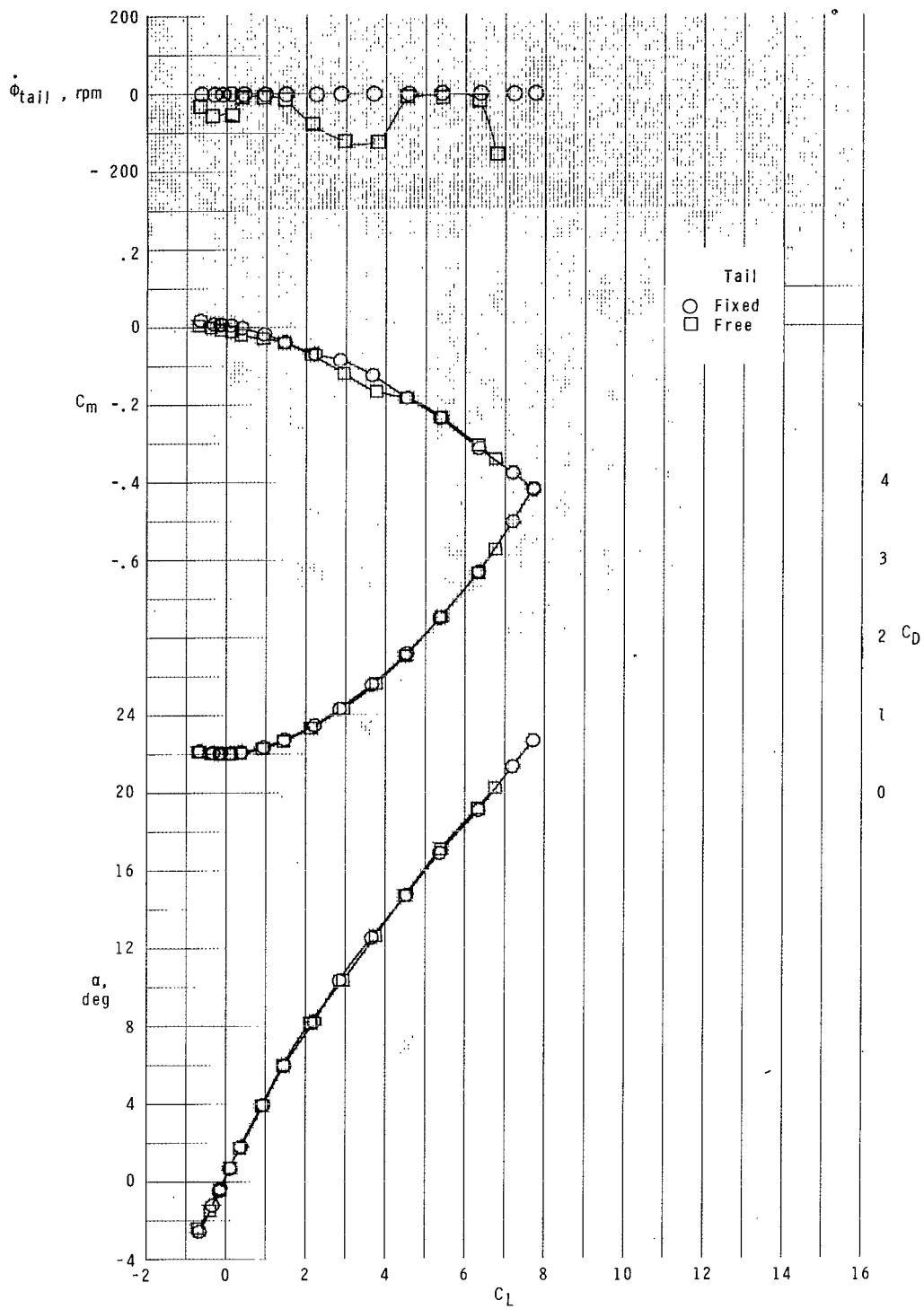
(c) Concluded.

Figure 5.- Continued.



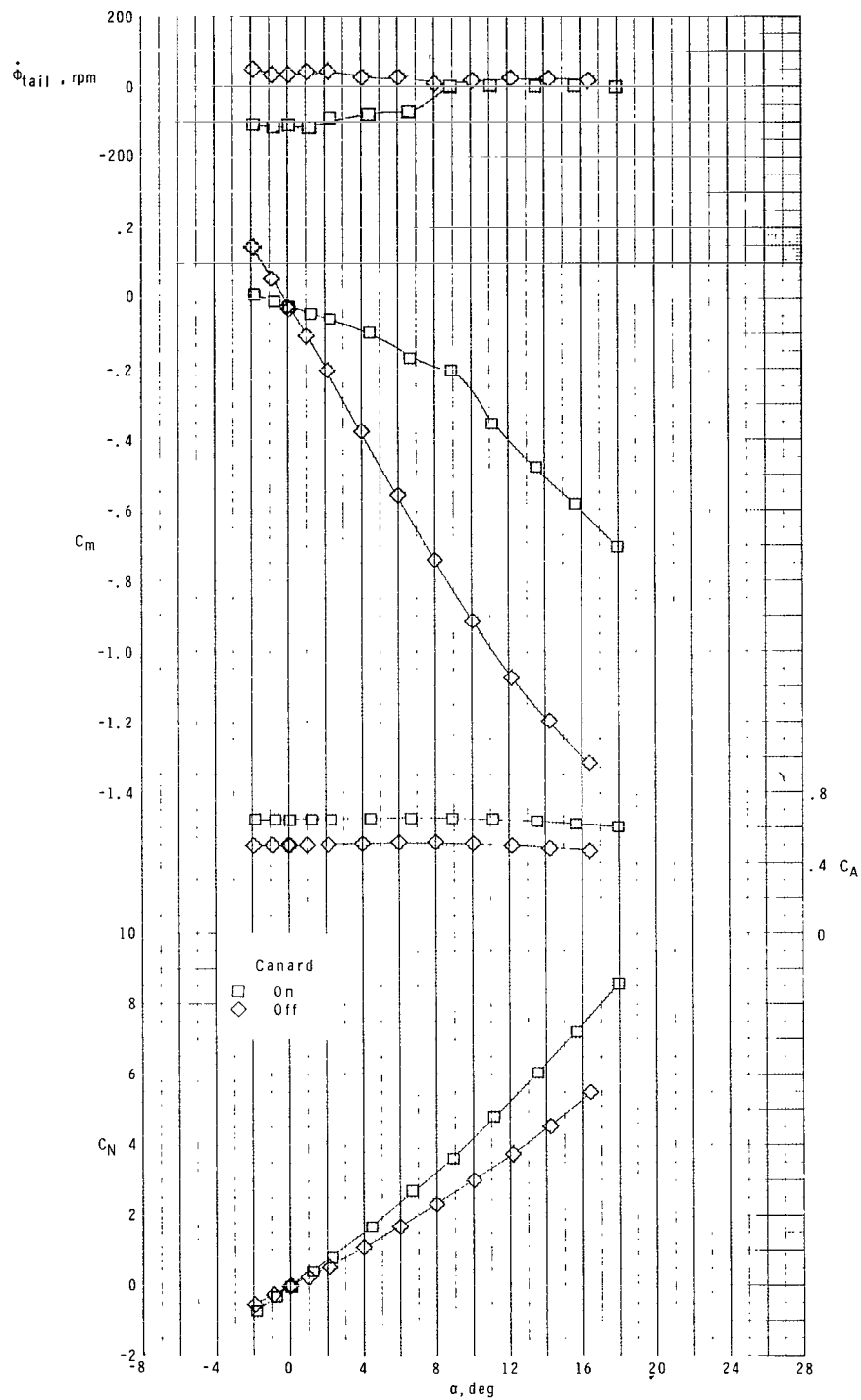
(d) $M = 2.86$

Figure 5.- Continued.



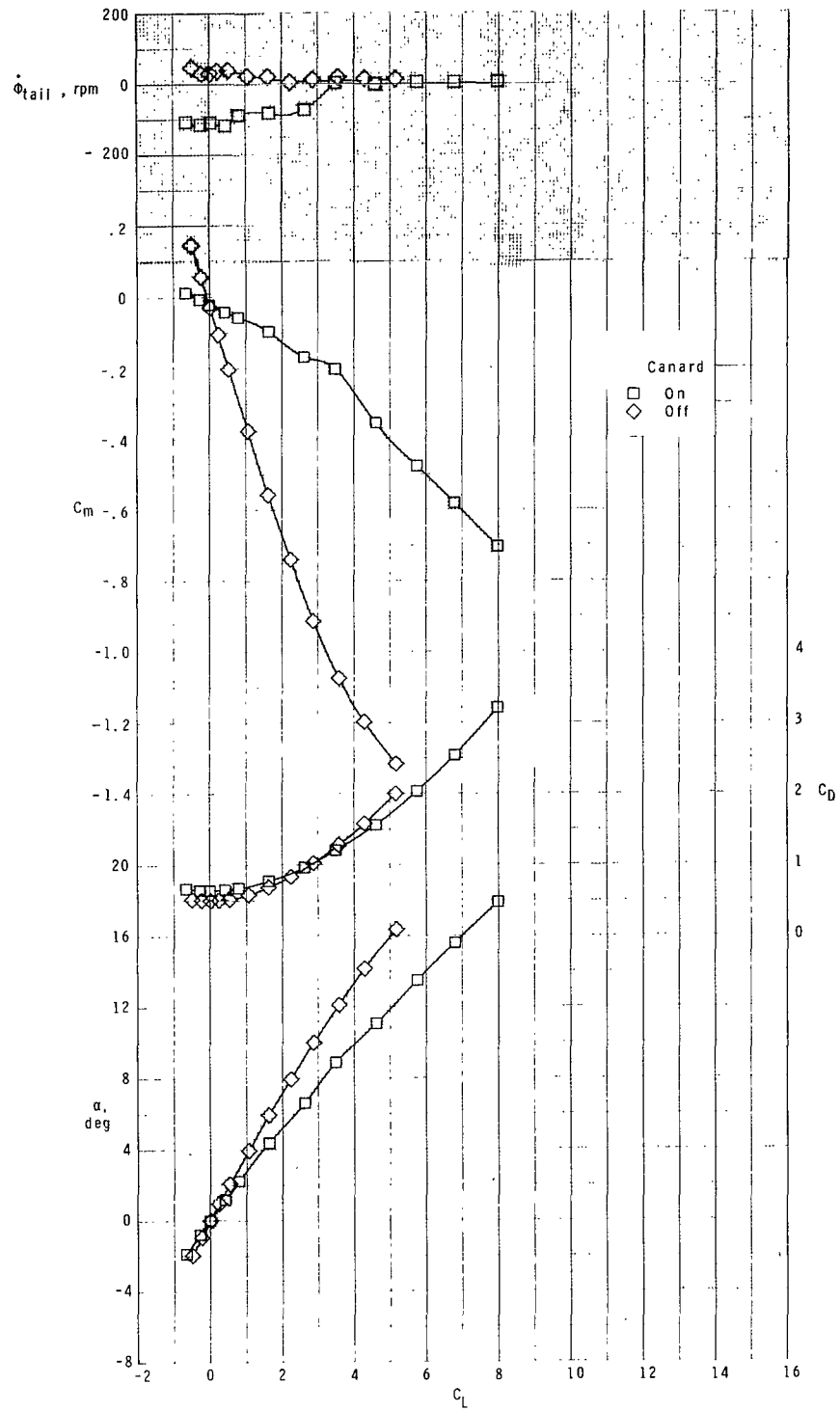
(d) Concluded.

Figure 5.- Concluded.



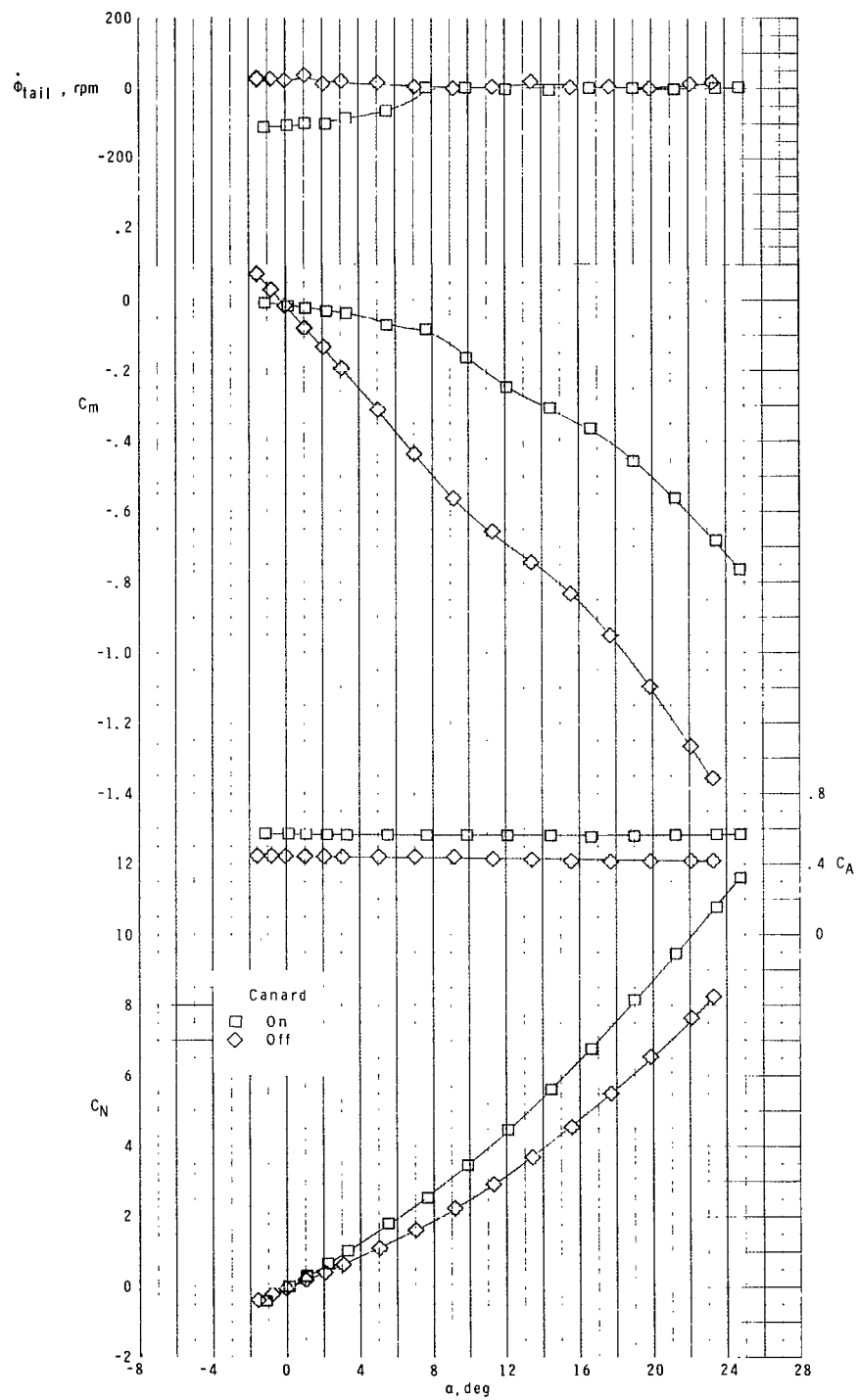
(a) $M = 1.70$.

Figure 6.- Effect of canards on longitudinal aerodynamic characteristics of model with free-rolling tail at $\phi_C = 0^\circ$.



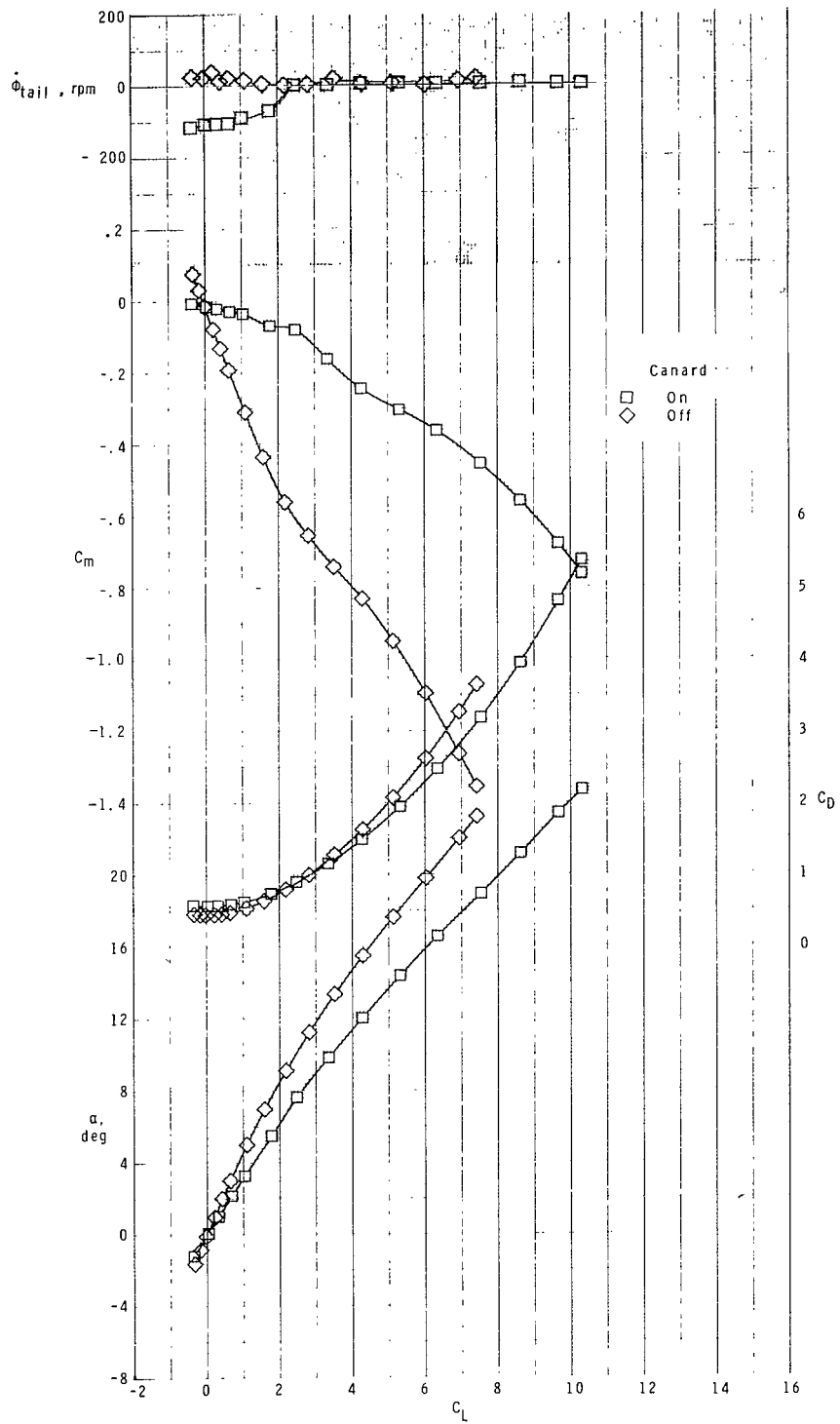
(a) Concluded.

Figure 6.- Continued.



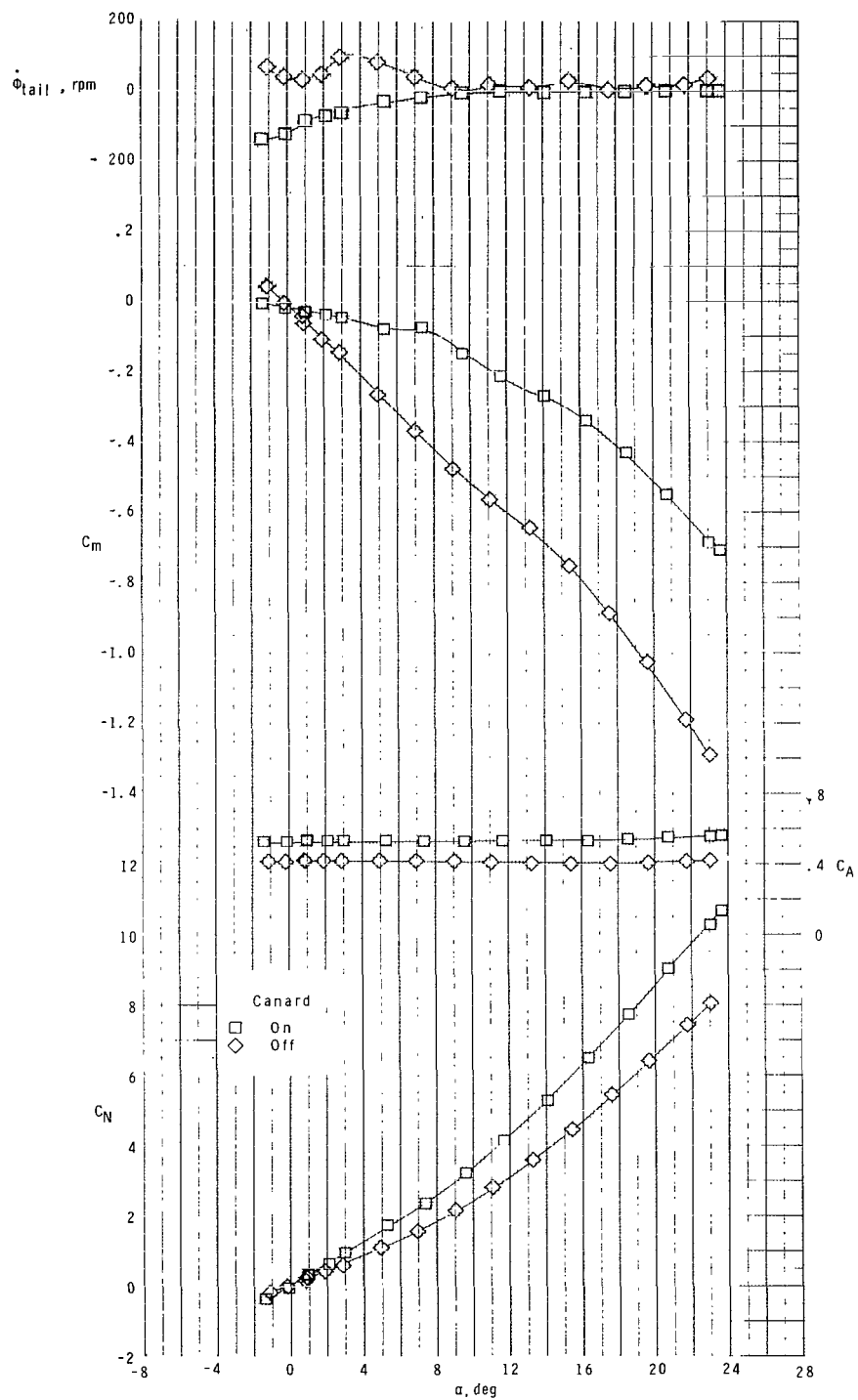
(b) $M = 2.16$.

Figure 6.- Continued.



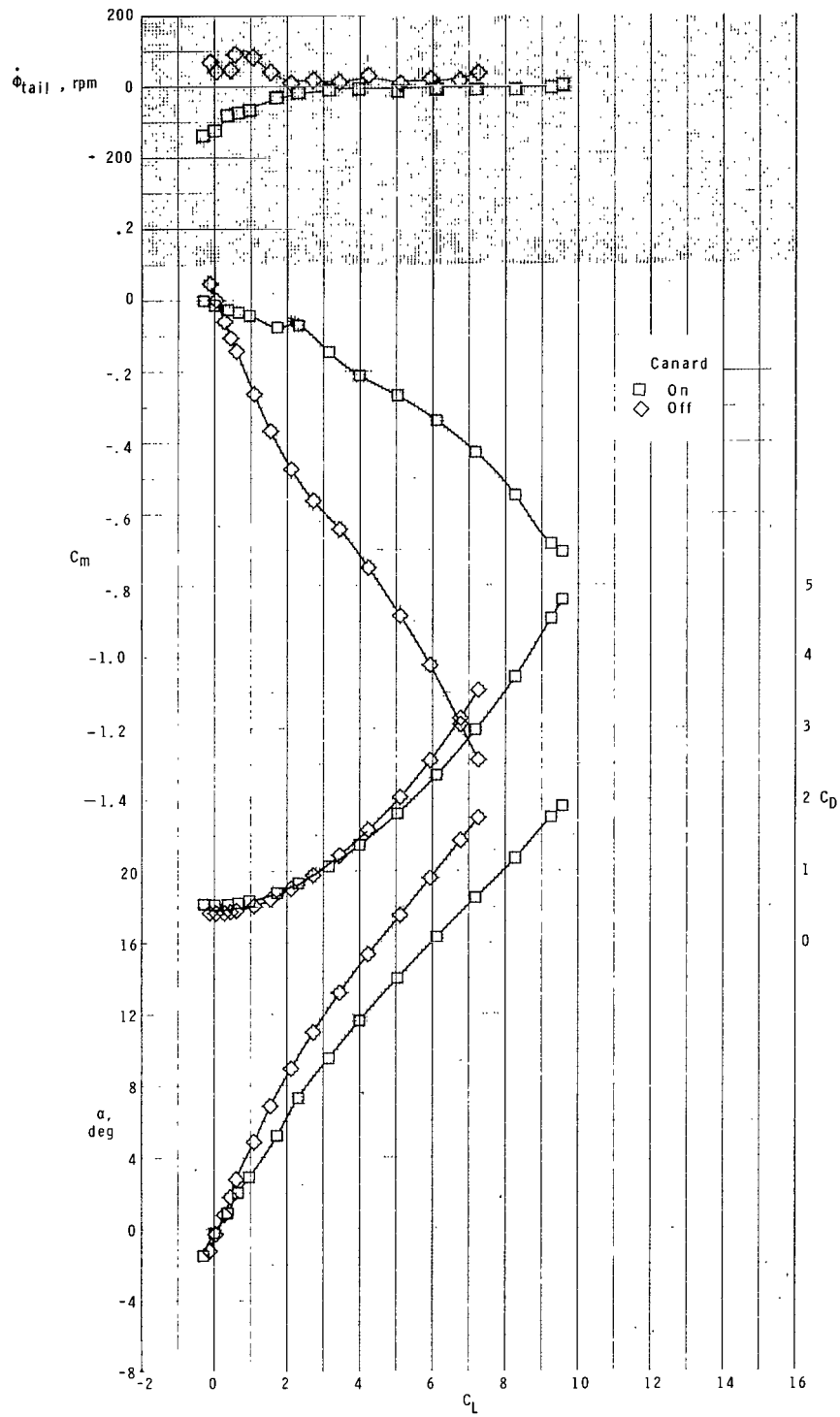
(b) Concluded.

Figure 6.- Continued.



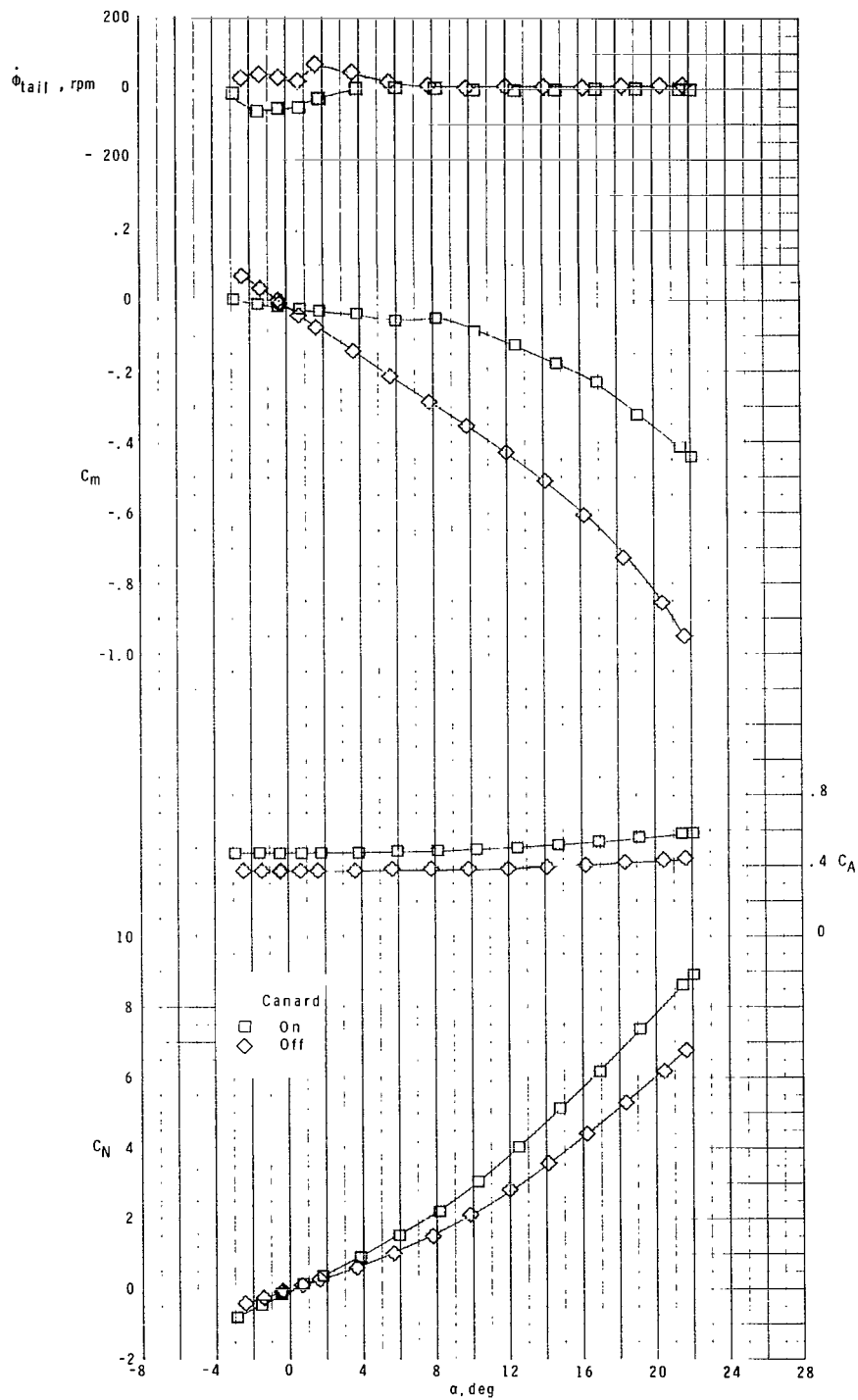
(c) $M = 2.36$.

Figure 6.- Continued.



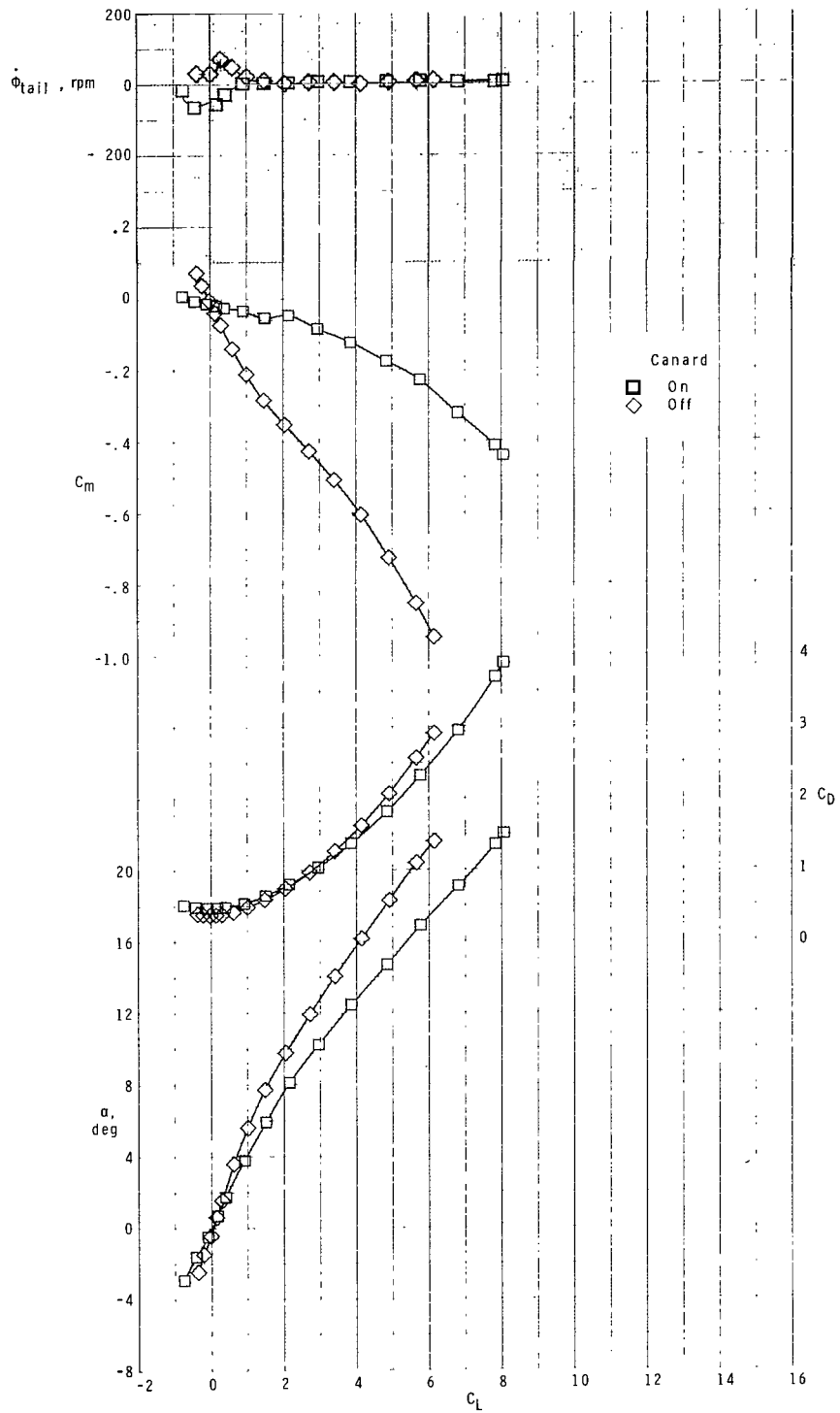
(c) Concluded.

Figure 6.- Continued.



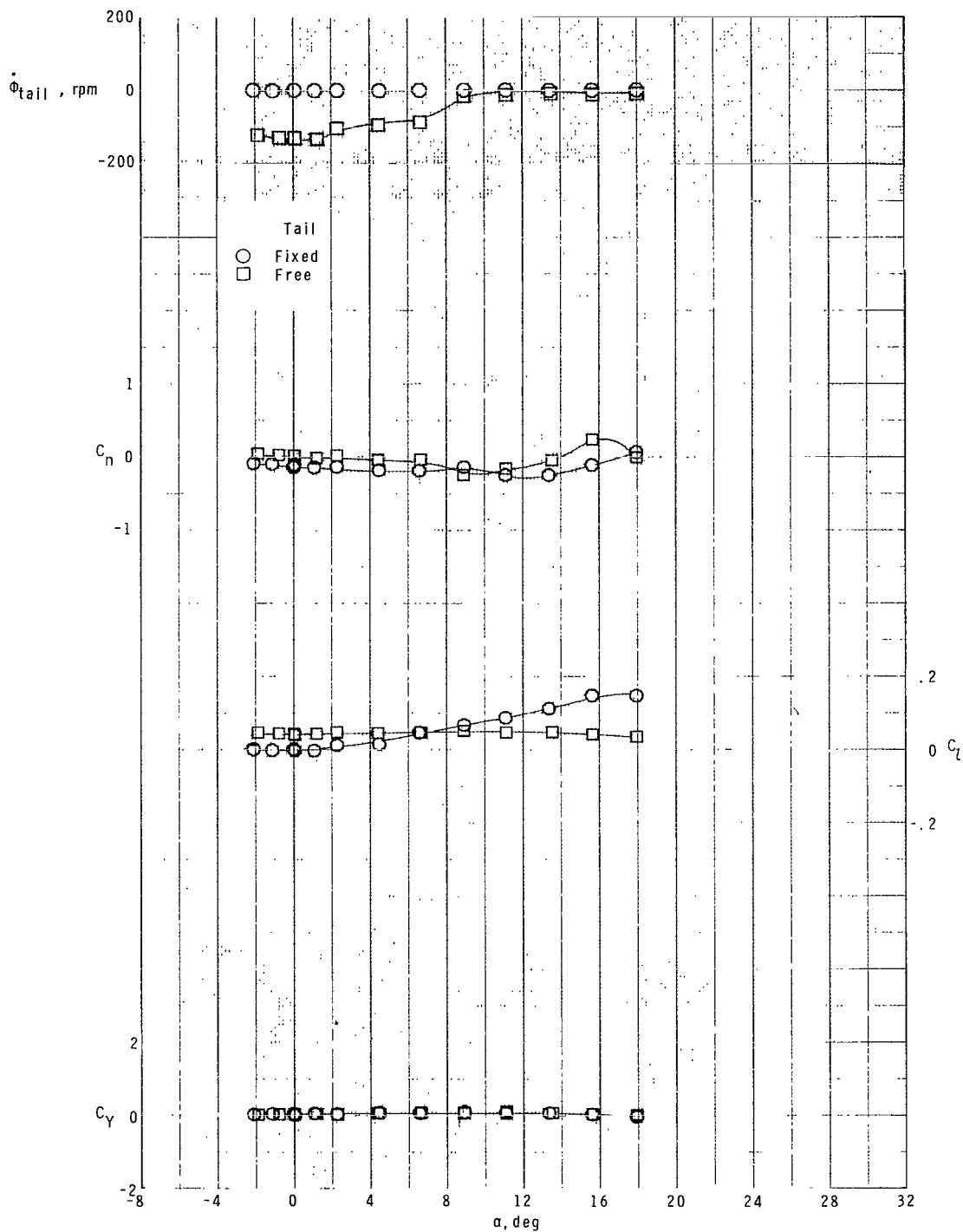
(d) $M = 2.86$.

Figure 6.- Continued.



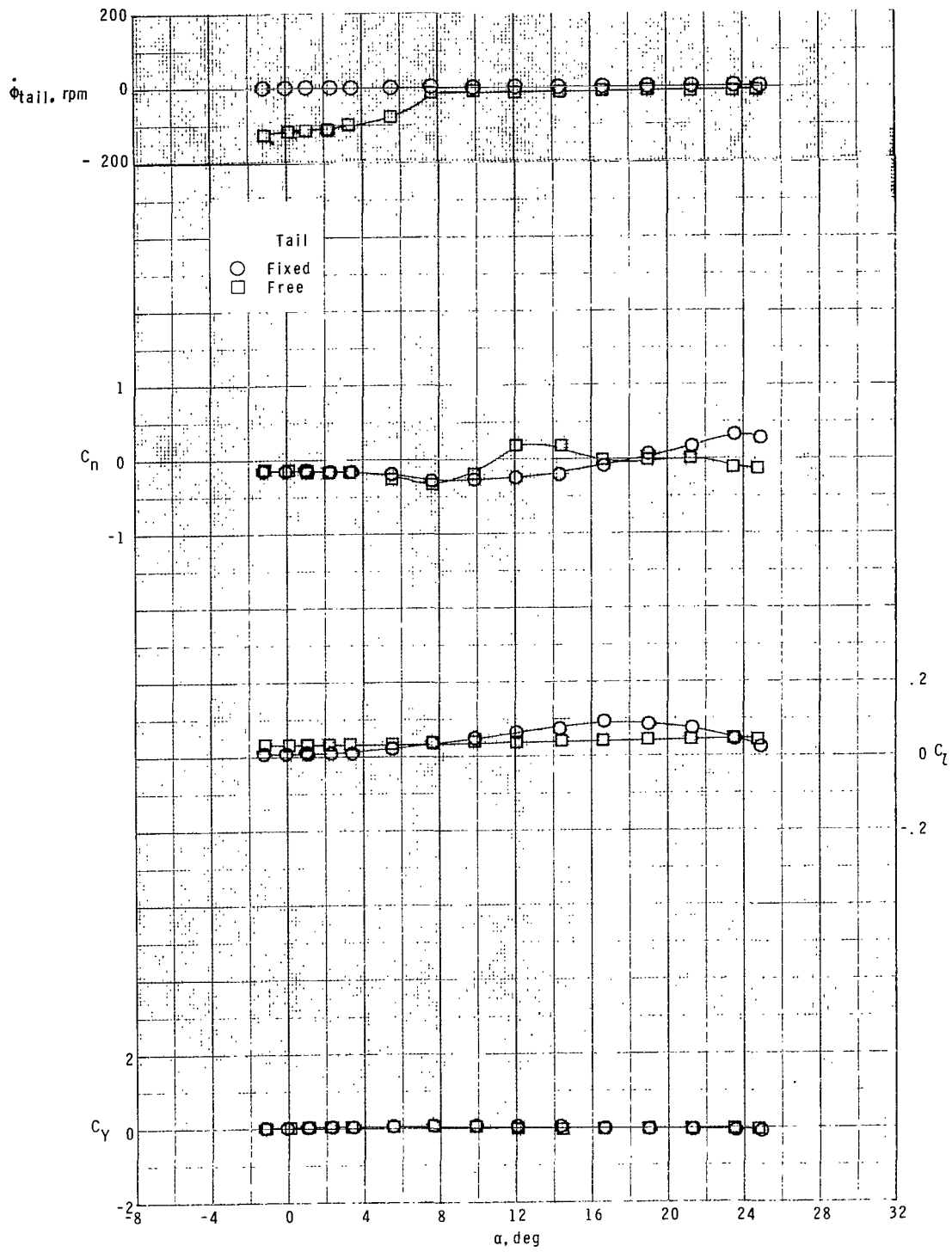
(d) Concluded.

Figure 6.- Concluded.



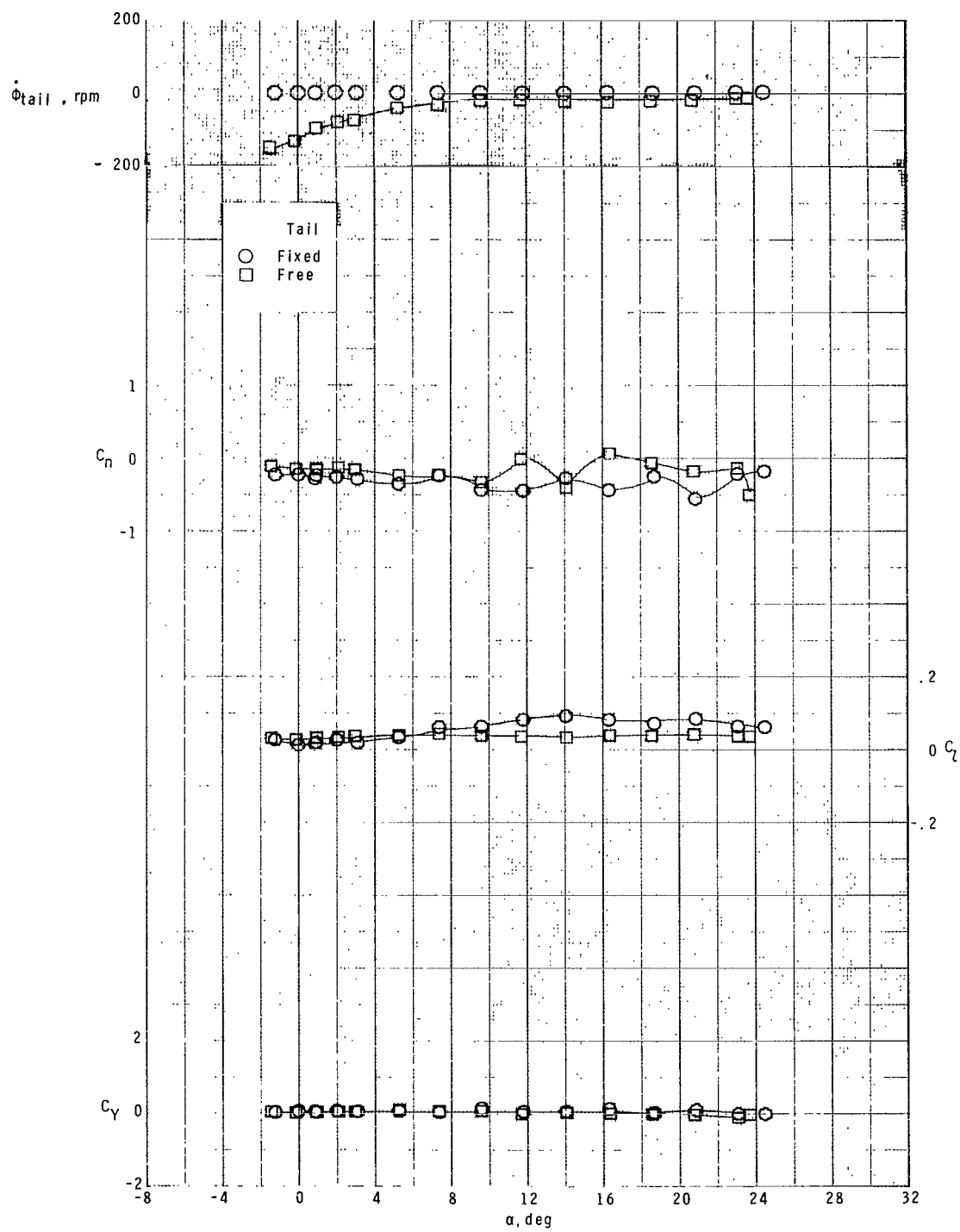
(a) $M = 1.70$.

Figure 7.- Effect of free-rolling tail on lateral aerodynamic characteristics of model with zero control deflection at $\phi_C = 0^\circ$.



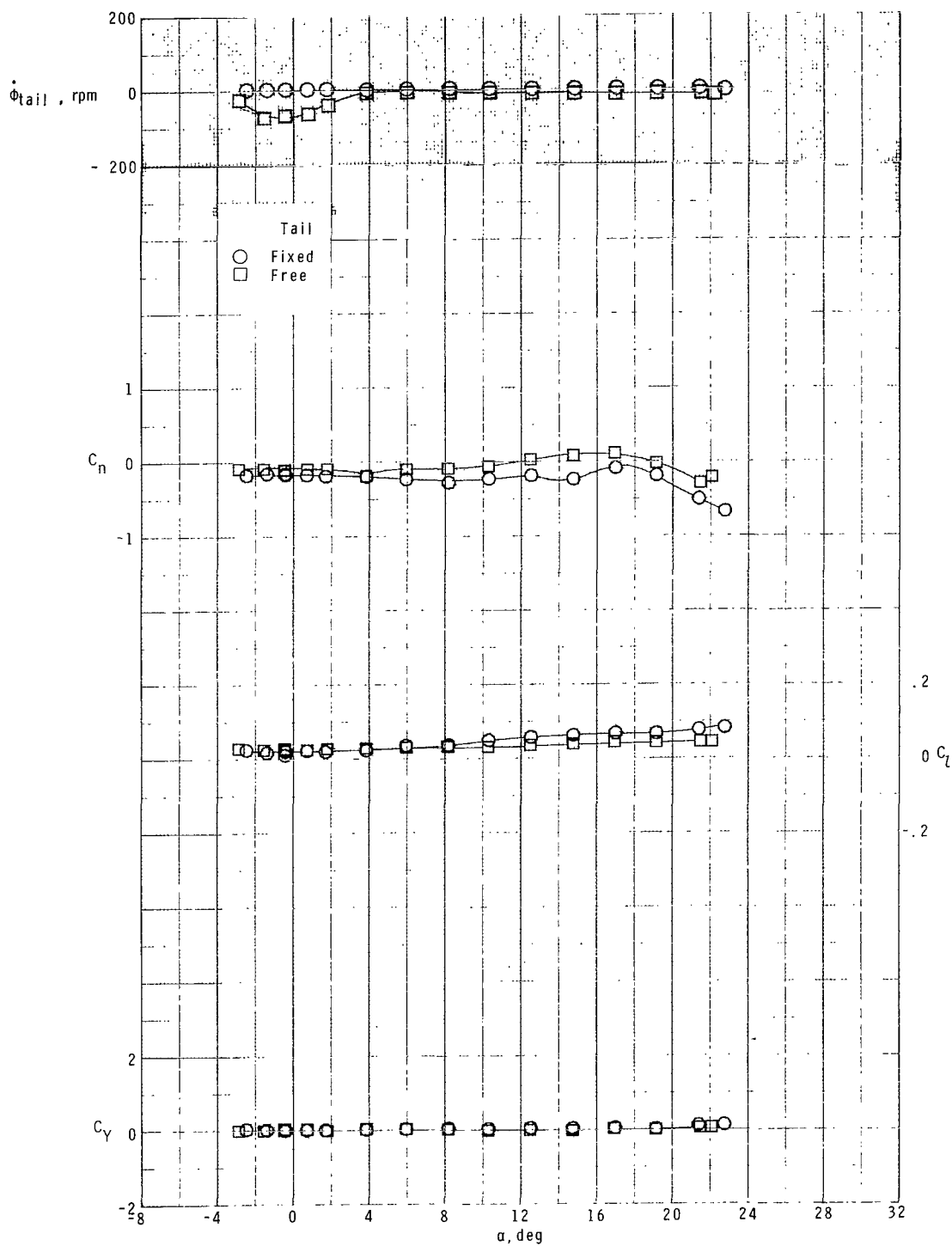
(b) $M = 2.16$.

Figure 7.- Continued.



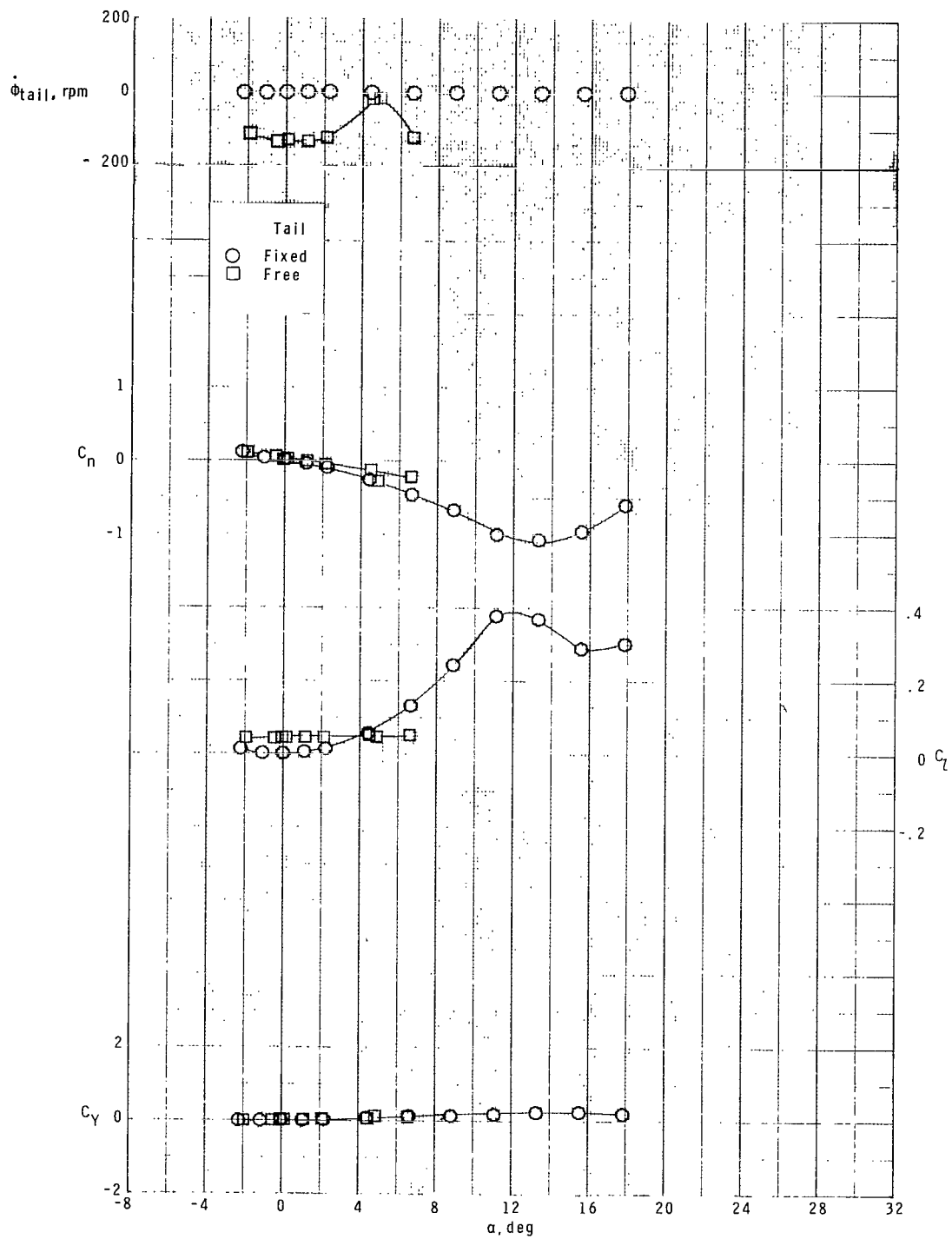
(c) $M = 2.36$.

Figure 7.- Continued.



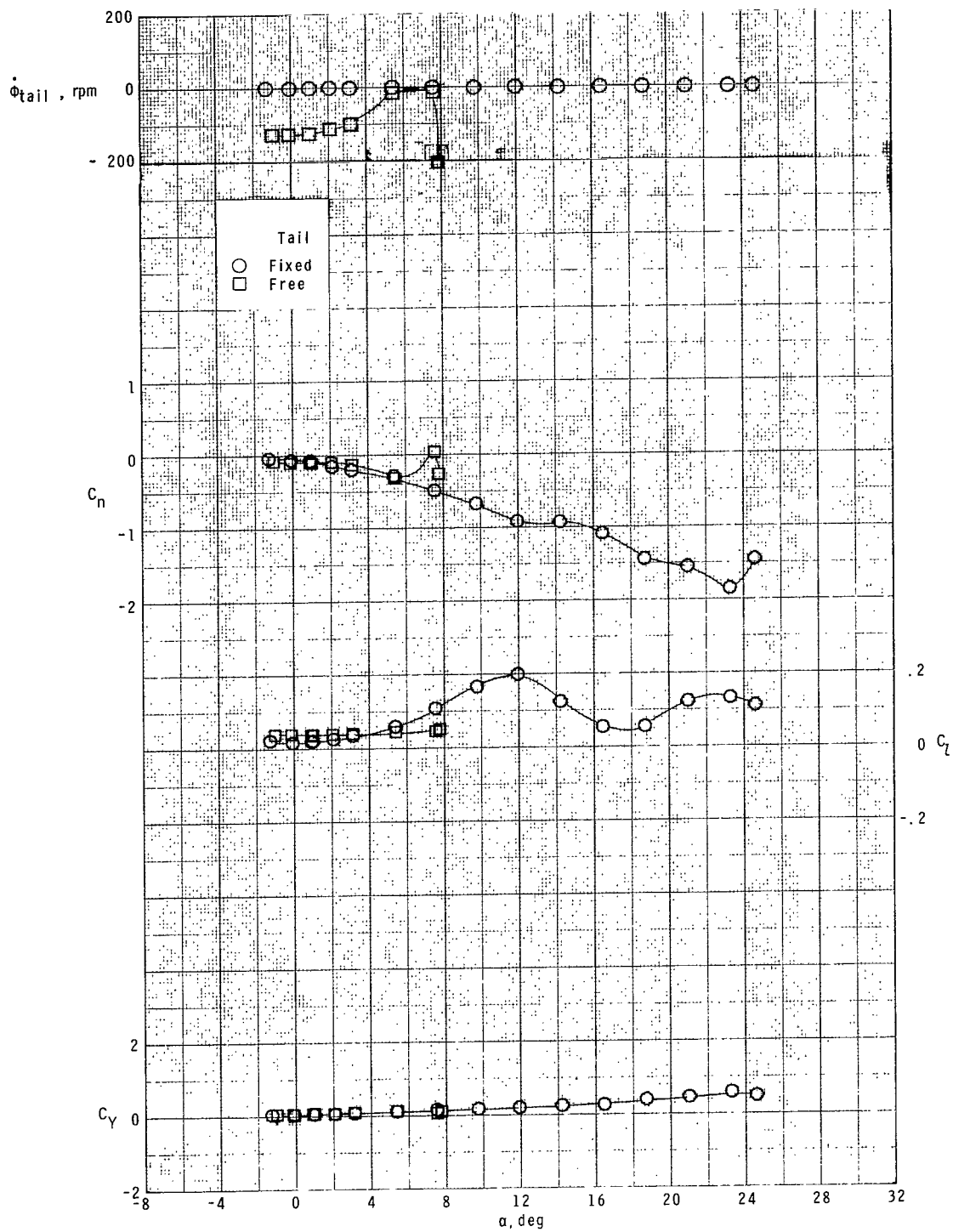
(d) $M = 2.86$.

Figure 7.- Concluded.



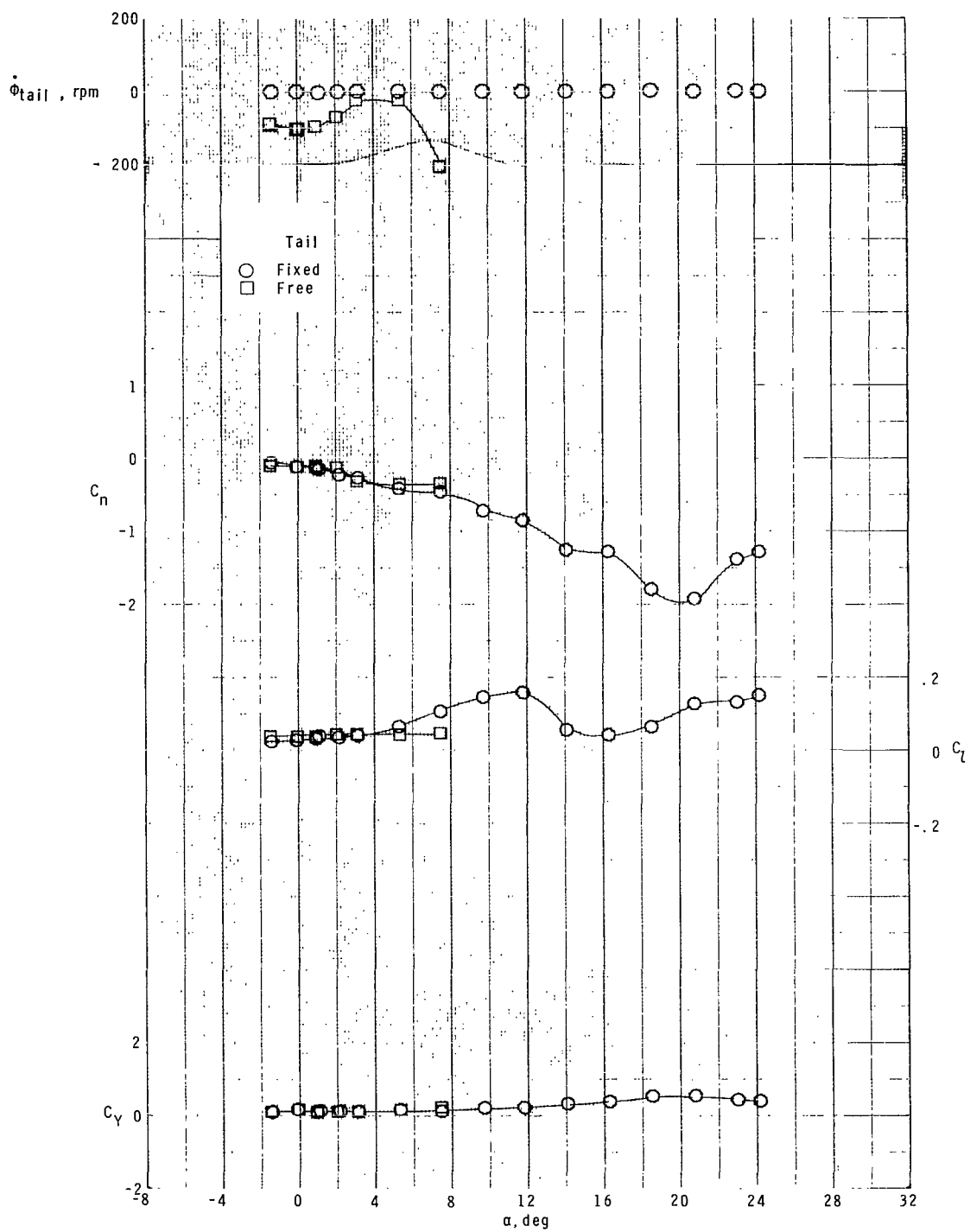
(a) $M = 1.70$.

Figure 8.- Effect of free-rolling tail on lateral aerodynamic characteristics of model with zero control deflection at $\phi_c = 26.6^\circ$.



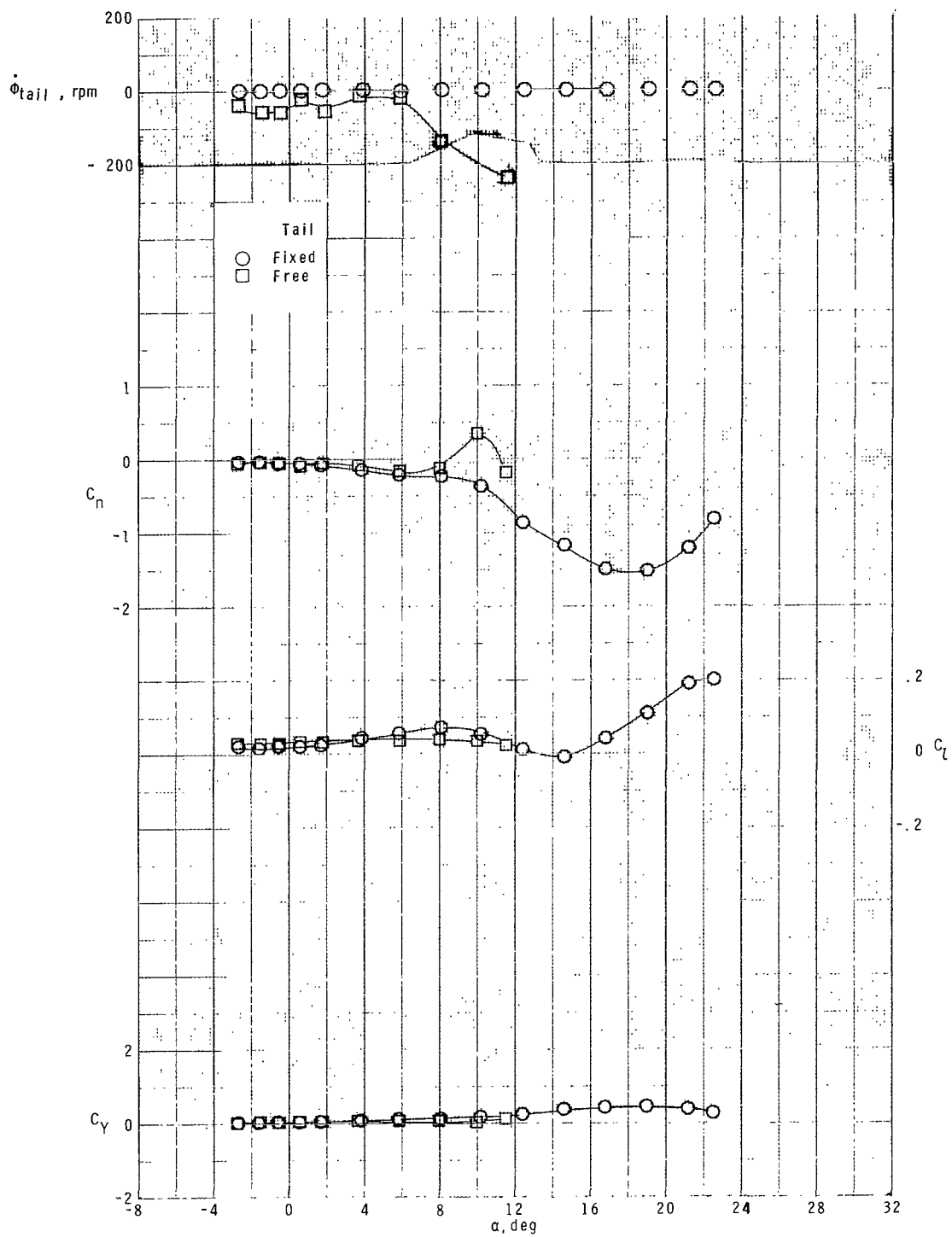
(b) $M = 2.16$.

Figure 8.- Continued.



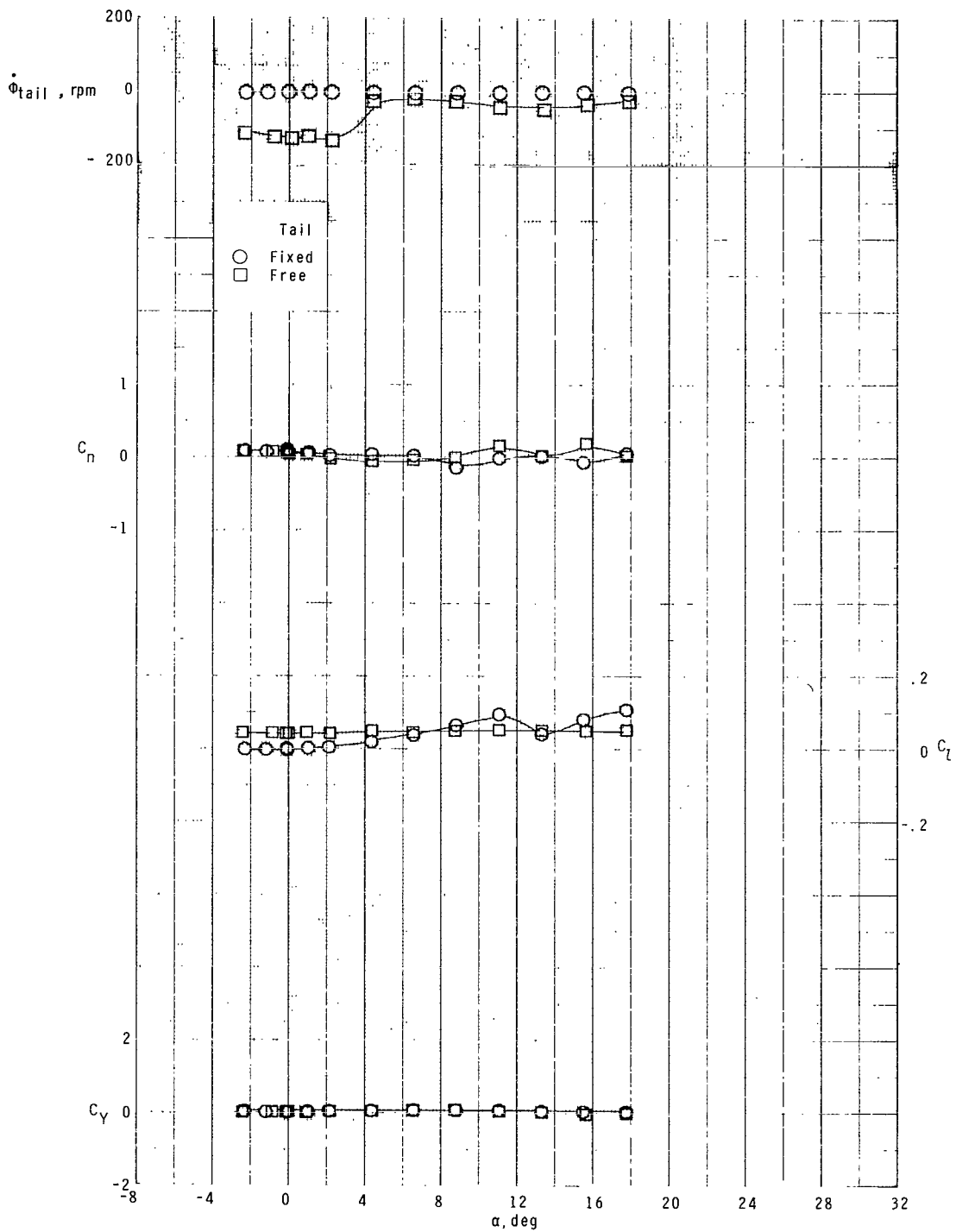
(c) $M = 2.36$.

Figure 8.- Continued.



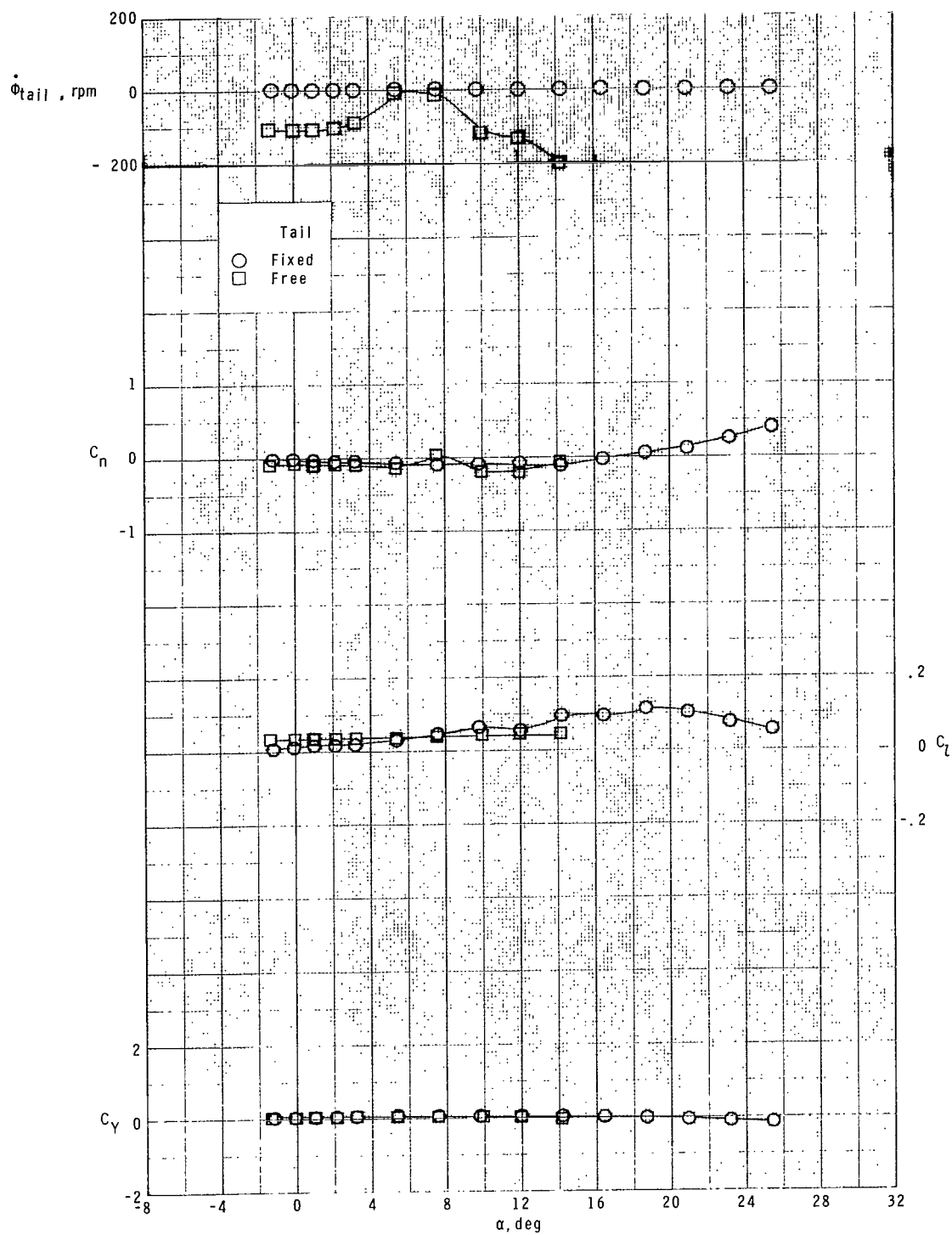
(d) $M = 2.86$.

Figure 8.- Concluded.



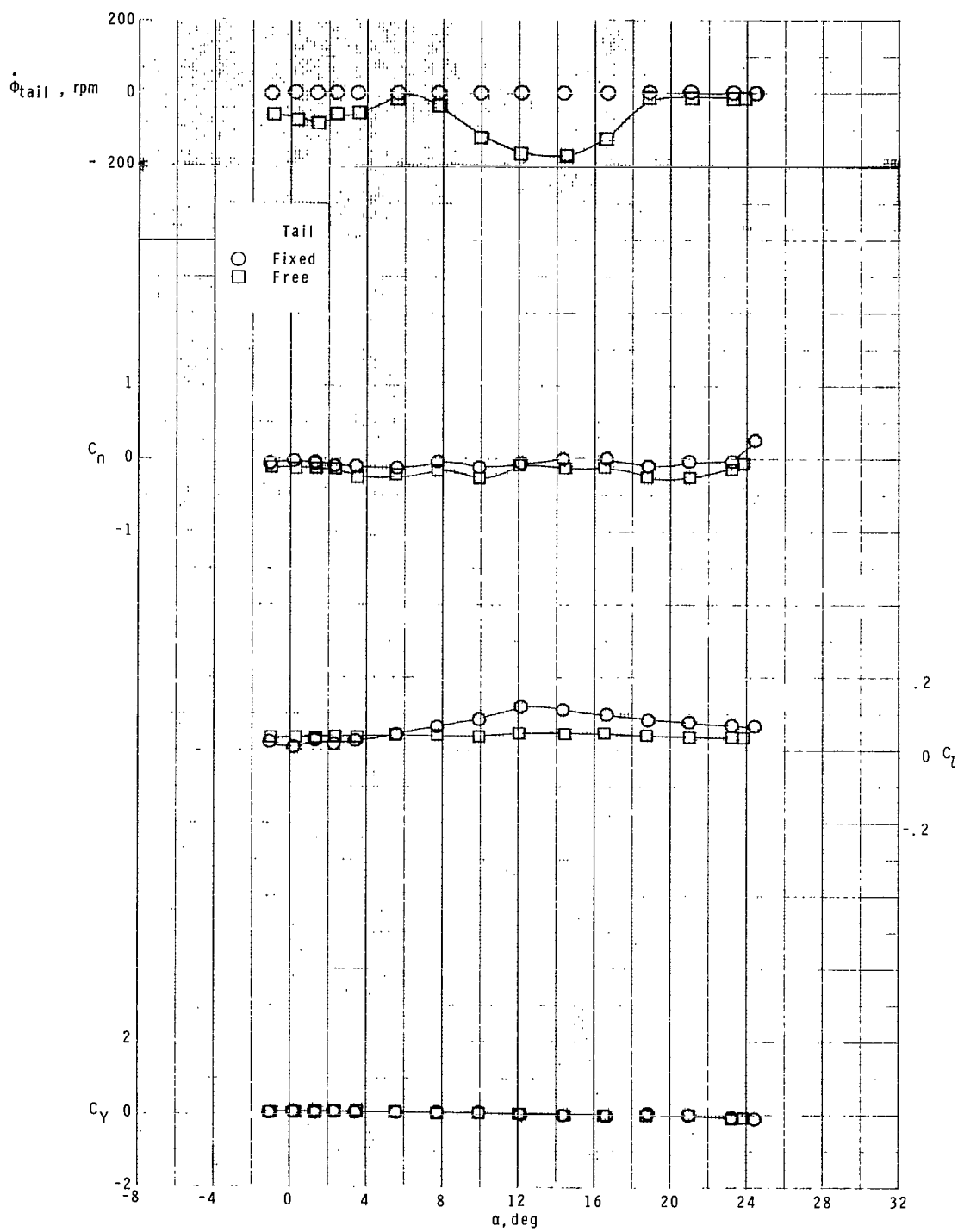
(a) $M = 1.70$.

Figure 9.- Effect of free-rolling tail on lateral aerodynamic characteristics of model with zero control deflection at $\phi_C = 45^\circ$.



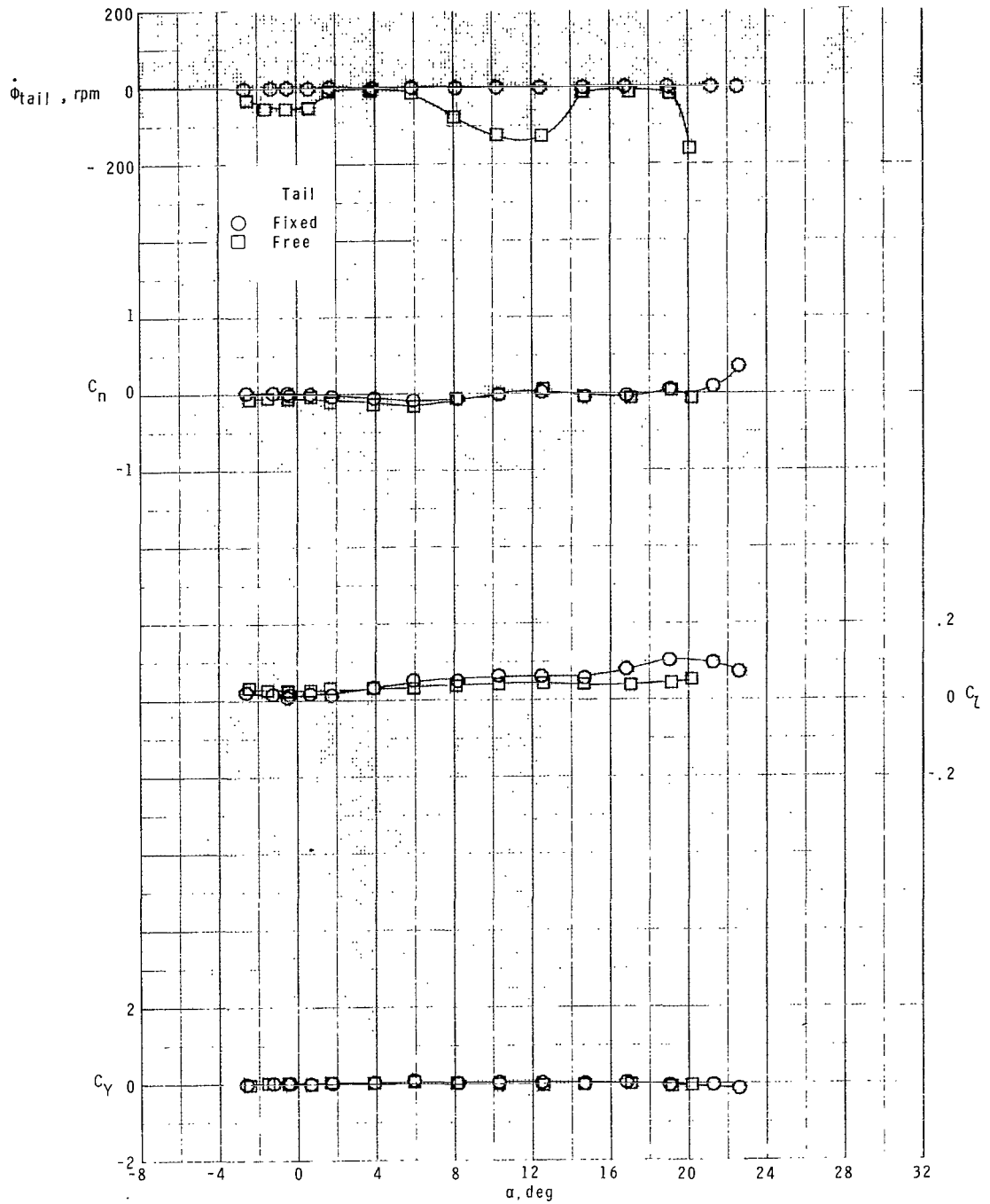
(b) $M = 2.16$.

Figure 9.- Continued.



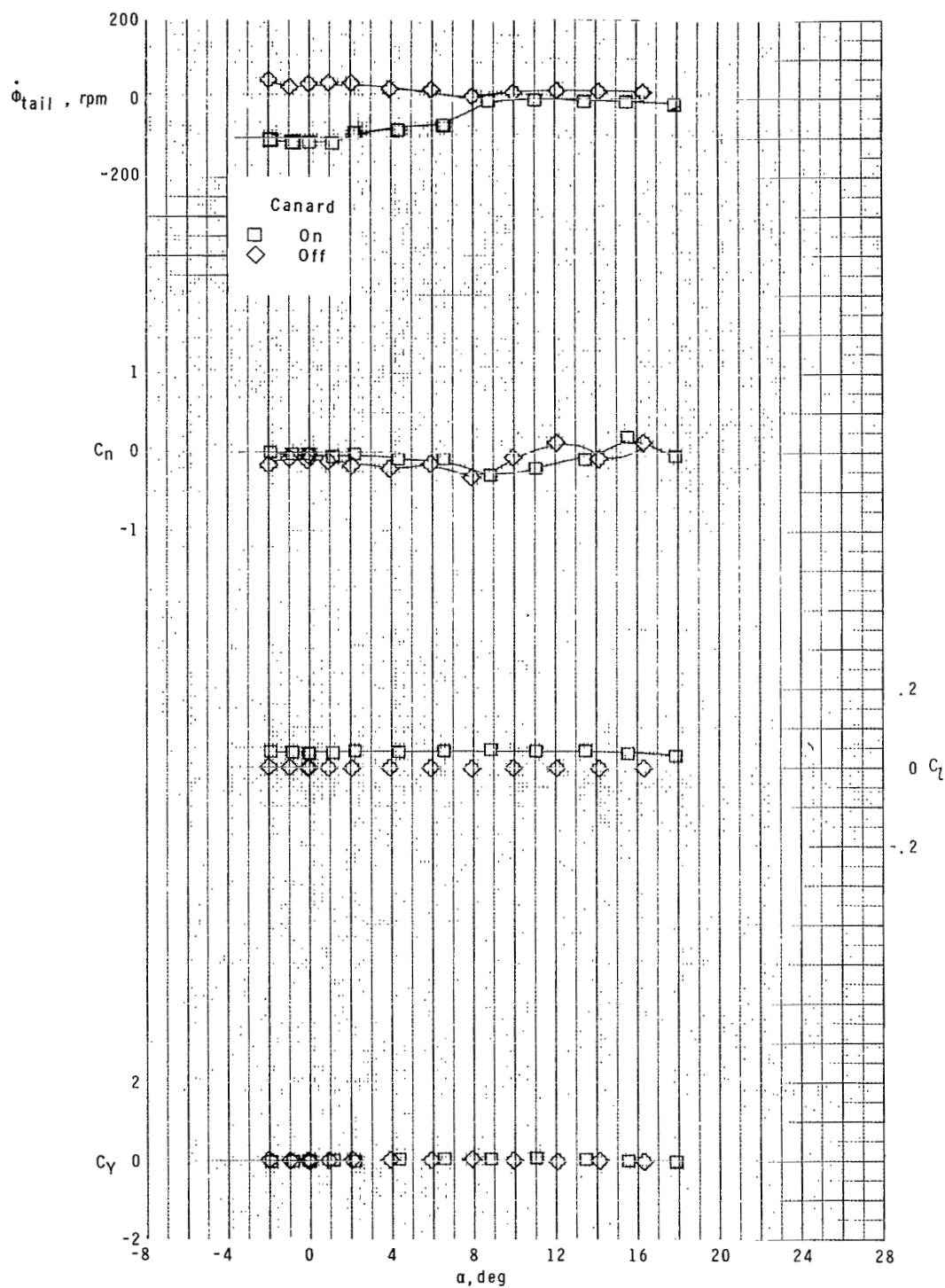
(c) $M = 2.36$.

Figure 9.- Continued.



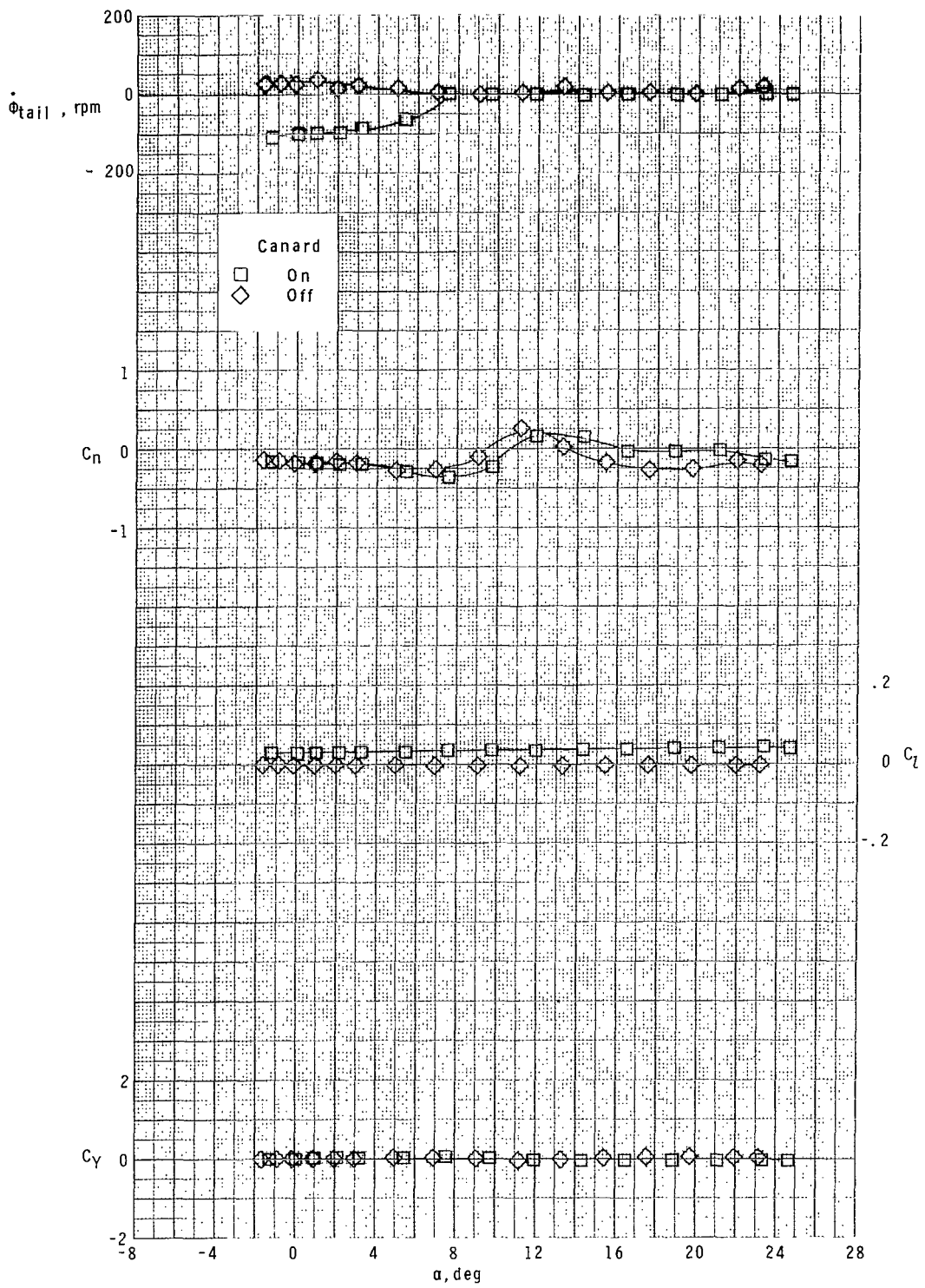
(d) $M = 2.86$.

Figure 9.- Concluded.



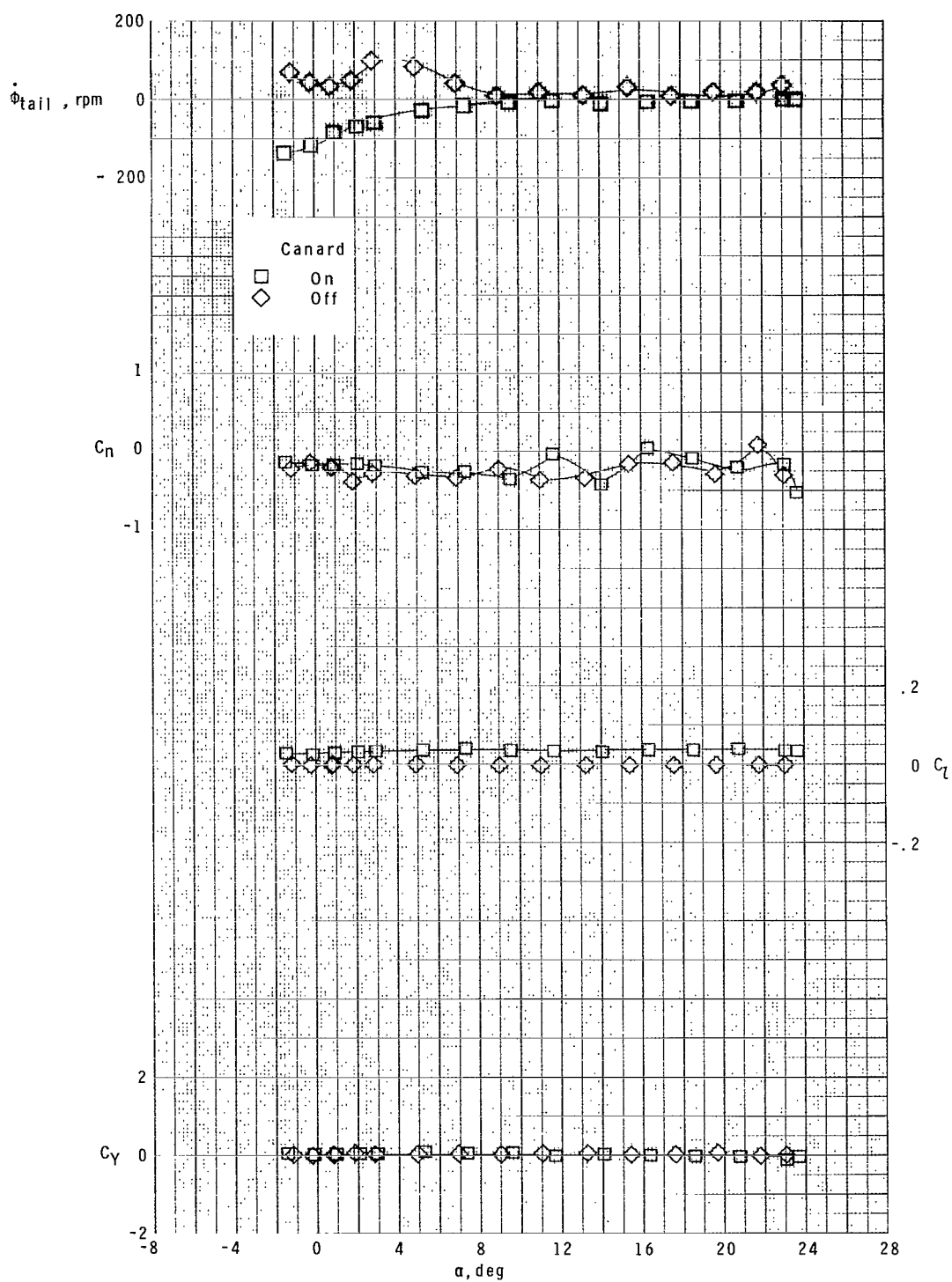
(a) $M = 1.70$.

Figure 10.- Effect of canards on lateral aerodynamic characteristics of model with a free-rolling tail at $\phi_C = 0^\circ$.



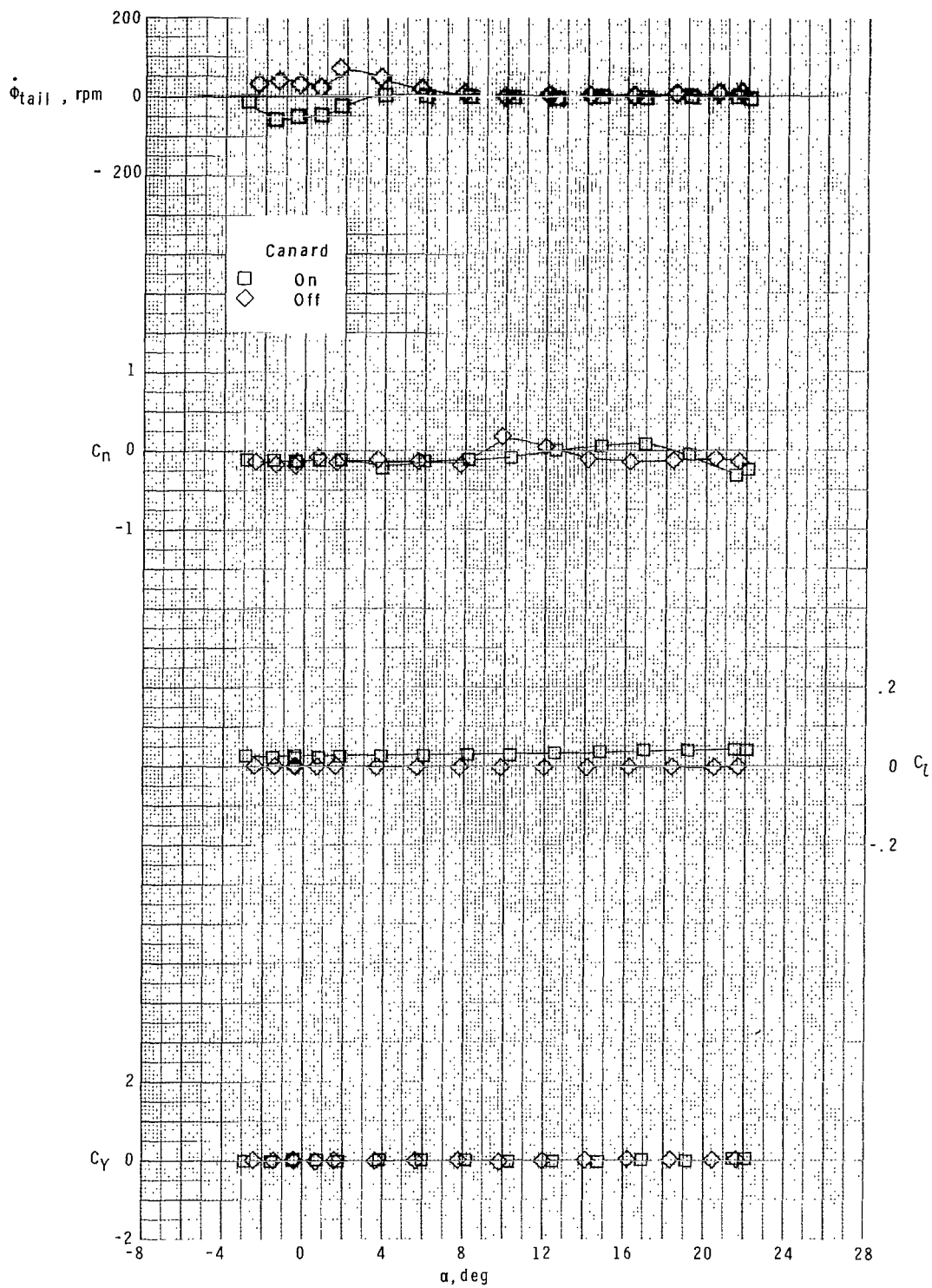
(b) $M = 2.16$.

Figure 10.- Continued.



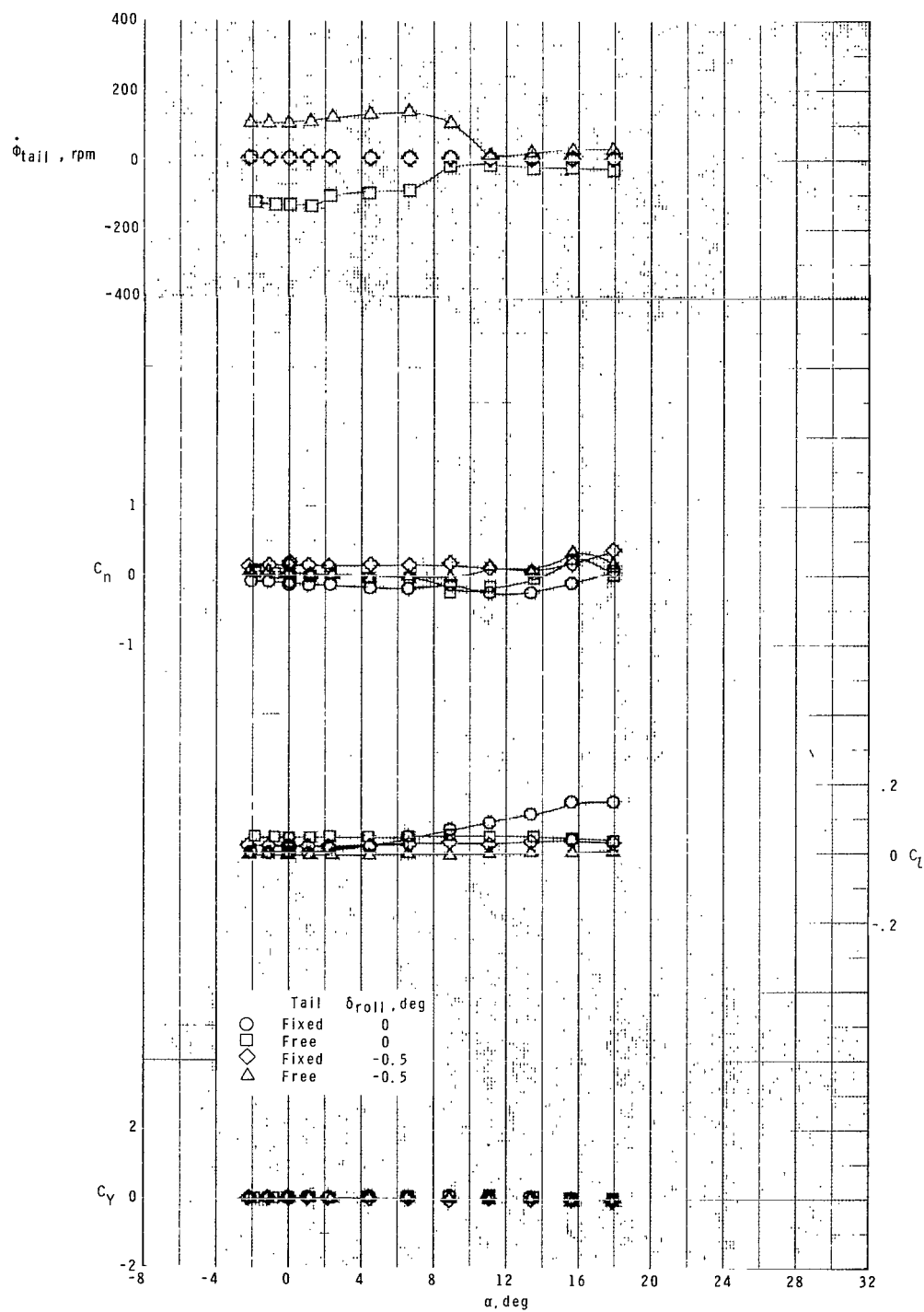
(c) $M = 2.36$.

Figure 10.- Continued.



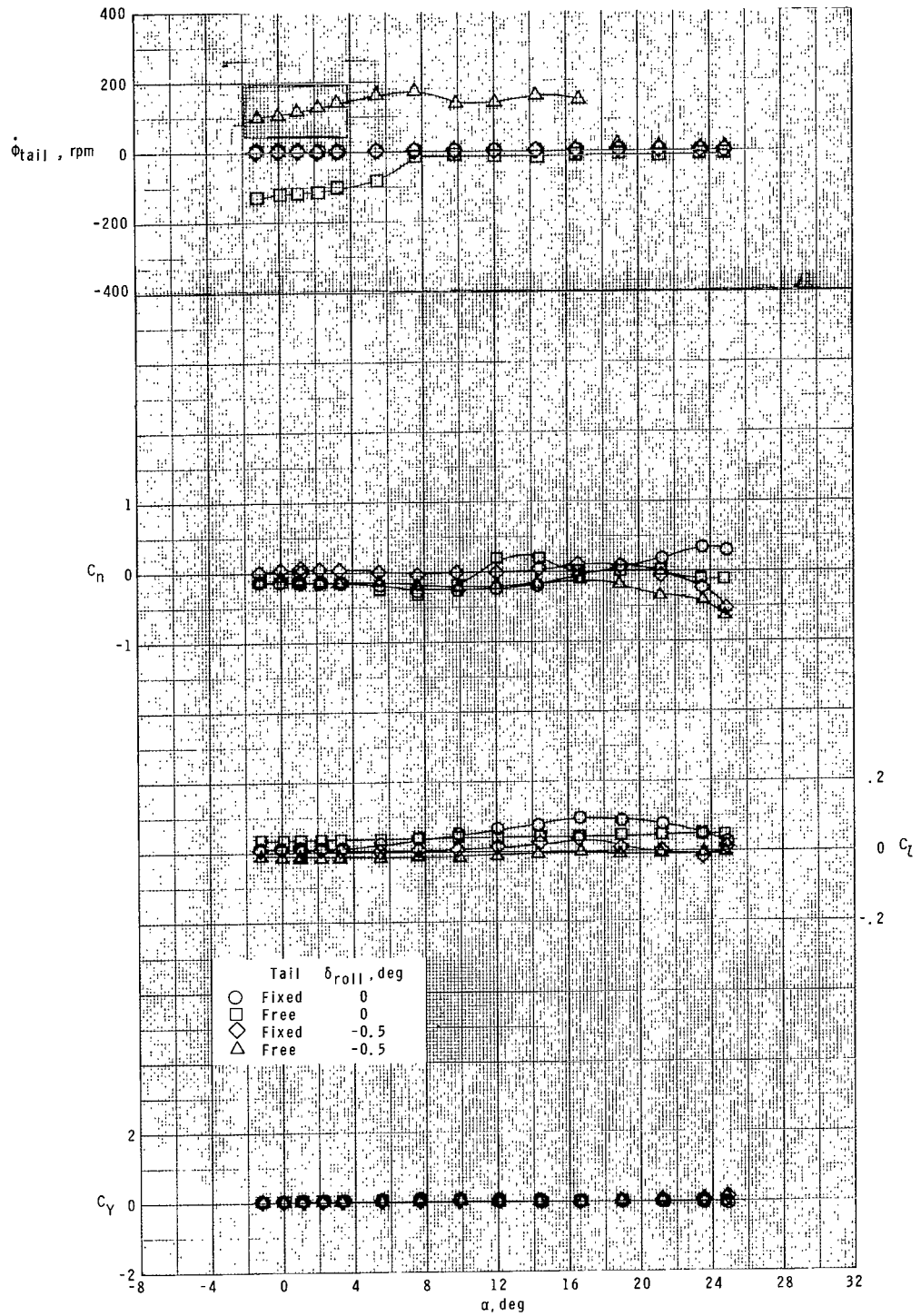
(d) $M \approx 2.86$.

Figure 10.- Concluded.



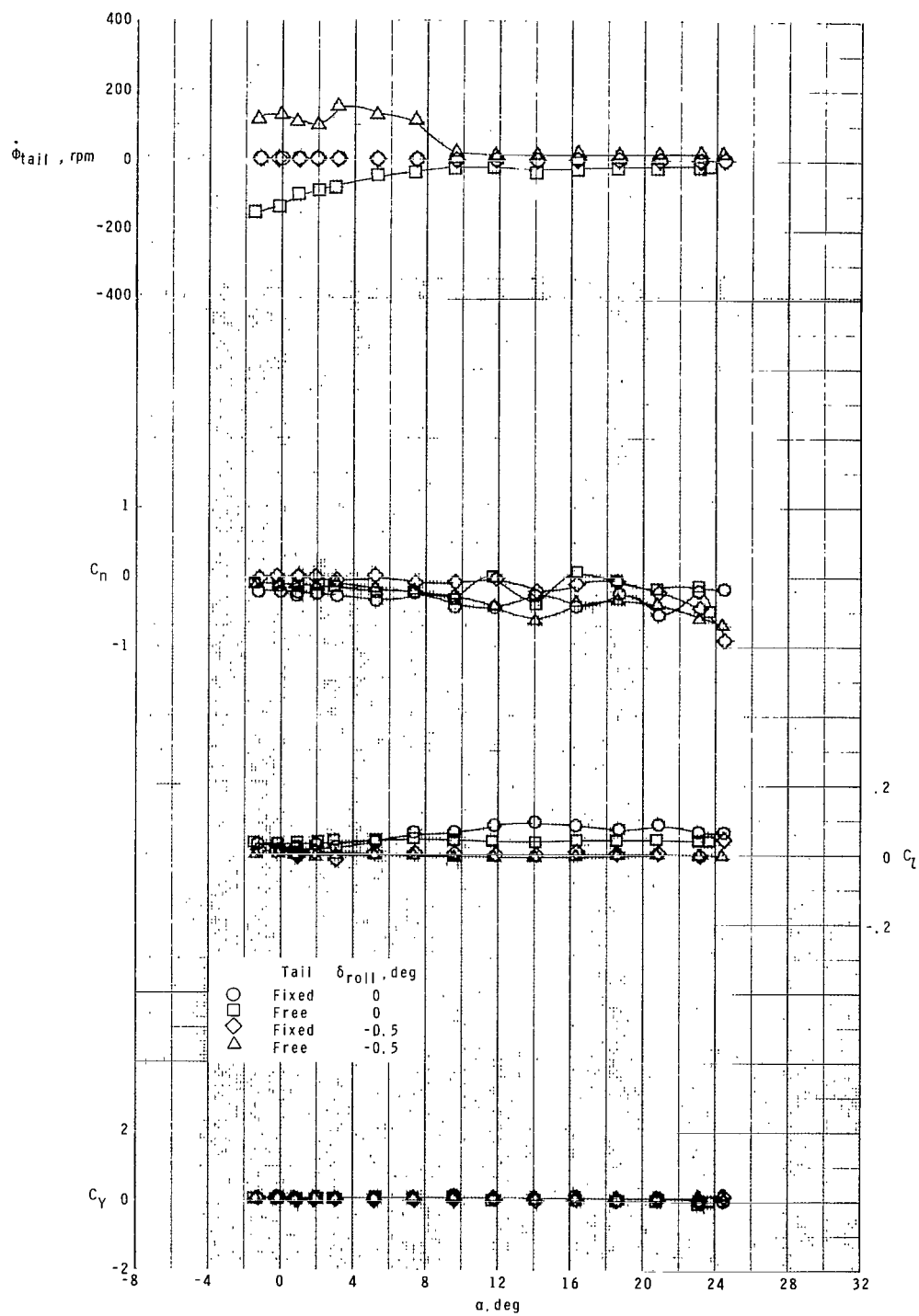
(a) $M = 1.70$.

Figure 11.- Roll-control characteristics of model with fixed and free-rolling tail at $\phi_C = 0^\circ$. Two canards deflected.



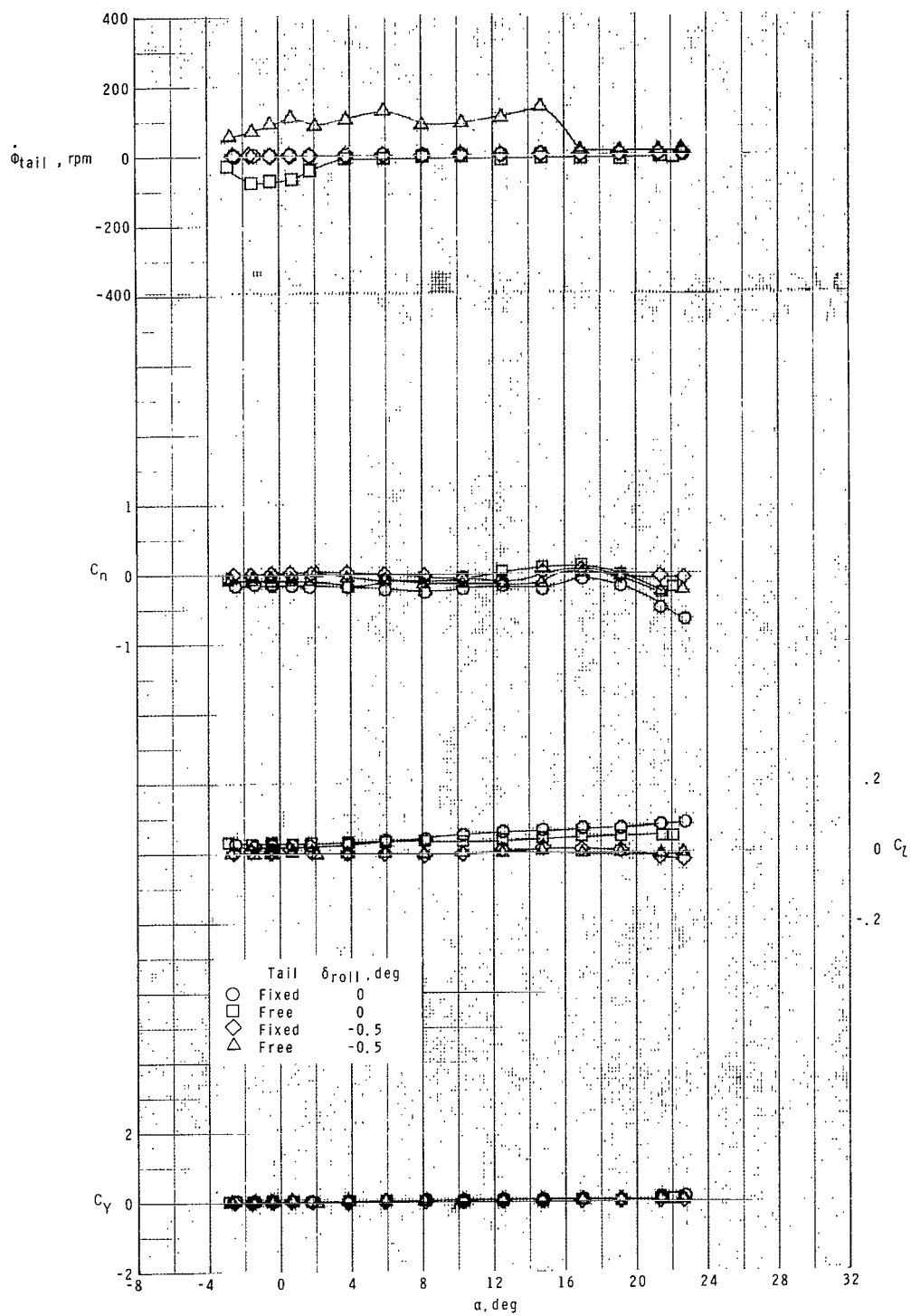
(b) $M = 2.16$.

Figure 11.- Continued.



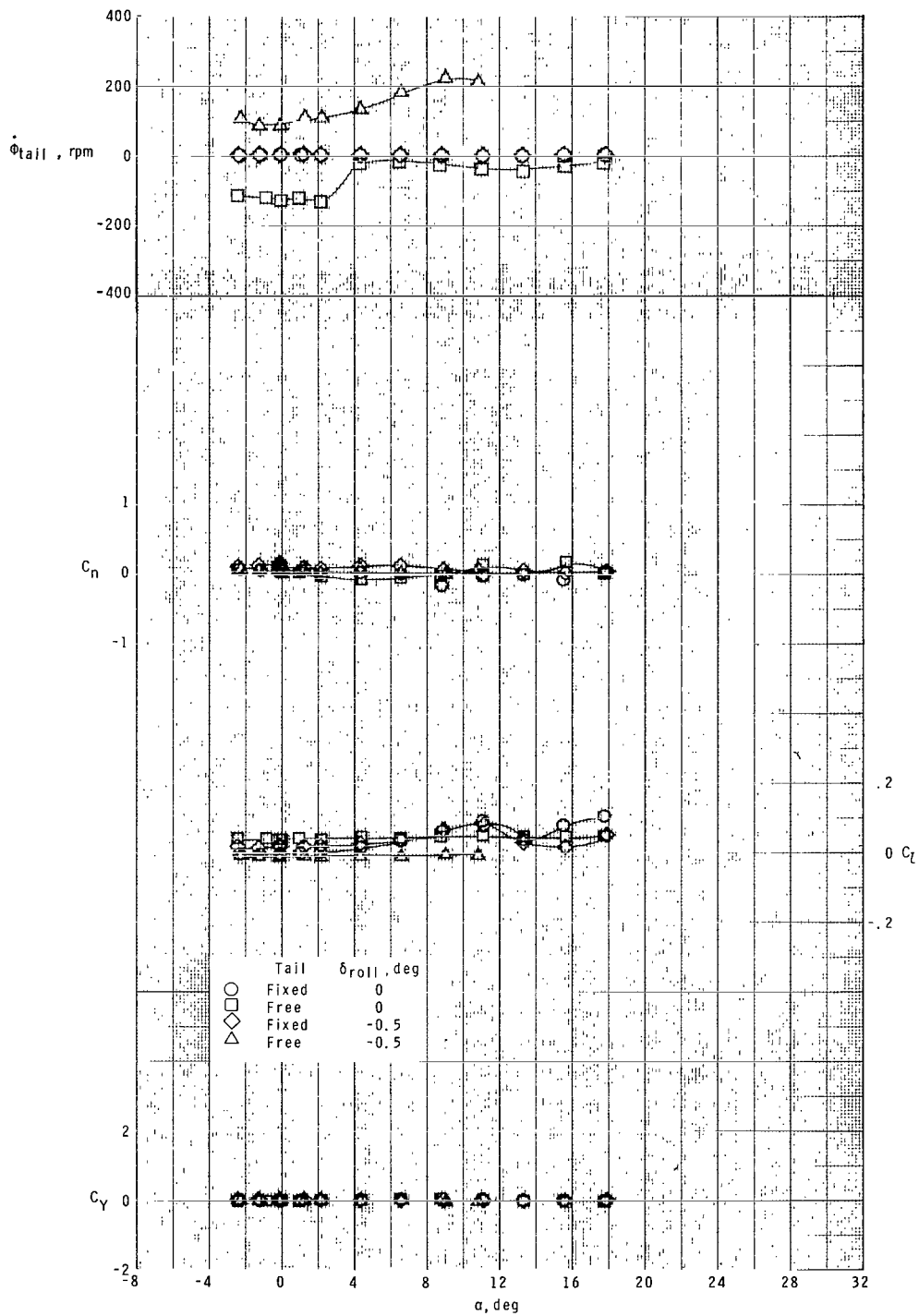
(c) $M = 2.36$.

Figure 11.- Continued.



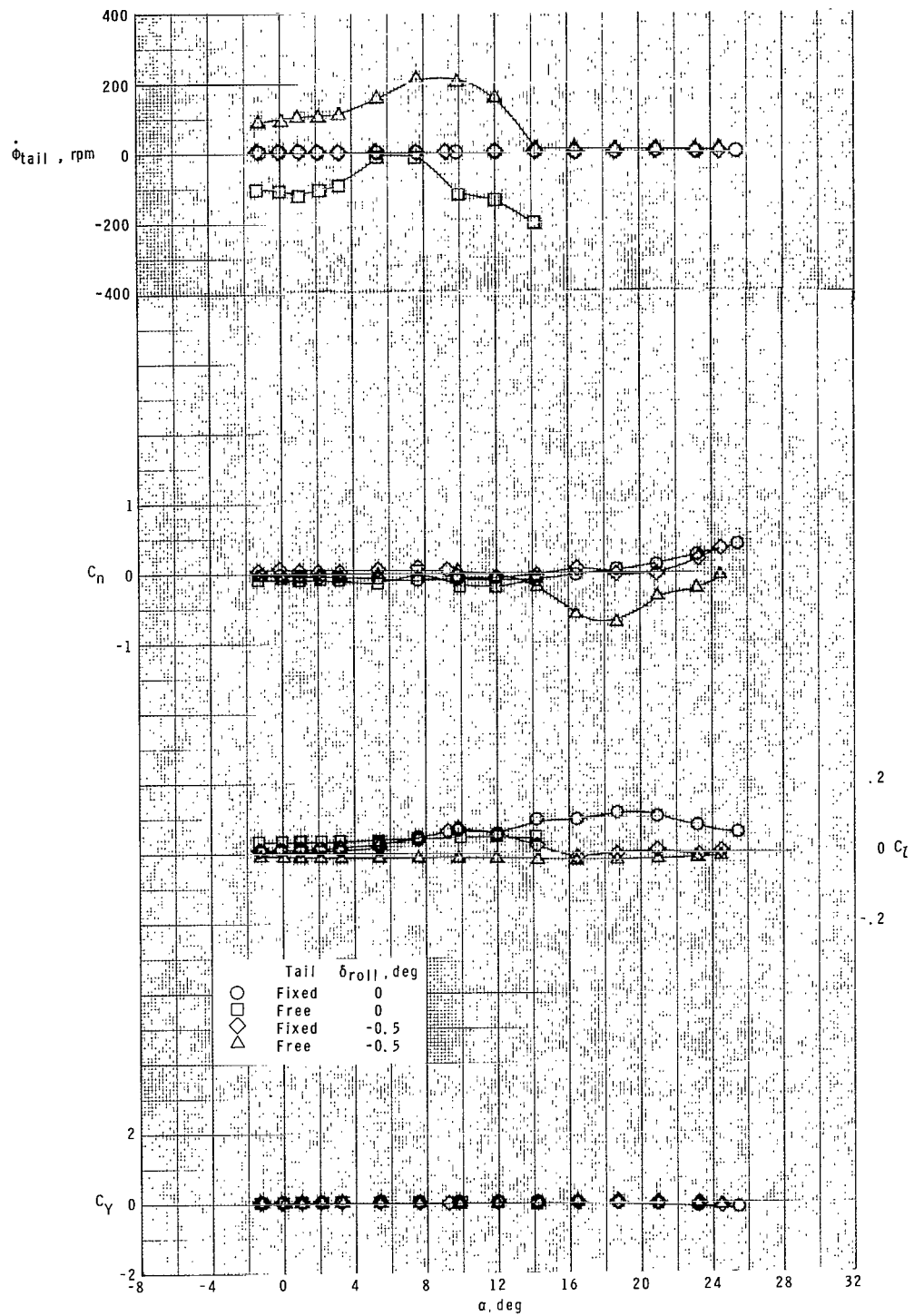
(d) $M = 2.86.$

Figure 11.- Concluded.



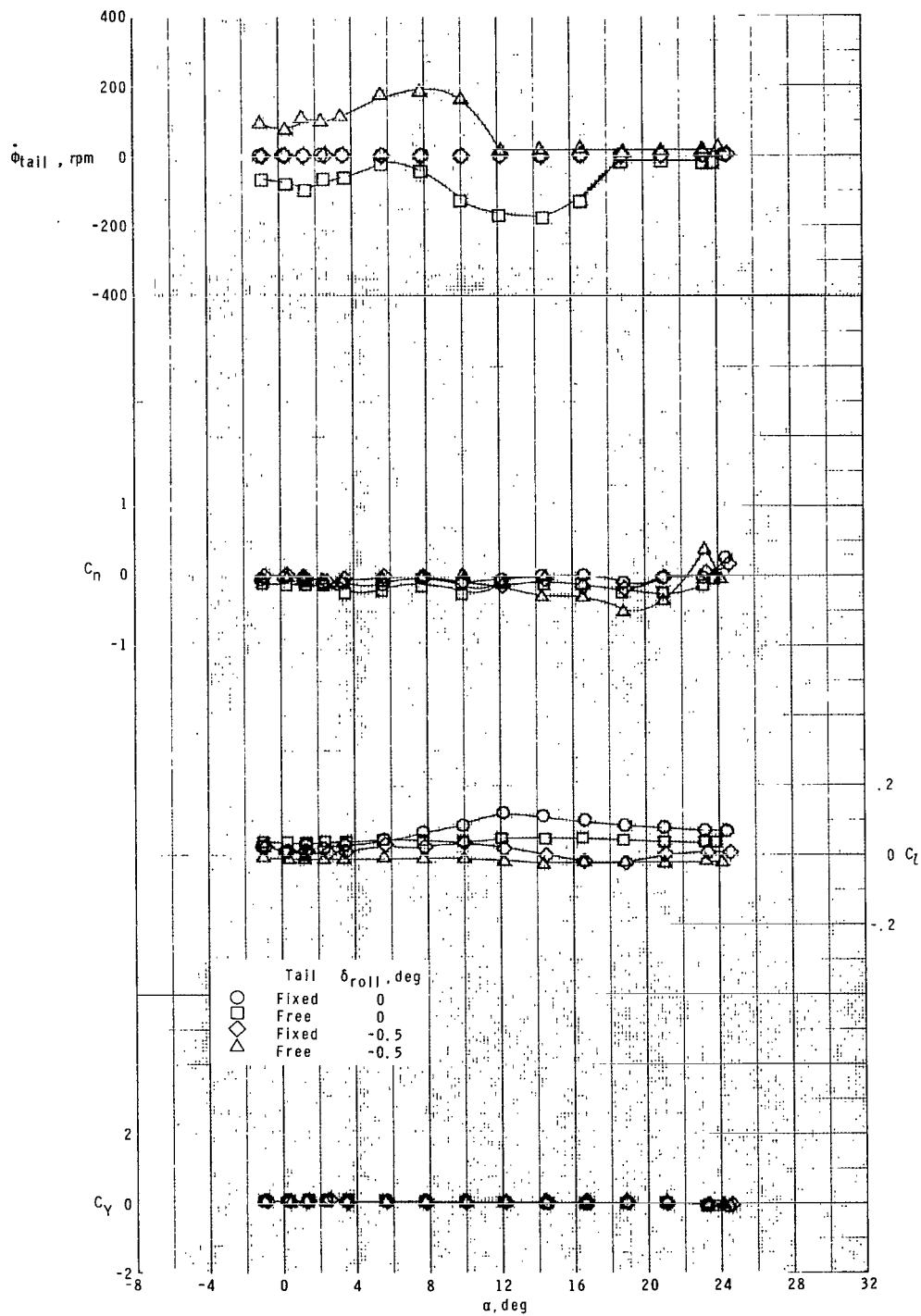
(a) $M = 1.70$.

Figure 12.- Roll-control characteristics of model with fixed and free-rolling tail at $\phi_c = 45^\circ$. Two canards deflected.



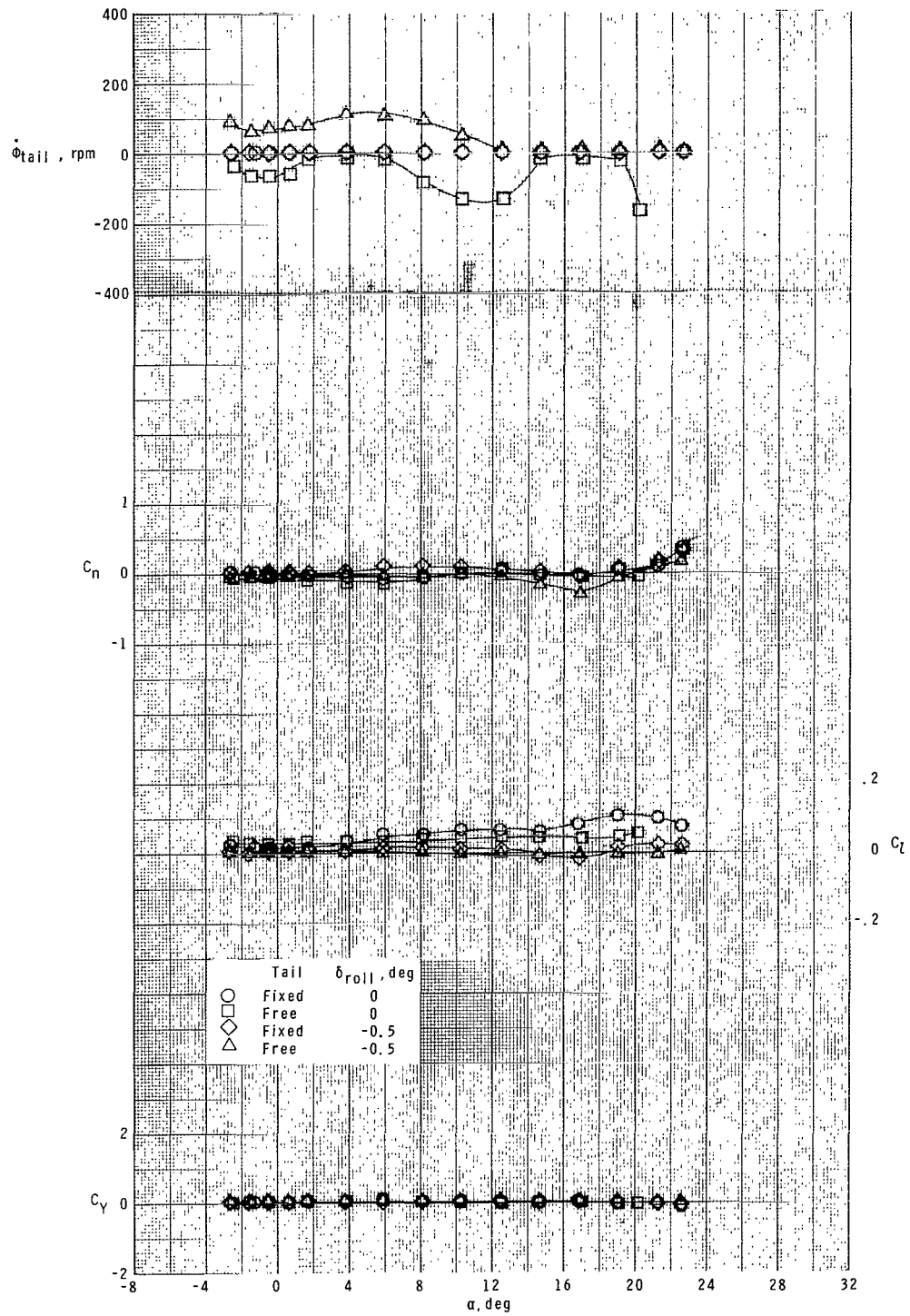
(b) $M = 2.16$.

Figure 12.- Continued.



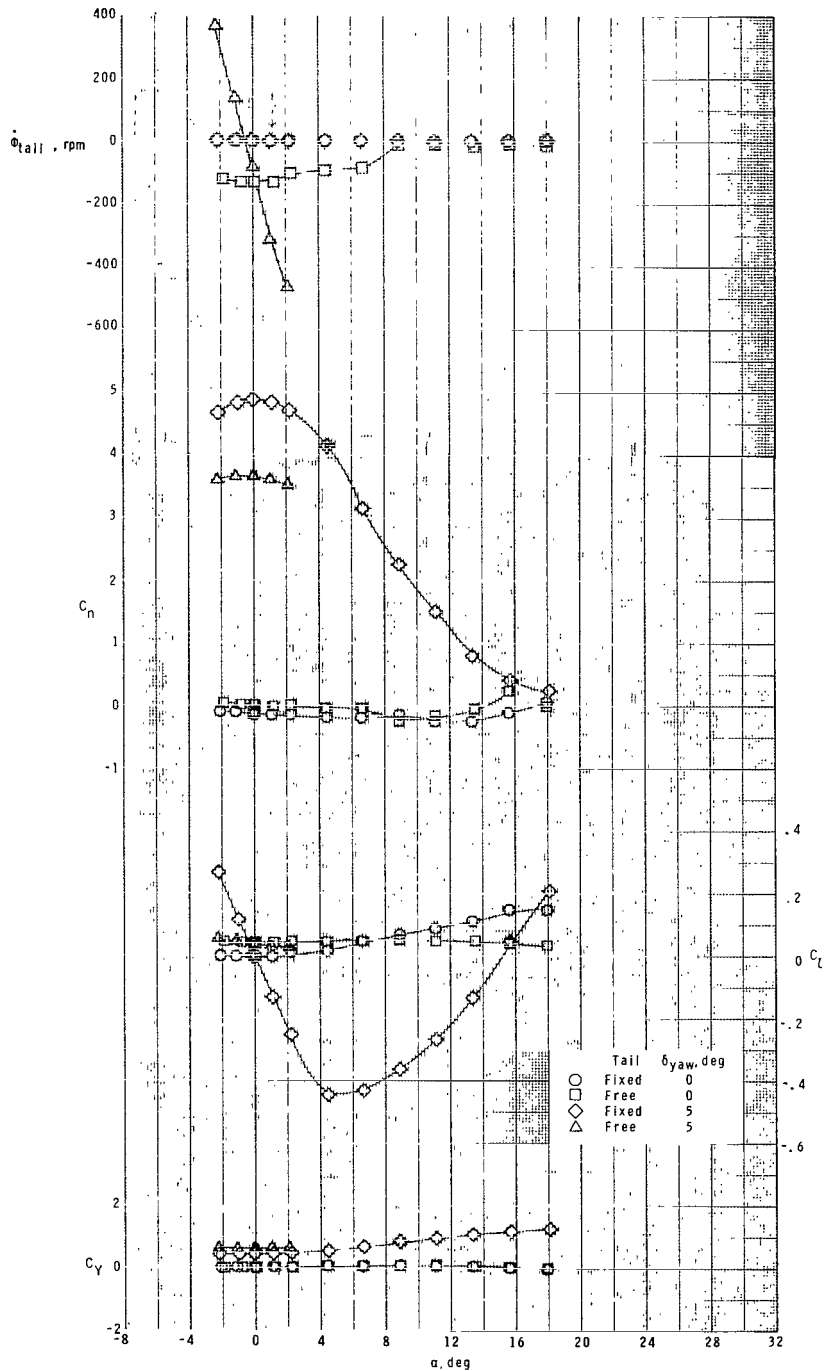
(c) $M = 2.36$.

Figure 12.- Continued.



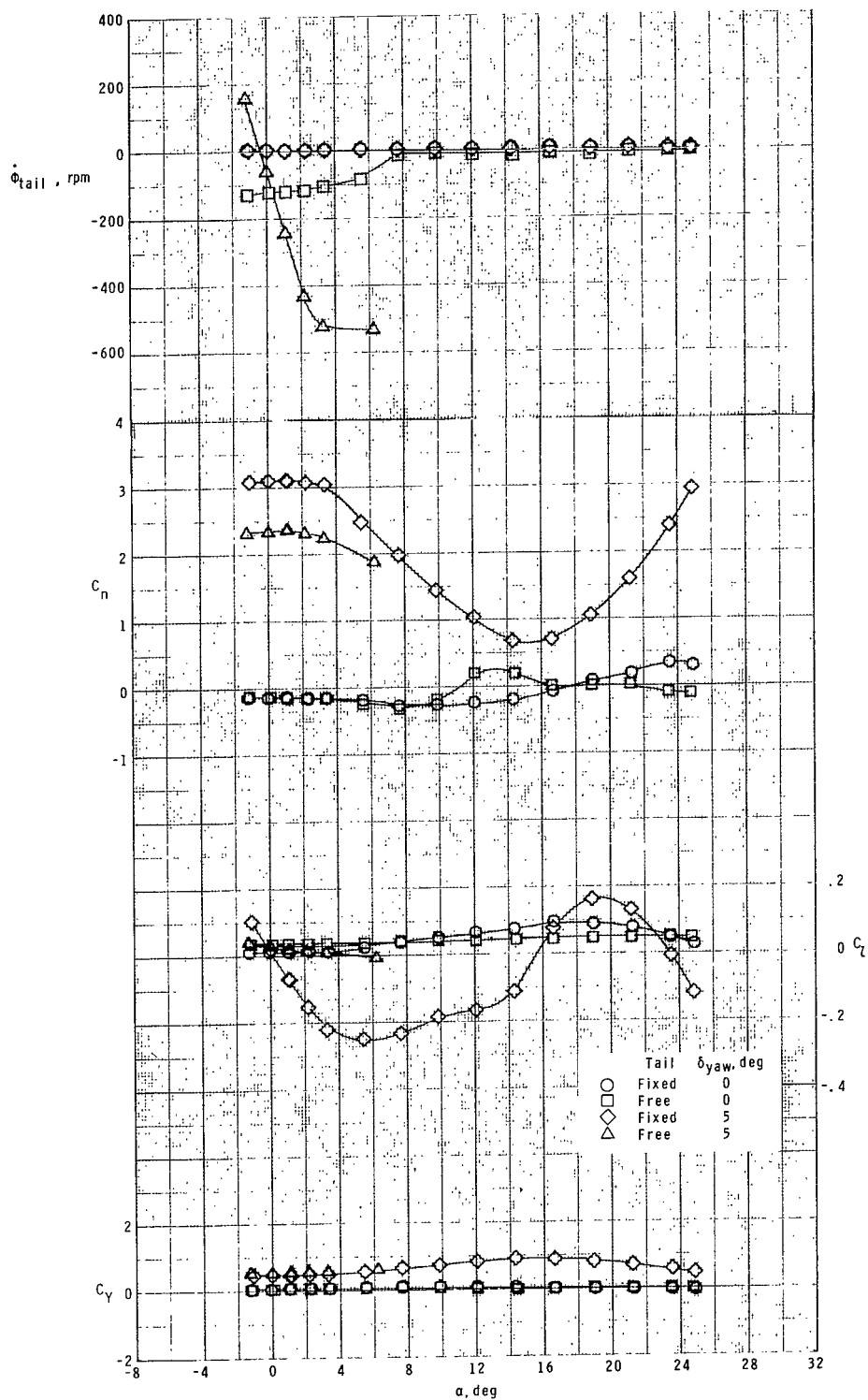
(d) $M = 2.86$.

Figure 12.- Concluded.



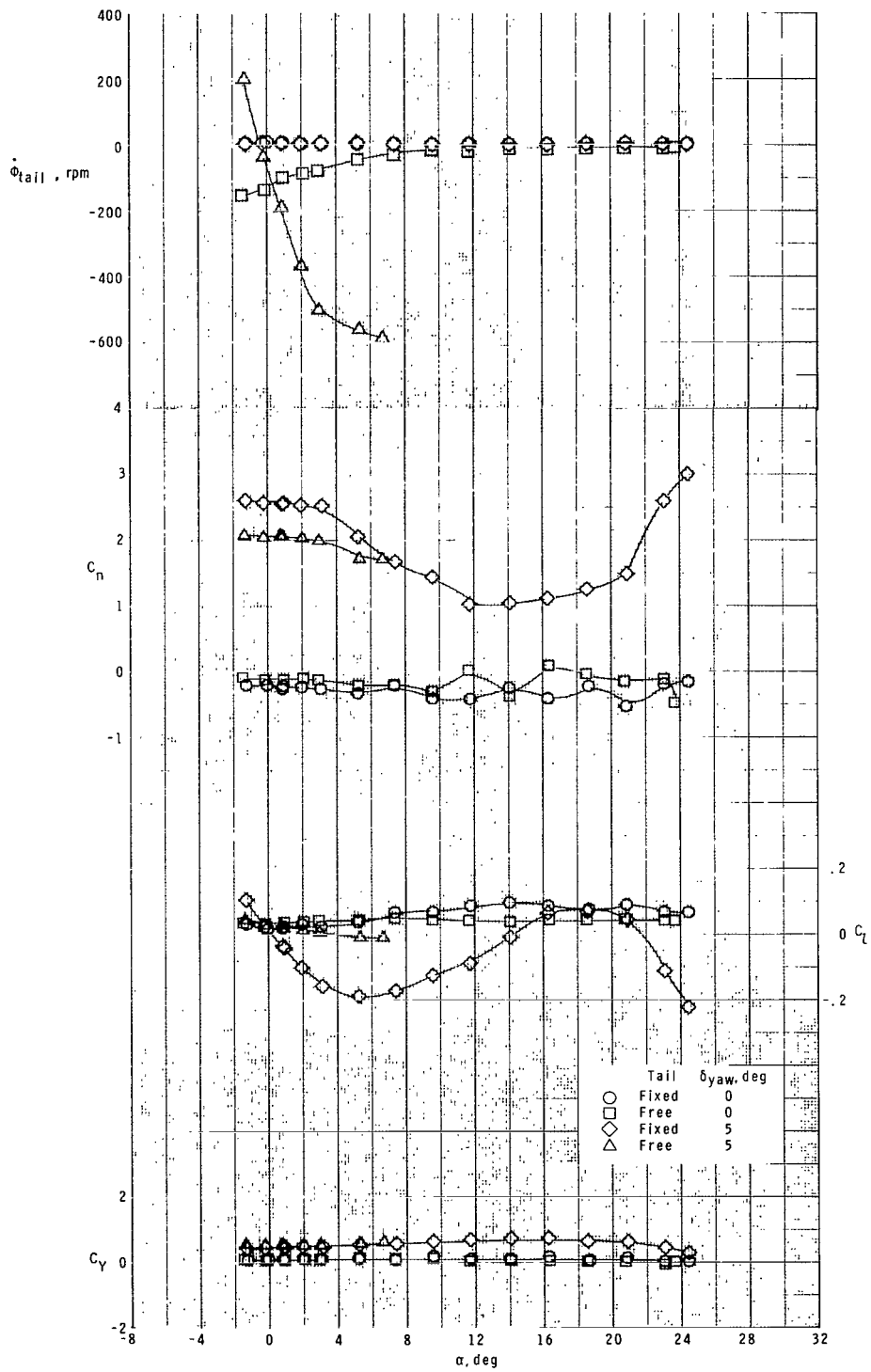
(a) $M = 1.70$.

Figure 13.- Yaw-control characteristics of model with fixed and free-rolling tail at $\phi_C = 0^\circ$. Vertical canards deflected.



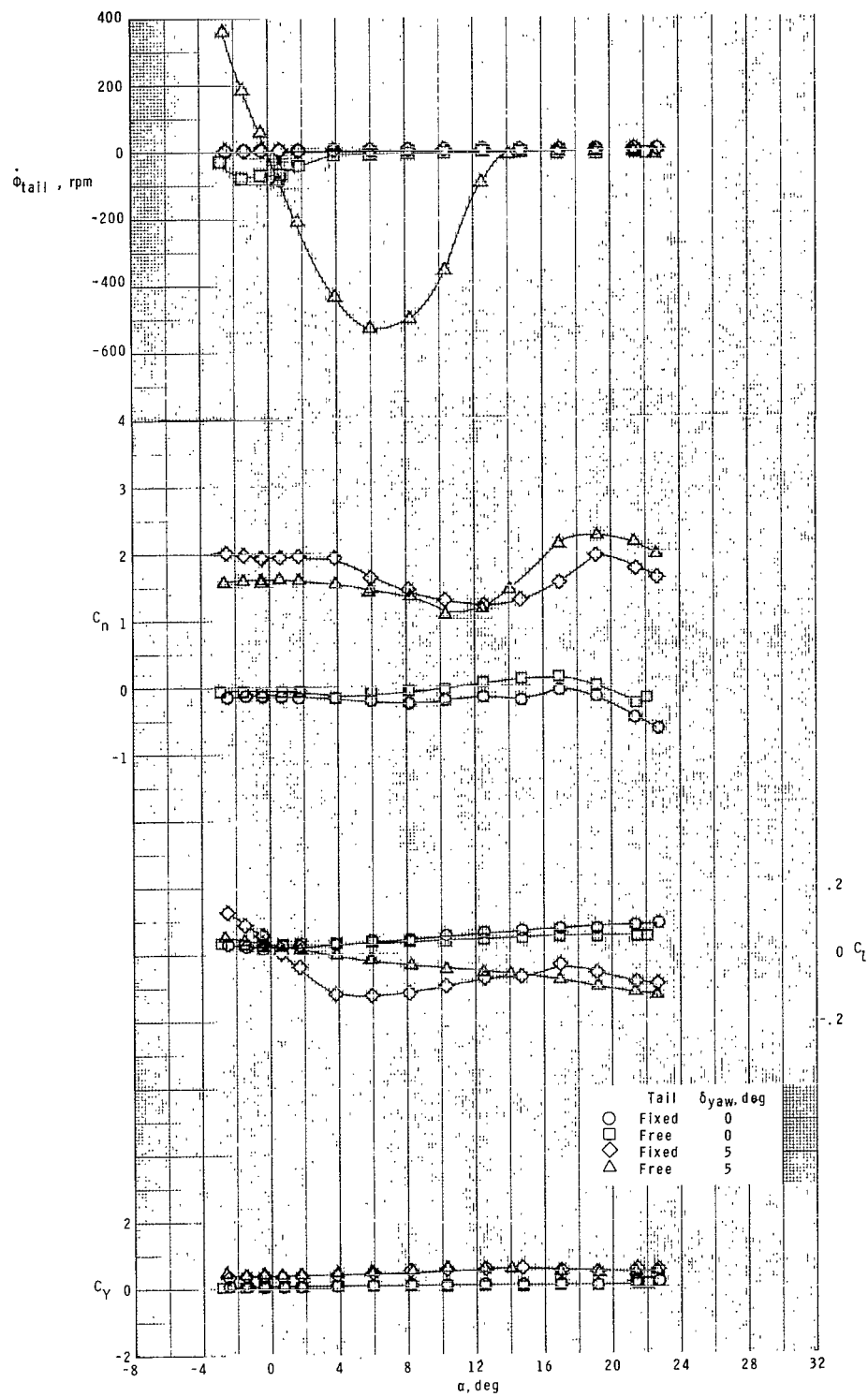
(b) $M = 2.16$.

Figure 13.- Continued.



(c) $M = 2.36$.

Figure 13.- Continued.



(d) $M = 2.86$.

Figure 13.- Concluded.

1. Report No. NASA TP-1316		2. Government Accession No.		3. Recipient's Catalog No.	
4. Title and Subtitle WIND-TUNNEL INVESTIGATION AT SUPERSONIC SPEEDS OF A CANARD-CONTROLLED MISSILE WITH FIXED AND FREE-ROLLING TAIL FINS				5. Report Date September 1978	
				6. Performing Organization Code	
7. Author(s) A. B. Blair, Jr.				8. Performing Organization Report No. L-12297	
9. Performing Organization Name and Address NASA Langley Research Center Hampton, VA 23665				10. Work Unit No. 505-11-23-03	
				11. Contract or Grant No.	
12. Sponsoring Agency Name and Address National Aeronautics and Space Administration Washington, DC 20546				13. Type of Report and Period Covered Technical Paper	
				14. Sponsoring Agency Code	
15. Supplementary Notes					
16. Abstract <p>A wind-tunnel investigation was made at free-stream Mach numbers from 1.70 to 2.86 to determine the effects of fixed and free-rolling tail-fin afterbodies on the static longitudinal and lateral aerodynamic characteristics of a cruciform canard-controlled missile model. The effect of small canard roll- and yaw-control deflections was also investigated. The results indicate that the fixed and free-rolling tail configurations have about the same lift-curve slope and longitudinal stability level at low angles of attack. For the free-rolling tail configuration, the canards provide conventional roll control with no roll-control reversal at low angles of attack. The free-rolling tail configuration reduced induced roll due to model roll angle and canard yaw control.</p>					
17. Key Words (Suggested by Author(s)) Cruciform missile Canard control Free-rolling tail			18. Distribution Statement Unclassified - Unlimited		
			Subject Category 02		
19. Security Classif. (of this report) Unclassified	20. Security Classif. (of this page) Unclassified	21. No. of Pages 76	22. Price* \$6.00		

* For sale by the National Technical Information Service, Springfield, Virginia 22161

NASA-Langley, 1978

National Aeronautics and
Space Administration

THIRD-CLASS BULK RATE

Postage and Fees Paid
National Aeronautics and
Space Administration
NASA-451



Washington, D.C.
20546

Official Business

Penalty for Private Use, \$300

8 1 1U,A, 090878 S00903DS
DEPT OF THE AIR FORCE
AF WEAPONS LABORATORY
ATTN: TECHNICAL LIBRARY (SUL)
KIRTLAND AFB NM 87117

NASA

POSTMASTER:

If Undeliverable (Section 158
Postal Manual) Do Not Return

S